#### MTBE SYNTHESIS IN A RISER SIMULATOR

by

Pierre Fournier

Faculty of Engineering Science Department of Chemical and Biochemical Engineering

> Submitted in partial fulfilment of the requirement for the degree of Master of Engineering Science

Faculty of Graduate Studies The University of Western Ontario London, Ontario, Canada August, 1997

© Pierre Fournier 1997



## National Library of Canada

Acquisitions and Bibliographic Services

395 Wellington Street Ottawa ON K1A 0N4 Canada

#### Bibliothèque nationale du Canada

Acquisitions et services bibliographiques

395, rue Wellington Ottawa ON K1A 0N4 Canada

Your file Votre reférence

Our file Notre reférence

The author has granted a nonexclusive licence allowing the National Library of Canada to reproduce, loan, distribute or sell copies of this thesis in microform, paper or electronic formats.

The author retains ownership of the copyright in this thesis. Neither the thesis nor substantial extracts from it may be printed or otherwise reproduced without the author's permission. L'auteur a accordé une licence non exclusive permettant à la Bibliothèque nationale du Canada de reproduire, prêter, distribuer ou vendre des copies de cette thèse sous la forme de microfiche/film, de reproduction sur papier ou sur format électronique.

L'auteur conserve la propriété du droit d'auteur qui protège cette thèse. Ni la thèse ni des extraits substantiels de celle-ci ne doivent être imprimés ou autrement reproduits sans son autorisation.

0-612-28568-5

# Canadä

### Abstract

In the last decade the demand for cleaner fuels has been increasing steadily. New legislation such as the Amendment to the Clean Air Act of the United States has enforced the use of reformulated gasolines. Methyl tertbutyl ether, MTBE, an ether synthesized from methanol and isobutylene is proposed as a chemical species for the replacement of the more polluting and hazardous gasoline components.

Methanol and isobutanol are considered to complement the current methanol and isobutylene feedstocks used in MTBE synthesis reactors. Using these feedstocks two reaction paths are possible: a) direct coupling of methanol to isobutanol, b) dehydration of isobutanol to isobutylene followed by the reaction of isobutylene with methanol. A H-ZSM-5 zeolite was employed in this present work to study the promotion of the direct coupling of methanol and isobutanol and the reaction of methanol and isobutylene.

The direct coupling of methanol to isobutanol was attempted in the 100-300 °C temperature range. The direct reaction was unsuccessful as it only led to the formation of MIBE an isomer of MTBE.

iii

The MTBE synthesis from methanol and isobutylene was studied between 80 to 160 °C with different catalyst/reactants ratios and reaction times. An injection of methanol, with enough time for methanol to reach adsorption equilibrium, followed by an isobutylene injection was found to be the best operating mode to achieve 100% selectivities toward MTBE with 4-6.8 % isobutylene conversions.

With the gathered experimental data, a reaction rate model based on the Rideal-Eley kinetic model was successfully developed. This model was then applied for the prediction of the reaction rates in the context of future potential industrial applications using riser and downer reactors.

## Dedication

"Vingt fois sur le métier remettez votre ouvrage; Polissez-le sans cesse et le repollissez; Ajoutez quelquefois, et souvent effacez."

Boileau, Chants I, verset 171

I dedicate this work to my mother, Emilienne, and my father, Sylvio, who constantly supported me through my student days.

## Acknowledgment

I want to express my sincere gratitude to Dr Hugo de Lasa for giving me the opportunity to accomplish graduate studies under his supervision. I appreciate his constant guidance and support during the sunny and rainy days of this long journey.

I would like to express my sincere appreciation to Dr A. Prakash, coadvisor of my thesis.

Next I would like to thank Mr Souheil Afara for his friendship, his encouragement, and his continual support during the technical phase of the project.

And last but not the least, thanks to all my fellow graduate students for their friendship, their patience and their help through the realisation of this project.

My last thanks are for the people I may have forgotten in this limited list.

## Table of Contents

Certificate of Examination	ii
Abstract	iii
Dedication	v
Acknowledgment	vi
Table of Contents	vii
List of Tables	xi
List of Figures	xii
List of Appendices	xiv
Nomenclature	xv

## Chapter I - Introduction

٠.

1.1 Reformulated Gasoline	.1
1.2 History of MTBE	.4
1.3 Other Advantages of MTBE	.6
1.4 Needs for the Development of a New Process	.9
1.5 Conclusion	11
Chapter II - Scope of the Study1	12
Chapter III - Literature Review1	4
3.1 Introduction1	14
3.2 Industrial Process Currently Used1	14
3.3 Alternative Routes Proposed for the Production of MTBE1	9

3.3.1 Isomerization of Linear Butene to Isobutylene	19
3.3.2 Butane Isomerization to Isobutane and its	
Dehydrogenation to form Isobutylene	20
3.3.3 Methanol to Produce Isobutylene	20
3.3.4 MTBE from Tert-Butyl Alcohol	
3.3.5 MTBE from a Mixture of Methanol and Isobutanol	21
3.4 Thermodynamic of the Reaction	22
3.5 Potential Byproducts Formed during the MTBE Reaction	25
3.6 Kinetics of the Reaction on Amberlyst-15	26
3.7 Catalyst Investigated for the Production of MTBE	
3.7.1 Use of Two Reactors in Series	
3.7.2 The Dehydration of Isobutanol	
3.7.3 The Etherification Reaction	35
3.8 Effects of the Catalyst Acidity on the Production of MTBE	38
3.9 ZSM-5 and its Major Characteristics	39
3.10 Conclusion	42
Chapter IV - Synthesis, Pelletization and Characterisation of H-ZSM-5	43
4.1 Introduction	43
4.2 Synthesis of Na-ZSM-5	43
4.3 Ion Exchange of the Catalyst	45
4.4 Spray Drying of the Catalyst	47
4.5 Characterisation	
4.5.1 X-ray Diffraction (XRD)	51
4.5.2 Temperature Program Desorption Analysis (TPD)	55
4.5.3 BET Analysis	
4.5.4 Scanning Electron Microscopy (SEM EDX)	
4.5.5 Sieving of The Final Products	
4.6 Conclusion	61

Chapter V - Experimental Methods	.63
5.1 Introduction	.63
5.2 The analytical method 5.2.1 Chemicals to be Analyzed	65 65
5.3 The Riser Simulator. 5.3.1 Details of the Riser Simulator. 5.3.2 The Sampling System.	69
5.4 The experimental Procedure 5.4.1 Different Feedstocks	
5.5 Analysis of the GC Results 5.5.1 Argon as the Internal Standard 5.5.2 Pressure at Sampling Time as the Reference Value	.76
5.6 Temperature and Pressure Profile	.77
5.7 Molar Balances	78
5.8 Experimental Design	.78
5.9 Repeatability of the Results.	79
5.10 Conclusion	79
Chapter VI - Results and Discussion	80
6.1 Introduction.	80
6.2 Methanol and Isobutanol Feedstock	81
6.3 Dehydration of Isobutanol	83
<ul> <li>6.4 Methanol and Isobutylene Feedstock-Three Modes of Operation</li> <li>6.4.1 Mode 1 of Operation</li></ul>	86 89 92 96

6.5 Reaction Mechanism	99
6.6 Reactions Testing at Different Conditions of Temperatures, Catalyst/Reactant ratios, and Reaction Times	
6.7 Model of the Reaction	109
6.8 Fitting Results	114
6.9 Prediction using the Model	118
6.10 Conclusions	122
Chapter VII - Conclusions and Recommendations	123
References	129
Appendix A - BET Analysis: Results and Calculations	134
Appendix B - Calibration of the Reactor Volume	140
Appendix C - Calibration of the Gas Chromatograph and Calculation of the Concentration from the Chromatogram Results	143
Appendix D - List of the experimental observations used to plot Figures 6.7 and 6.8. Calculation of the average conversion for the different conditions.	150
Appendix E - Adsorption Experiments and Related Calculations	152
Appendix F - Equilibrium Conversion Calculation	159
Appendix G - Fitting of the Data to the Rate Model	162
Appendix H - Carbon Balances	166
Curriculum Vitae	

## List of Tables

Table 1.1 Properties of Some Components of Gasoline (Seddon, 1992)4
Table 3.1: Typical Composition of a C <sub>4</sub> 's in a Processed Stream (Hutchings, 1992)17
Table 3.2: Composition of a MTBE Stream (Hutchings, 1992)         18
Table 3.3: Rate Equations Proposed in the Literature         28
Table 3.4: Energy of Activation of the MTBE Reaction on Amberlyst 15         from Different Literature Sources.         29
Table 3.5: Results Reported for Zeolite H-ZSM-5 and H-ZSM-11Compared with Amberlyst-15 (Chu et al, 1987)37
Table 4.1: BET Analysis Results for Zeolite Powder         and Pellets Compared to a Literature Value         58
Table 4.2: Results of the Surface Composition of the Zeolite H-ZSM-5
Table 6.1 Direct Coupling of Methanol and Isobutanol         82
Table 6.2: Dehydration of Isobutanol to Isobutylene
Table 6.3: MTBE Yields for Different Methanol/Isobutylene Ratio         98
Table 6.4: Conversion of Isobutylene toward MTBE at a Reaction         Time of 120 Seconds
Table 6.5: Equilibrium Constants and Conversion of Isobutylene into MTBE107
Table 6.6: Final Partial Pressure of MTBE when the Partial Pressure of         Isobutylene is Increased121

## List of Figures

Fig 1.1: Evolution of the Production of MTBE in the United States	6
Fig 1.2: Schematic of the OXY-CREC concept	10
Fig 3.1: Typical Layout of a MTBE plant(Hutchings et al, 1992)	17
Fig 3.2: Schematic of the two Reactors System: Dehydration Reactor and Etherification Reactor (Nicolaides et al, 1993)	33
Fig 3.3: Structure of ZSM-5 Zeolite (from: Zeolite Catalysis: Principles and Applications, 1990)	41
Fig 4.1: Basic Building Blocks of Zeolites	44
Fig 4.2: Different Ionic Form of the Zeolite H-ZSM-5	46
Fig 4.3: Schematic of the Spray Dryer available at CREC Laboratory	49
Fig 4.4: XRD Pattern for the Zeolite Powder. a) theoretical Pattern (Zeolites, 1996, numbers 5-6), b) Experimental XRD Pattern (Wenyang et al, 1989), and Experimental XRD from the Present Study.	53
Fig 4.5: XRD Pattern for: a)Kaolin, b)Kaolin and H-ZSM-5 in Pellets, and c) After Calcination of the pellets	54
Fig 4.6: Results of the TPD Analysis of the H-ZSM-5	56
Fig 4.7: Picture of the Pellets	61
Fig 5.1: Temperature Program for the Poropak Q Column	66
Fig 5.2: Schematic of the Riser Simulator	69
Fig 5.3: Schematic of the Sampling System	72
Fig 6.1: Temperature and Pressure Profiles for Mode 1, Run 1	87
Fig 6.2: Comparison between the Temperature Profiles of Three Subsequen Runs after Regeneration of the Catalyst for Mode 1	
Fig 6.3: Temperature and Pressure Profiles for Mode 2, Run 1	90

Fig 6.4: Comparison between the Temperature Profiles of the first three Runs afterRegeneration for Mode 2	
Fig 6.5: Temperature and Pressure Profiles for Mode 3, Run 1	93
Fig 6.6: Temperature and Pressure Profiles for Mode 3, Run 3	93
Fig 6.7: Conversion of Isobutylene toward MTBE for a Catalyst/Reactant Ratio of 5	104
Fig 6.8: Conversion of Isobutylene toward MTBE for a Catalyst/Reactant Ratio of 1	104
Fig 6.9: Representation of the Model against the Experimental Results for a Catalyst/Reactant Ratio of 5	115
Fig 6.10: Representation of the Model against the Experimental Results for a Catalyst/Reactant Ratio of 1	115
Fig 6.11: Comparison between the Experimental and the Theoretical Conversion	116
Fig 6.12: Arrhenius Plot of the Forward Kinetic Constant	118
Fig 6.13: Effect on the Conversion of Changing the Catalyst Weight. ( $W_{met} = 0.0157 \text{ g}$ , $V_{iso} = 11 \text{ ml}$ , $T_R = 80 \text{ °C}$ )	120
Fig 6.14: Effect of Changing the Methanol to Isobutylene Ratio on the Equilibrium Conversion ( $W_{cat} = 1 \text{ gram}, p_{met} = 0.0157 \text{ g}, T_R = 80 \text{ °C}$ ).	120

## List of Appendices

Appendix A -	BET Analysis: Results and Calculations1	34
Appendix B -	Calibration of the Reactor Volume1	40
Appendix C -	Calibration of the Gas Chromatograph and Calculation of the Concentration from the Chromatogram Results1	43
Appendix D -	List of the experimental observations used to plot Figures 6.7 and 6.8. Calculation of the average conversion for the different conditions	50
Appendix E -	Adsorption Experiments and Related Calculations1	52
Appendix F -	Equilibrium Conversion Calculation1	59
Appendix G -	Fitting of the Data to the Rate Model1	62
Appendix H -	Carbon Balances1	66

## Nomenclature

- A Methanol
- B isobutylene
- C MTBE
- a, Activity of species i
- $\vec{k}$  Forward reaction kinetic constant ( $W_{cat}^{-1}$  s<sup>-1</sup>)
- $\bar{k}$  Reverse reaction kinetic constant (mol  $W_{cat}^{-1} s^{-1}$ )
- $K = \vec{k} K_A (kPa^{-1} W_{cat}^{-1} s^{-1})$
- K<sub>A</sub> Adsorption constant of methanol (kPa<sup>-1</sup>)
- K<sub>B</sub> Adsorption constant of isobutylene (kPa<sup>-1</sup>)
- K<sub>c</sub> Adsorption constant of MTBE (kPa<sup>-1</sup>)
- Keq Reaction equilibrium constant (kPa<sup>-1</sup>)
- N. Mole of Chemical i in the Reactor
- N<sub>\*</sub> Mole of Argon in the Reactor
- N<sub>m</sub> Total Mole of Reactant and Products in the Reaction Mixture
- n. Mole of Chemical i in the Sample
- n<sub>as</sub> Mole of Argon in the Sample
- p<sub>AR</sub> Partial pressure of Argon (kPa)
- p<sub>A</sub> Partial pressure of Methanol (kPa)
- p<sub>8</sub> Partial pressure of Isobutylene (kPa)
- p<sub>c</sub> Partial pressure of MTBE (kPa)
- p\* Equivalent Partial Pressure of the Adsorbed Methanol and the Methanol in the Gas Phase(kPa)
- p<sub>N</sub> Partial Pressure of Nitrogen (mm Hg)
- p<sub>m</sub> Saturation Pressure of Nitrogen (mm Hg)
- p<sub>sr</sub> Pressure of the reactor at the sampling time (kPa)
- Patm Atmospheric Pressure (mm Hg)
- q quantity of methanol adsorbed on the catalyst surface by unit mass of catalyst (mole/g cat)

- quantity of methanol adsorbed on the catalyst when the monolayer is saturated (mole/g cat)
- R Universal gas constant (cm<sup>3</sup> kPa mol<sup>-1</sup> K<sup>-1</sup>)
- T Temperature (K)
- T<sub>room</sub> Room Temperature (°C)
- V<sub>8</sub> Reactor Volume (cm<sup>3</sup>)
- V<sub>m</sub> Volume of the Monolayer of Nitrogen (cm<sup>3</sup>)
- $V_{N}$  Volume Nitrogen (cm<sup>3</sup>)
- V<sub>srp</sub> Volume of Nitrogen at Standard Temperature and Pressure (cm<sup>3</sup>)
- x Conversion of isobutylene (-)
- y. Molar Fraction of Chemical i in the Gas Phase
- W<sub>cat</sub> Weight of Catalyst (g)
- $\alpha$  P<sub>A</sub>/P<sub>A0</sub>, coefficient of the methanol in the gas phase over the total quantity of methanol in the reactor (-)
- MIBE Methyl Isobutyl ether
- MTBE Methyl tert Butyl Ether
- DME Dimethyl Ether
- TBA Tert-Butyl Alcohol
- DIB Diisobutylene

#### Subscript

- A Methanol
- B Isobutylene
- C MTBE
- exp experimental
- the theoretical
- 0 initial

### Chapter I

### Introduction

#### 1.1 Reformulated Gasoline

A major source of air pollution in North American cities is the result of gas emissions from the tailpipes of automobiles. In order to limit these emissions, a significant amount of research has been devoted over the last twenty years toward the development of cleaner fuels. To attain this objective one possible approach is to enforce the use of catalytic converters allowing the complete combustion of unburned hydrocarbons.

Supported platinum is the most frequently used catalyst in catalytic converters. A difficulty faced with platinum is the fact that it is susceptible of being deactivated by gasoline lead based compounds. Originally, lead based compounds were employed to increase the gasoline octane number. Eventually, they had to be replaced because of their negative effects on the platinum catalyst, the environment, and the public health. Refiners proposed replacing lead based compounds by other octane enhancers such as aromatics. Aromatics are mainly produced by the reforming of paraffins.

Unfortunately, during the mid 80's, and even with lead compounds not being part of the gasoline formulation, it became apparent that catalytic converters were not going to give the expected results. Gas emissions were still too high and complementary measures had to be taken. In this context the design of cleaner burning fuels or "reformulated gasolines" became an important issue.

Two main goals are currently set for the reformulated gasolines: a) low emission of carbon monoxide, b) low content of chemicals having photochemical activity. The photochemical activity is related to ozone production. These two goals are part of the amendment of the "Clean Air Act", a United States law adopted in November 1990.

In order to reach these goals several regulations are currently enforced. The Clean Air Act sets strict limits on aromatic content in gasoline with an emphasis on benzene. The total content of benzene should be lower than 1% (Seddon, 1992). Consequently, new approaches to lower the content of aromatics are currently being researched. A promising one is the use of new FCC catalysts that yield gasolines with higher olefin content. These new FCC catalysts also limit the content of aromatics with benzene being less than 1 wt% (Gianetto *et al.*, 1996). The Clean Air Act also enforces the utilisation of new blending components, such as oxygenates, to replace the current ones.

Oxygenates should have the following properties: a) high octane number, b) low vapour pressure, and c) low photochemical activity. Oxygenates, while offering a high octane number, also increase the level of oxygen in gasoline thus reducing the level of

carbon monoxide emissions. Two main classes of oxygenates are proposed: alcohols and ethers.

Alcohols such as methanol, ethanol and tert-butanol, while valuable for gasoline blending, show potential problems. First, in the case of methanol and ethanol, they must be blended with a higher alcohol, as co-solvent, to avoid phase separation in the presence of water. If not properly blended, these alcohols while in contact with water separate from gasoline and water may accumulate in the gasoline tank. Also, given the relatively high Reid vapour pressures of 414 kPa for methanol and 117 kPa for ethanol, vapour locks in gasoline lines are a frequent problem. Furthermore, tert-butanol shows relatively low research octane number and is less interesting overall.

Three ethers are proposed for reformulated gasoline: methyl-tert-butyl ether (MTBE), ethyl-tert-butyl ether (ETBE) and tert-amyl methyl ether (TAME). These three ethers possess octane numbers above 100, a Reid Vapour pressure below 69 kPa and an acceptable photochemical activity below 10. Note that some blending components in gasoline reach photochemical activities of 60 which is much larger than the proposed ethers. For more details about the properties of the ethers refer to Table 1.1. From the point of view of phase separation none of these ethers present the problems of methanol and ethanol.

Component	Research Octane Number (RON)	Motor Octane Number (MON)	Reid Vapour Pressure kPa	Photochemical Activity
methanol	123	93	414	1.0
ethanol	115		117	3.3
tert-butanol	100		62	1.1
MTBE	123	97	55	2.6
ETBE	111		28	8.1
TAME	113	97	14	7.9
iso-octane	100	110	11	3.15
1-butene	144	126	344	24.4
benzene	99	91	23	0.88
toluene	124	112	7	5.98

Table 1.1 Properties of Some Components of Gasoline (Seddon, 1992)

\*Photochemical activity is measured as rate of reaction with OH radicals, units cc/(molecule.sec) x 10<sup>12</sup>.

Finally, compared to the alcohols, the three ethers are superior in all respects. When the ethers are in turn compared to each other, MTBE appears, however, to be the best candidate for gasoline blending. Although MTBE has the highest Reid Vapour Pressure, it offers the highest octane number and the smallest photochemical activity. The fact that MTBE has been produced for over 20 years is also an advantage for its use. Refiners have already gathered significant experience with the handling of this chemical.

#### 1.2 History of MTBE

The first industrial production of MTBE took place in Italy by Snamprogetti/Ecofuel in 1973. The plant is still in operation and has a capacity of 100 000 tons/year. The reaction that leads to MTBE involves the simple coupling of methanol and isobutylene. This reaction is catalysed by an acidic resin. The MTBE plant uses the isobutylene contained in the C<sub>4</sub> as feedstock. This C<sub>4</sub> fraction may be produced in a steam cracker or a in catalytic cracking unit. The isobutylene fraction ranges between 35 and 53 wt % after removal of the

butadiene fraction (Hutchings *et al.*, 1992). The reaction is carried out in a fixed bed reactor where the temperature is maintained between 30 and 100 °C and the pressure between 7 and 14 atm. Ever since, other refiners have improved the original design of the MTBE process. By now, the production of MTBE is a well established industrial process and this ether is produced in several plants around the world.

MTBE was first used to increase the octane number of gasolines that would not otherwise reach the targeted gasoline specification. MTBE was also used to produce premium gasoline or high octane gasoline. At the present time, with the amendment to the Clean Air Act in the United States, the use of MTBE is becoming very popular. Figure 1.1 shows the steady increase of the production of MTBE in the United States for the period of 1985-1995. This increase in MTBE production is expected to reach a plateau by the year 2000 when the new law will be fully enforced. By that time, the level of MTBE in gasoline will be 2 wt % or 12.7 vol %. It is expected that other countries will eventually adopt policies which will be similar to those of the United States. Japan, for example, recently approved the addition of up to 7 vol % of MTBE in gasoline.

Thus, with new legislation expected to be adopted in the very near future in several countries, the demand for MTBE can only steadily increase.

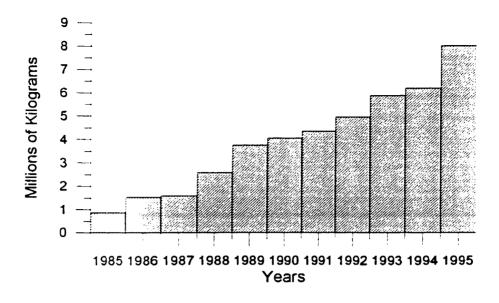


Figure 1.1: Evolution of the Production of MTBE in the United States. (Chemical and Engineering News, 1996)

#### 1.3 Other Advantages of MTBE

Isobutylene, one of the reactants in the MTBE production, has a research octane number of around 140. Consequently isobutylene is used as an octane enhancer with other C4's. Considering the large quantity of isobutylene available in the C<sub>4</sub> cut of an FCC unit, up to 50% in some refineries, a large supply of iso C<sub>4</sub><sup>\*</sup>s is available. However, isobutylene is highly volatile and cannot be used as a major blending component. Depending on the seasons and the areas where the gasoline is to be distributed, refiners add a variable quantity of different butenes produced in either the FCC or the hydrocracking units. The amount of butenes is limited by their high vapour pressure which can cause vapour lock in the gas lines of cars or even worse end up in the atmosphere.

Through the use of MTBE, the amount of methanol and isobutylene for the production of gasoline can be increased. MTBE addresses two major problems: a) it does not have the high vapour pressure of iso-butylene and methanol mixed directly, and b) there is no phase separation problem as experienced with methanol in the presence of water. Note that methanol is usually produced from syngas which is the reaction product of methane and steam. In this manner, methane production in a refinery could also lead to the production of usable gasoline and increase the overall supply of gasoline range hydrocarbons. Thus, the production of MTBE extends the supply of hydrocarbons available from crude oil.

The C<sub>4</sub> fraction, mentioned earlier, is currently used for the alkylation processes in several refineries. The alkylation reaction takes place when isoparaffins, isobutane or isopentane, react with olefins in the presence of either sulphuric acid or hydrofluoric acid. The products of the reaction are high molecular weight isoparaffins such as isooctane, isoheptane and their isomers. If the reaction conditions are properly controlled, the motor octane number of the alkylates can reach 88 to 94 and the research octane number 94 to 99 (Gary *et al.*, 1984). Like MTBE, the alkylation process increases the fraction of crude oil available for gasoline blending by using highly volatile compounds to obtain heavier products with a lower Reid vapour pressure. In the case of a sulphuric acid unit, the most widely used process, the implementation of an MTBE unit has the overall effect of increasing the octane number of the combined product, i.e. MTBE plus alkylates compared to alkylates alone. The MTBE unit processes the C<sub>4</sub> stream before it enters the alkylation

unit, consuming up to 90 % of the isobutylene content (Schmitt, 1991). If the isobutylene were to be reacted in the alkylation unit, it would end up in a lower octane number product than MTBE. Consequently, the MTBE unit allows an increase of 0.75 to 1 points of the final alkylate octane number (Schmitt, 1991). In fact, the effect of adding an MTBE unit is two-fold. On one hand, it produces a higher octane product than would the alkylation process alone. On the other hand, it increases the time-on-stream of the alkylation unit, allowing the production of alkylates of higher quality with a higher octane number.

It is interesting to mention that MTBE not only leads to the production of higher quality gasoline, it can also be used to obtain pure isobutylene which is used as a feedstock for polymerisation processes. Once MTBE has been obtained, it can be easily separated to obtain a stream of highly concentrated MTBE. This stream of MTBE can then, be reacted to obtain a product stream composed of methanol and isobutylene. Then, isobutylene is easily extracted from MTBE, obtaining an almost pure stream for polymerisation.

#### 1.4 Needs for the Development of a New Process

As described above, the demand for MTBE will steadily increase in the near future and will exhaust the current feedstock used for the production of MTBE. Pressures will be placed on the industry to develop new processes. Thus, a first goal for chemical companies is to design processes that will use current feedstocks more efficiently. This can be achieved by the development of new catalysts which are appropriate for existing installations or by the development of new MTBE reactors. Another possibility is the development of new catalysts suitable for new reactor designs. The ultimate avenue will be to move to cheaper and more accessible feedstocks and this will require innovative processes.

The OXY-CREC concept developed by Hugo de Lasa, is one potential new design that could lead to a new generation of MTBE production units. Figure 1.2 presents a schematic diagram of the OXY-CREC concept. The core of this new design is a riser/downer reactor which offers several advantages over a conventional MTBE reactor. The more significant ones are: a) the capacity of controlling the contact time of the reactants with the catalyst in the order of few to several seconds; b) the ability of controlling the reaction temperature, thus, avoiding potential hot spots and catalyst deactivation; and c) the possibility of fully regenerating the catalyst on a continuous basis therefore keeping it in a highly active state.

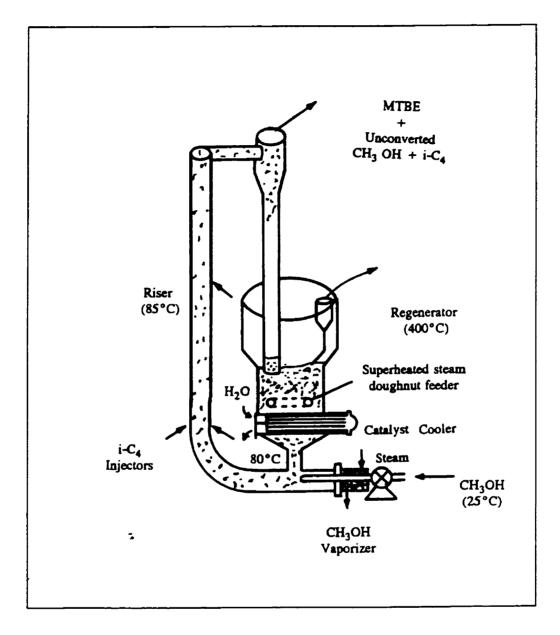


Figure 1.2: Schematic of the OXY-CREC Reactor Concept

#### 1.4 Conclusion

The latest trends related to MTBE manufacturing and its applications were reviewed in the present introductory chapter. The advantages of using oxygenates and particularly ethers in gasoline formulations were also highlighted.

The following chapters of the present study consider the various research steps undertaken: a) Literature Review, b) Synthesis, Pelletization and Characterisation of the H-ZSM-5, c) Experimental Methods, d) Results and Discussion, and, e) Conclusions and Recommendations.

### Chapter II

### Scope of The Study

The primary objective of this thesis is to demonstrate the feasibility of the OXY-CREC concept using the Riser Simulator available at the laboratories of CREC, Chemical Reactor Engineering Centre, at the University of Western Ontario. The Riser Simulator reproduces, at the laboratory scale, the conditions met in a riser reactor and thus provides an effective way of simulating riser/downer operations.

The catalyst considered in this study is a H-ZSM-5 zeolite. This catalyst provides strong acid sites and potentially a high selectivity toward MTBE. The synthesized catalyst crystals (about 1 micron) has to be pelletized in order to obtain particles with acceptable fluidization properties. An advantage of H-ZSM-5 for MTBE synthesis is given by its inherent thermal stability. This allows for easy regeneration and minimum catalyst deactivation during reaction conditions.

The goal of the present research is to test two alternative feedstocks for MTBE synthesis: methanol/isobutanol, and methanol/isobutylene. These feedstocks are going to be studied under different operating conditions such as temperature, catalyst/reactant ratios and residence times.

Finally, it is an objective of this study to propose a kinetic rate equation for the MTBE synthesis. This rate equation will be helpful to simulate riser/downer operations under conditions close to the ones investigated in the present study. This rate equation should also provide insights for a gas phase MTBE synthesis process.

## Chapter III

### Literature Review

#### 3.1. Introduction

This chapter is devoted to the review of technical information on the MTBE synthesis available in the scientific literature. These topics are covered in the following sequence:

- a) An overview of the actual industrial process,
- b) Available alternatives to replace or supplement the conventional process,
- c) Thermodynamics of the reaction involving methanol and isobutanol, and methanol and isobutylene,
- d) Possible processes using methanol and isobutanol feedstocks,
- e) Etherification and dehydration reactions,
- f) Catalysts currently used, as well as the effect of their acidity and shape selectivity properties,
- g) The H-ZSM-5 zeolite , catalyst of choice, for the present program.

#### 3.2 Industrial Process Currently Used

As stated in the introduction, MTBE was first produced in Italy in 1973. Ever since new processes which are more efficient have been developed. The purpose of this section is to explain the main features of this process, its advantages and its limitations.

The overall reaction stoichiometry for MTBE synthesis is quite simple: one mole of methanol is added to one mole of isobutylene.

$$CH_{,OH} + (CH_{,})_{,C} = CH_{,} \rightarrow CH_{,} - O - C(CH_{,})_{,}$$
(3.1)

This etherification reaction is catalyzed in an acidic medium. The reaction could be realized in an homogeneous reactor with the reactants being mixed with an acid to lower their pH. The use of a liquid acid requires, however, an additional separation step. Eventually, the use of solid acidic catalysts, easing the separation of the catalyst from the liquid phase, was advocated and this led to the development of heterogeneous reactors.

Nowadays the most common catalyst used is a strong ion-exchanged resin: Amberlyst-15. Amberlyst-15 shows a selectivity toward MTBE ranging from 92 to 98%. MTBE selectivity is directly related to the methanol/isobutylene ratio and increases when methanol is in slight excess. However, the resin is not heat resistant and must be used at temperatures lower than 120 °C.

The MTBE reaction is highly exothermic with a heat of reaction of -37.7 kJ/mole at 292 K. The reaction is thermodynamically controlled making it inadvisable to use reactor temperatures much higher than 90 °C. Above 90 °C, the yields of MTBE are less interesting, given the influence of the reverse reaction and the Amberlyst weak temperature resistance. These two problems led to the use of operating temperatures between 30 to 90 °C. Furthermore, the desire of operating the reactor in the liquid phase, where best results with Amberlyst-15 were obtained, made necessary the use of pressures ranging from 7 to 14 atm.

The classical feedstock for the reaction is a methanol and isobutylene mixture. Both chemicals can be produced on site using existing refinery capabilities. Methanol can be produced from synthesis gas, produced by the steam reforming of methane. Isobutylene is available from the  $C_4$  fractions produced by the catalytic cracking units or the hydrocracking units of existing refineries. The typical composition of a processed C4 stream is shown in Table 3.1.

Component	Composition wt %
C <sub>3</sub> 's	0.04
n-butane	5.12
isobutane	1.80
1-butene	14.50
isobutylene	22.63
trans-2-butene	6.16
cis-2-butene	3.66
1,3-butadiene	45.74
1,2-butadiene	0.22
propyne	32 ppm
vinylacetylene	350 ppm
1-butyne	210 ppm
C <sub>5</sub> 's	0.10

Table 3.1: Typical composition of  $C_4$ 's in a process stream (Hutchings, 1992)

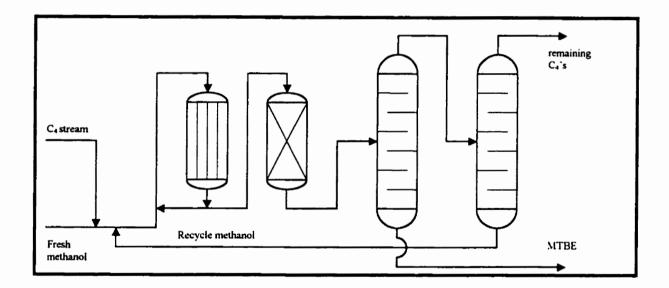


Figure 3.1: Typical Layout of a MTBE plant (Hutchings et al, 1992).

Component	Composition wt %
MTBE	99.10
methanol	0.01
tert-butyl alcohol	0.20
3-methoxy-1-butene	0.47
1-methoxy-2-butene	0.18
2-methoxybutane	0.01
heavy products	0.02
water	5-10 ppm
peroxydation inhibitor	200 ppm

 Table 3.2: Typical Composition of a MTBE Stream (Hutchings, 1992)

Figure 1.1 shows a typical layout of a MTBE plant. First, fresh and recycled methanol are mixed with the C4 stream. This combined stream is first fed to a packed bed reactor which is usually operated close to isothermal conditions. Uniform temperature avoids hot spots leading to fast catalyst decay. Thus, temperature control is a significant concern in this first reactor. The reaction stream from the isothermal reactor is directed to a second reactor, packed bed type, to complete the MTBE synthesis. The reaction takes place in this second stage adiabatically. Using such a train of reactors, isobutylene conversion can reach 95%.

The following step in the process is the separation of MTBE from the remaining  $C_{4's}$ , methanol, and byproducts. Following this operation, unconverted methanol is separated from the C4 stream and recirculated to the first reactor. Table 3.2 shows the composition of a typical stream where the purity of MTBE reaches 99.1%.

#### 3.3 Alternative Routes Proposed for the Production of MTBE

Several routes have been proposed to produce MTBE. Since the quantity of isobutylene produced by catalytic cracking and hydrocracking is limited a major technical challenge is to develop new routes to produce isobutylene. Two of these new approaches also consider direct etherification of two alcohols. This section will review the various alternatives currently being proposed.

#### 3.3.1 Isomerization of Linear Butene to Isobutylene.

Equilibrium studies show that, at low temperature the most favored butene isomere is isobutylene. For example, at 400 K, isobutylene can compose as much as 60 % of a butene mixture (Butler *et al.*, 1993). Zeolites with their strong acid sites can, in the proper temperature range, catalyze isomerization reactions. Narrow pores zeolites add a shape selectivity effect, thus limiting the formation of unwanted dimers. Moreover, in the case when regeneration is needed, zeolites can withstand the high temperatures required. In all these respects, the most promising zeolite is the ferrierite.

Confirming this trend a new large scale demonstration isomerization plant was announced in 1993 (Butler *et al.*, 1993).

# 3.3.2 Butane Isomerization to Isobutane and its Dehydrogenation to Form Isobutylene.

In order to increase the octane number of the butane feedstock through the alkylation process, butane isomerization has been used quite extensively for over 30 years. By now, this is a well known and established process. Over the years new catalysts have been developed to catalyze the isomerization reaction at temperatures below 200 °C where isobutane formation is thermodynamically favored (Frischkorn *et al.* 1988).

Following isomerization, the next process step is the dehydrogenation of isobutane. Isobutane is circulated through a furnace where it is catalytically converted to isobutylene. Typical byproducts such as methane and propylene are also formed (Monfils *et al.*, 1992).

#### 3.3.3 Methanol to Produce Isobutylene

Isobutylene can also be produced from methanol. Methanol is reacted on silicate titanium oxides impregnated catalysts producing a stream containing up to 15 wt % of isobutylene, 20 wt % of isobutane, 5 wt % of linear butane and 10 wt % linear butene (Anthony *et al.*, 1984). Reaction conditions are 410 °C and 1 atm. Then, this stream can be reacted with methanol to obtain MTBE. The main

advantage of this process is the possibility of producing MTBE from methanol, with methanol readily available from synthesis gas.

# 3.3.4 MTBE from Tert-Butyl Alcohol.

Tert-Butyl Alcohol (TBA) is a byproduct of the production of propylene oxide. This by-product is available in large quantities. TBA could be coupled directly to methanol to form MTBE. However, there is strong indication that direct coupling of TBA to methanol is not viable (Matouq *et al.*, 1994). Matouq *et al.* showed that isobutylene is necessary for the formation of MTBE from methanol and TBA. Therefore, the other option is to dehydrate TBA first to obtain isobutylene. Then, the isobutylene is reacted with methanol to produce MTBE. Dehydration of TBA to isobutylene shows significant potential as the TBA dehydration can be carried out at 315 °C with a 99.7% conversion (Abraham *et al.*, 1992).

# 3.3.5 MTBE from a Mixture of Methanol and Isobutanol

Methanol and isobutanol are two main alcohols obtained from the reaction of synthesis gas. The composition of the product mixture reached 48% for methanol and 20% for isobutanol. The catalysts studied contained copper, manganese, zinc, chromium and potassium oxide (Stiles 1991). The ratio of methanol to isobutanol and their quantity could eventually be controlled by modifying the catalyst, the reaction conditions and the composition of the syngas (Stiles 1991).

Of the alternative routes for MTBE, and considering the large availability of natural gas, syngas has excellent potential to produce MTBE. Most of the other alternatives use products which are mostly available through refining and are already in high demand for other chemical processes. Considering these facts, the remainder of this literature review will focus on the alternative processes for MTBE from synthesis gas.

## 3.4 Thermodynamics of the Reaction

When methanol and isobutanol are being used as the MTBE feedstock, two reaction paths can be followed. The first one is the direct etherification reaction of methanol and isobutanol to obtain MTBE.

$$CH_3OH + (CH_3)_2CHCH_2OH \rightarrow CH_3 - O - C(CH_3)_3$$
(3.2)

The second path begins with the dehydration of isobutanol to obtain isobutylene. This is followed by the addition of methanol to the dehydration product.

First Step

$$(CH_3)_2 CHCH_2 - OH \rightarrow (CH_3)_2 C = CH_2 + H_2 O$$
 (3.3)

Second Step

$$(CH_3)C = CH_2 + CH_3OH \rightarrow CH_3 - O - C(CH_3)_3$$
(3.4)

The direct synthesis of MTBE from methanol and isobutanol is the most interesting of the two described routes as only one reaction step is involved, the etherification reaction eq(2.2). Unfortunately the main product of the reaction from methanol and isobutanol is methyl isobutyl ether, MIBE, an isomer of MTBE. It appears that thermodynamic equilibrium does not prevent the isomerization of MIBE toward MTBE and that kinetic limitations may explain this behavior; i.e. the isomerization reaction rate is very slow when compared to the etherification reaction rate (Klier *et al.*, 1991).

The synthesis of MTBE from methanol and isobutylene, eq(2.4), is strongly influenced by thermodynamic limitations. The reaction is exothermic with  $\Delta H$ = -37.7 kJ/mole at 298 K (Rehfinger *et al.*, 1990). As expected the

equilibrium is shifted to the product side when temperature is lowered and to the reactants side when the temperature is increased.

To predict equilibrium conditions different theoretical equations have been developed. An example of these equations is the one derived using the UNIFAC model for the case of MTBE synthesis in the liquid phase (Colombo *et al.*, 1983).

$$\ln K_{\star}^{T} = -10.0982 + \frac{4254.05}{T} + 0.2667 \ln T - \frac{1}{RT} \sum_{i=1}^{4} 0.0242 v_{i} v_{i}^{i} (P - P_{i}^{i}) \quad (3.5)$$

Methanol has a non-ideal behavior because of its polar nature displaying activity coefficients higher than one while isobutylene and MTBE activity coefficients are closer to unity. The fourth term of the right hand side of eq (2.5) represents the influence of pressure on fugacity and it was found to be negligible for pressures below 20 atm. However, Colombo *et al.* 1983 expressed concerns of using eq(2.5) to predict equilibrium for high methanol concentrations.

As eq (2.5) is only adequate for liquid phase MTBE reaction, another equation was developed for gas phase reactors (Tejero *et al.*, 1988):

$$\ln K = 7340T^{-1} - 4.749(\ln T) + 1.169 \times 10^{-2}T$$
  
-4.339 × 10<sup>-2</sup> T<sup>2</sup> + 2.514 × 10<sup>-4</sup> T<sup>2</sup> + 4.65 (3.6)

In the case of the gas phase MTBE synthesis, fugacity coefficients for various components are very close to unity. Consequently, the equilibrium constant can be computed using directly the gas fractions of each of the components and the total pressure of the system. Equilibrium constants obtained from various experiments were compared to the theoretical ones and good agreement was found (Tejero *et al.* 1988).

# 3.5 Potential Byproducts Formed During the MTBE Reaction

While methanol and isobutylene are reacted together to form MTBE other parallel reactions, producing undesirable byproducts may take place. The three main byproducts are: a) dimethyl ether (DME), b) tert-butyl alcohol (TBA), c) diisobutylene isomers (2,4,4-trimethyl-1-pentene (2,4,4-TMP-1), and 2,4,4-trimethyl-2-pentene (2,4,4-TMP-2).

The various reactions leading to byproducts formation can be summarized as follows:

$$2CH_3OH \to CH_3 - O - CH_3 + H_2O \tag{3.7}$$

$$(CH_3)_2 C = CH_2 + H_2 O \rightarrow (CH_3)_3 C - OH$$
 (3.8)

$$2(CH_3)_2 C = CH_2 \to CH_3 = C(CH_3)CH_2C(CH_3)_3 (2,4,4-\text{TMP-1})$$
(3.9)

$$2(CH_3)_2 C = CH_2 \to CH_3 C(CH_3) = CHC(CH_3)_3 (2,4,4-\text{TMP-2}) \quad (3.10)$$

Although these byproducts have potential to contribute to the final octane number of gasoline, they are less interesting than MTBE because of their lower octane number (Ali *et al.*, 1990).

Several strategies have been used to reduce the production of these undesirable byproducts. First, the ratio of methanol/isobutylene is kept above 1 to suppress the dimerization of butene. Reaction temperatures below 100 °C diminish the formation of DME. Finally, the pretreatment of the feed stream, removing water, prevents the formation of TBA.

#### 3.6 Kinetics of the Reaction on Amberlyst-15

Amberlyst-15 is the most used catalyst for the synthesis of MTBE. Several studies have been published to explain the kinetics of MTBE formation. Most of the studies consider that the MTBE synthesis is an heterogeneous reaction occurring on a solid catalyst. The reaction takes place in several steps. For a porous catalyst, reactants have to diffuse through the pores, adsorb on the

surface of the catalyst and react forming products. Products have to subsequently desorb and diffuse out of the catalyst.

In the case of the MTBE reaction, Zhang *et al.* (1995) reported that, below 333 K and for particles smaller than 0.74 mm, no mass transfer limitations were observed. Al-Jarallah *et al.* (1988) indicate that stirring the mixture of MTBE and Amberlyst-15 above 1000 RPM eliminated mass transfer limitations for all experimental conditions, i.e. 70-100 °C. Ali *et al.*, 1990 argued that the use of particle size, 0.32 and 0.60 mm, had no effect on fractional conversion at 333 K and conclude that intraparticle diffusion was negligible. Therefore, diffusion inside the catalyst was not a limiting step in the reaction process. Taking into account the absence of diffusional limitations, Zhang *et al.* (1995) described the reaction as being a pseudohomogeneous process.

As a result of this, the approach adopted by different authors is the use of models that consider the following hypothesis:

- a) the overall reaction rate is controlled by the intrinsic reaction rate,
- b) methanol and/or isobutylene are adsorbed on the catalyst surface,
- c) the reaction takes place between the adsorbed reactant proceeds on the surface of the catalyst,
- d) MTBE desorbs from the surface of the catalyst.

The reaction between two adsorbed molecules can be described by the Langmuir-Hinshelwood mechanism. The reaction between an adsorbed molecule and a second one in the gas phase can be described by the Rideal-Eley mechanism. The controlling step can either be the adsorption of the reactants on the surface, methanol and/or isobutylene, the reaction occurring on the surface or the desorption of the product (MTBE).

Ali *et al.* (1990); Al-Jarallah *et al.* (1988); Rehfinger *et al.* (1990); Zhang *et al.* (1995) agreed that a model describing the reaction as the limiting step with methanol being the only adsorbed reactant better fit the experimental data. A list of proposed rate equations is given in Table 2.3.

Reference	Equation
Al-Jaraliah (1988)	$r_{s} = \vec{k} K_{A}^{a} \left[ \frac{C_{A}^{a} C_{B}^{b} - C_{c}^{c} / K_{a}}{\left(1 + K_{A} C_{A} + K_{c} C_{c}\right)^{a}} \right]$
Ali <i>et al.</i> (1990)	$r_{r} = \frac{\vec{k}C_{A}C_{B} - \vec{k}RC_{c}}{C_{A} + RC_{c}}$
Rehfinger <i>et al.</i> (1990)	$r_{r} = K \left[ \frac{a_{s}}{a_{s}} - \frac{1}{K_{rq}} \frac{a_{c}}{a_{s}^{2}} \right]$
Zhang <i>et al.</i> (1995)	$r_{r} = K \left[ \frac{a_{s}}{a_{s}} - \frac{1}{K_{s}} \frac{a_{c}}{a_{s}^{2}} \right]$

 Table 3.3: Rate Equations Proposed in the Literature

Note: indices are A = methanol; B = isobutylene; C = MTBE; a = order of methanol; b = order of isobutylene; c= order of MTBE

C = bulk concentration; a = bulk activities

R = ratio of MTBE to methanol adsorption constant

Ali *et al.* (1990) employed a model developed by Gickel *et al.* (1983) assuming: a) a negligible number of free sites, b) a high value for the RC<sub>c</sub> term, and, c) a high methanol surface concentration. In agreement with this, Rehfinger *et al.* (1990) et Zhang *et al.* (1995) both assumed that the number of free sites were negligible and that the adsorbed fraction of other chemicals species but methanol was insignificant. While various models assume the reaction to be first order for all the chemicals involved, Al-Jarallah *et al.* (1988) reported the reaction to be first order for methanol, half order for isobutylene and 1.5 order for MTBE.

Regarding the apparent energy of activation, Table 3.4, the values reported are, with only one exception, in a quite similar range.

References	Energy of Activation kJ/mol		
Gicquel and Torck (1983)	82.0		
Al-Jarallah et al. (1988)	87.9		
Ali <i>et al.</i> (1990)	68.9		
Rehfinger et al. (1990)	92.4		
Zhang et al. (1995)	85.4		

 Table 3.4: Energy of Activation of the MTBE Reaction on Amberlyst 15 from

 Different Literature Sources.

Note that Ali et al. (1990) obtained a value which is significantly lower than the other literature references. This could be explained by the fact that Ali *et al.* (1990) performed experiments for MTBE synthesis in a gas phase reacting system while all the other authors developed studies in the liquid phase.

#### 3.7 Catalyst Investigated For the Production of MTBE

Since methanol and isobutanol can be readily available in a mixture, refer to section 3.3.5, it is interesting to develop a process where the two chemicals would not need to be separated thus reducing the cost for the MTBE synthesis. Keeping this concept in mind, two processes have been proposed:

- 1) direct coupling of methanol and isobutanol
- dehydration of isobutanol to isobutylene followed by methanol to isobutylene coupling

As it is described before, the first process is not allowed due to kinetic limitations. Moreover it is shown by Nicolaides *et al.* (1993), that the main product of the reaction with methanol and isobutanol is MIBE. The two catalysts compared in their study were Amberlyst-15 and H-ZSM-5 zeolites. The experiments were conducted in the gas phase at ambient pressure using a tubular stainless steel reactor. The temperature of reaction for Amberlyst 15 was 84 to 121 °C and for H-ZSM-5 was 75 to 100 °C. The catalyst giving best results for these conditions was Amberlyst 15 with a yield of MTBE and MIBE of 3.3%

and a MTBE/MIBE ratio of 1 to 9. Several other byproducts, such as TBA, DIB and C<sub>8</sub>, were also present.

Results from Klier *et al.* (1993) corroborate Nicolaides *et al.* (1993) findings. Klier *et al.* (1993) experimented four different ion exchanged resins: Amberlyst-15, BioRad, Nafion MS and Purolite; and five inorganic catalysts: H-ZSM-5,  $\gamma$ -alumina, H-Modernite, Montmorillonite, Silica-Alumina and Sulfated ZrO<sub>2</sub>. In the case of the resins, the reaction conditions were 90 °C and 1 atm. These conditions led to the formation of MIBE and a smaller quantity of MTBE with about the same MIBE/MTBE ratio as found by Nicolaides *et al.* (1993). Most of the inorganic catalysts gave similar results. H-Mordernite did not show any sign of activity toward MIBE or MTBE and  $\gamma$ -alumina led to the production of MIBE only.

Nunan *et al.* (1993) reported a kinetic study of the direct coupling of the alcohols using Nafion H resin. Several products were identified: methyl isobutyl ether (MIBE), diisobutyl ether, diisobutylene, dimethyl ether and butene. The selectivity toward MIBE was higher than toward dimethyl ether or diisobutylene ether. Moreover, the direct coupling of methanol and isobutylene was also experimented with Nafion H resin. MTBE was found to be the only ether present in the product stream with a selectivity greater than 99.9%. In light of these

results, the authors proposed that the presence of isobutylene was necessary for the formation of MTBE but not for the formation of MIBE.

Knowing that the main product from the direct coupling of methanol and isobutanol is MIBE another process could be proposed. The first step could involve the coupling of the two alcohols followed by the isomerization of MIBE to MTBE. However, the possibility to realize this process is limited given the lack of technical information available on ethers isomerization.

## 3.7.1 Use of Two Reactors In Series

Nicolaides *et al.* (1993) conclude from their results that isobutylene is a necessary precursor to MTBE synthesis. They consider the potential use of a train of two reactors: a) the first reactor dehydrating isobutanol, b) the second reactor performing the MTBE synthesis. Between the two reactors a condenser removes the excess water from the dehydration reactor preventing the formation of tert-butyl alcohol in the second reactor.

According to Nicolaides *et al.* (1993), the difference of optimal temperature between the isobutanol dehydration and the methanol to isobutylene coupling justifies the use of more than one reactor. These authors argue that the dehydration reaction necessitates a temperature above 150 °C

while the temperature for the etherification reaction must be below 100 °C because of equilibrium limitations.

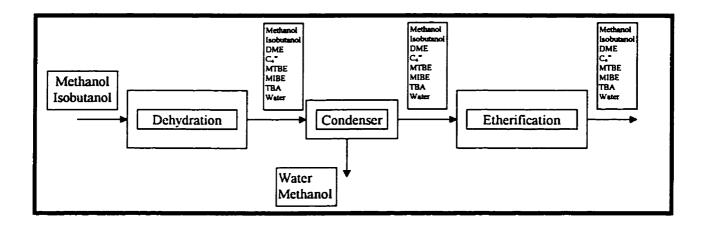


Figure 3.2: Schematic of the Two Reactor System: Dehydration Reactor and Etherification Reactor. (Nicolaides *et al.*, 1993)

Nicolaides *et al.* (1993) found that the more suitable catalyst for the dehydration of isobutanol was silica-alumina while Amberlyst 15 was the best for MTBE synthesis. In fact, dehydration of isobutanol forms four butene isomers. The highest isobutylene selectivity based on isobutanol was 69.2 % at 225 °C. With this selectivity, the total conversion of the isobutanol toward butenes reached 96%. The etherification reactor temperature was maintained at 50 °C.

Compositions of the stream coming out of each reactor were analyzed and MTBE along with MIBE were positively identified in both cases. The mass fraction of MTBE and MIBE at the outlet of the first reactor was 4.8% and at the outlet of the second one, 27.8 %. The MTBE/MIBE ratio were respectively 1/14 and 11.7/1.

#### 3.7.2 The Dehydration of Isobutanol

The dehydration of isobutanol is a fairly straightforward reaction but it can also lead to the formation of several byproducts. These reactions are the etherification of the alcohols to obtain disobutanol, the dimerization of the butenes or the formation of higher hydrocarbons.

The dehydration reaction is a more energy demanding reaction than the etherification and an increase in the temperature favors the formation of butenes (Nunan *et al.* 1993). The partial pressure of isobutanol also plays an important role in the case of Nafion H resin. An adsorbed atom of isobutanol is assisted by a free acid site to complete the dehydration (Nunan *et al.* 1993).

Contrary to Nicolaides *et al.* (1993), who argue that the dehydration of isobutanol using  $\gamma$ -Alumina formed a whole array of butenes, section 3.7.1, Knözinger *et al.* (1972) reported that, while using alumina catalyst, the only butene detected was isobutylene. The range of temperatures considered varied from 150 to 300 °C.

Makarova *et al.* (1990) reported, however, that reaction temperatures between 100 to 150 °C can be used with H-ZSM-5 and this is well below the 225°C reported by Nicolaides *et al.* (1990).

From these results, it appears that no general conclusion can be drawn about optimum conditions for the dehydration reaction. Furthermore, optimum conditions to obtain the largest amount of isobutylene seem to be catalyst sensitive. In this context, different combinations of reaction conditions and catalysts could probably be used in the future to obtain better results.

# 3.7.3 The Etherification Reaction

Although the actual process to produce MTBE has been already used for over 20 years not much is known about it besides some of the kinetics features discussed earlier. New catalysts and reaction conditions are currently being investigated.

Most of these recent studies have been conducted in the vapor phase and this contrasts with the currently used liquid phase industrial process. Studies with the new macroreticular ion exchange resin Amberlyst-35 appear to be the exception (Ladish *et al.* 1993). Resins such as Purolite and BioRad (Klier 1993) were also studied. Also various types of zeolites were investigated: Modernite, Beta, REHY (RE stands for rare earth), REAIY, ZSM-5 and ZSM-11 (Chu 1987). In order to have a basis for comparison, experiments were normally developed in parallel with tests using the industrial catalyst Amberlyst 15.

Concerning resins, experiments were typically conducted at a pressure of 1 atm, and a temperature of 75 °C. In the case of the Amberlyst 35, the selected pressure was either 10 or 20 atm, and the temperature 55 °C which closely match industrial conditions. For Amberlyst 35 a feed comparable to an industrial one was used while the reactant mixtures for other catalyst were composed of methanol and isobutylene. The BioRad resin did not present any reactivity (Klier 1993).. The Purolite resin was active with a conversion of 15.8% which is lower than the 24.6 % found with Amberlyst 15 (Klier 1993). Amberlyst 35 gave a conversion of isobutylene of 95.5 % and this was higher than Amberlyst 15 for the same conditions (Ladish *et al.* 1993). The selectivity of both Amberlyst 15 and 35 toward MTBE was 99%.

Other tests with varying temperatures and space velocities were performed with the BioRad resin. While varying the temperature, the highest conversion observed was 19.2 % at 85°C. In the case of the space velocity, the temperature was kept constant at 75 °C. Doubling the space velocity decreased the conversion by half to reach 7.4%. Diminishing the space velocity by half more than doubled the conversion bringing it up to 36% (Klier *et al.*, 1993).

The six zeolites mentionned earlier in this section, were first tested in order to find out which ones give best results (Chu 1987). Reaction conditions were 1 atm, and the inlet temperatures were 82 °C and 93 °C. Modernite and Beta displayed, in all the cases, a selectivity toward MTBE lower than 58% with an isobutylene conversion lower than 37%. REHY and REAIY gave a selectivity toward MTBE ranging between 85 and 98.8 % with a maximum conversion for REHY of 12.5% and for REAIY of 25.6%. The two best catalysts were H-ZSM-5 and H-ZSM-11 with a selectivity toward MTBE over 99% and a conversion of 30.5%. Further experiments were developed with these two zeolites and with Amberlyst-15 as a basis of comparison. Results are presented in Table 3.4.

Table 3.4: Results Reported for	Zeolite H-ZSM-5	and H-ZSM-11	Compared with
Amberlyst-15 (Chu et al., 1987).			

Methanol/isobutylene	H-ZSM-5		H-ZSM-11			Amberlyst-15			
	1.00	1.05	1.10	1.00	1.05	1.10	1.00	1.05	1.10
Temperature °C	78	80	82	N/A.	78	79	65	58	51
Conversion of isobutylene %	89.6	89.8	90.1	N/A.	88.7	90.2	93.1	93.4	94.5
Yield of MTBE %	89.6	89.8	90.1	N/A.	88.7	90.2	86.0	89.4	92.7
Selectivity %	100	100	100	N/A.	100	100	92.4	95.7	<del>9</del> 8.1

The two zeolites tested gave 100% selectivity towards MTBE at any of the methanol/isobutylene ratios considered. The highest selectivity that Amberlyst-15 could reach was 98.1 and this selectivity was influenced by the methanol/isobutylene ratio.

#### 3.8 Effects of Catalyst Acidity on the Production of MTBE

The concentration and the strength of acid sites have effects on the production of MTBE from methanol and isobutylene. As shown in the case of Amberlyst-35 versus Amberlyst-15, Ladisch *et al.* (1993), an increase in the density of acid sites having the same strength increased the conversion of isobutylene toward MTBE. Ladisch *et al.* (1993) reported that the equilibrium concentrations of Amberlyst 35 was different from the ones obtained with Amberlyst-15. They proposed as an hypothesis that catalysts with different gelphase properties affect the activity coefficients differently. This translates, for Amberlyst-35, in an increase in the equilibrium constant based on molar fractions.

In the case of zeolites the acid strength of the catalyst can be varied by ion exchange. NaY zeolite can be ion exchanged to obtain HY zeolite which in turn can be partially ion exchanged with alkali nitrates of Li, Na, and Rb (Kogelbauer *et al.* 1994). The result was a group of four different catalysts having the same number of acid sites but with different strengths. The highest site strength belonged to HY followed by LiHY, NaHY and RbHY. For the four catalysts considered, the initial rate of reaction was mostly the same but changed with time-on-stream. The degree of coking for the four catalyst was also different: HY 6.1 wt %, LiHY 5.2 wt %, NaHY 4.4 wt %, and, RbHY 3.2 wt %.

38

At steady state LiHY had the highest rate of reaction then came NaHY, HY and RbHY. In the case of RbHY, the higher size of the Rb ion impeded the pore diffusion of reactants and explained its diminishing activity. For the other parent catalysts, the size of the ion could not explain the catalyst deactivation. The formation of isobutylene dimers which were strongly bonded upon reaction onto the catalyst surface was advanced as a possible factor causing deactivation (Kogelbauer *et al.* 1994).

Another method to modify the strength of the acid sites, in the case of zeolites, is to proceed through the dealumination of the catalyst increasing the acid strength but decreasing the number of sites (Nikolopoulos *et al.* 1994). Dealumination of HY zeolite was effectuated and the activity of the catalyst toward MTBE was increased (Nikolopoulos *et al.* 1994). Different methods of dealumination were used but the samples dealuminated by ammonium hexfluorosilicate or steam dealumination showed the higher increase in catalyst activity (Nikolopoulos *et al.* 1994).

## 3.9 ZSM-5 and its Major Characteristics

ZSM-5 has characteristics that made it one of the most interesting industrial catalyst. ZSM-5 is formed by a network of pores that offers shape selective capabilities (see fig 2.3). The pore sizes of ZSM-5 are 5.4 x 5.6 and 5.1

39

x 5.5 Å. In the case of the MTBE synthesis, these sizes of pores offer rapid diffusion of methanol,  $3.7 \times 4.2$  Å, while hindering the diffusion of isobutylene,  $3.9 \times 5.4$  Å (Chu *et al.* 1987). As explained in Chu *et al.* (1987), a molecule of isobutene diffusing through the zeolite pores would more likely have to react with methanol, already adsorbed onto the acid sites, to form MTBE

ZSM-5 also offers, after ion exchanged, a strong acid catalyst called H-ZSM-5. In Kogelbauer *et al.* (1995), this characteristic was enlightened by the selective adsorption of different reactants onto the acid sites. The acid sites provide a higher affinity for methanol. Experiments where methanol was preadsorbed on the catalyst showed an increase in the rate of reaction and on the selectivity toward MTBE. When isobutylene is preadsorbed on the catalyst, it led to the formation of diisobutylene which tended to poison the catalyst given its high adsorption energy. Moreover, when methanol was preadsorbed, no catalyst deactivation was observed even after two hours on stream. From these results, preadsorption of methanol seems to be a main factor for H-ZSM-5 high selectivity toward MTBE. Nevertheless, Kogelbauer *et al.* (1995) do not exclude the fact that the shape selectivity properties could cause some mass transfer limitations and this can favorably influence selectivity toward MTBE.

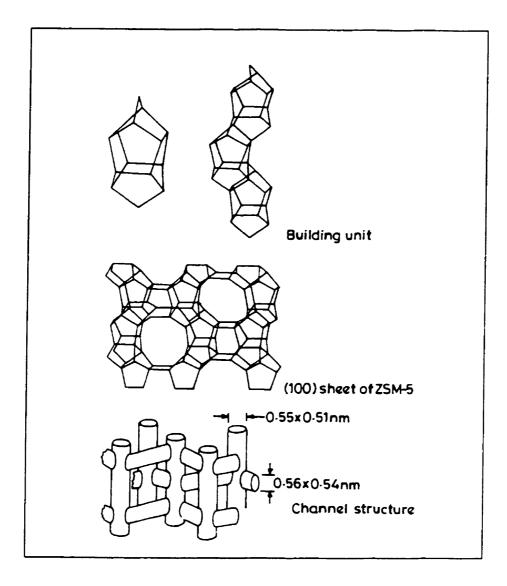


Fig 3.3: Structure of ZSM-5 Zeolite (from: Zeolite Catalysis: Principles and Applications, 1990).

# 3.10 Conclusion

Although the production of MTBE seems to be a well established process, the introduction of new legislation such as the Amendment to the Clean Air Act of the United States open doors to new research opportunities. The improvement of existing processes is the most promising solution to the problem. Nevertheless, new sources for the MTBE process feedstock are needed to meet future MTBE demands.

The most promising MTBE feedstock is certainly synthesis gas from which methanol and isobutanol can be obtained. As a result, new processes involving new catalysts and new reactor designs are required to take advantage of this potential path. Catalysts such as H-ZSM-5 may lead the way for these potential innovations and will certainly serve as basis of future processes.

# Chapter IV

# Synthesis, Pelletization, and Characterisation of H-ZSM-5

## 4.1 Introduction

This chapter describes the synthesis of the H-ZSM-5 catalyst used in this project. Several steps are involved in the preparation of such a catalyst:

- a) the synthesis of the catalyst to obtain the Na<sup>+</sup> form,
- b) the ion-exchange of the catalyst followed by a calcination to obtain the H<sup>\*</sup> form,
- c) the pelletization of the catalyst into 60 microns pellets.

Through all these steps different techniques of catalyst characterisation are used to establish the quality of the zeolite obtained. These techniques and the results of the various analyses are presented in the last section of this chapter.

# 4.2 Synthesis of Na-ZSM5

The synthesis of this type of zeolite requires moderate conditions of temperature and pressure which are respectively: 150 °C and 690 kPa. An autoclave, available at the CREC's laboratories, was employed to achieve these conditions. The autoclave is a vertical insulated vessel with a heating element embedded into the walls. A cover equipped with orifices for a pressure gauge, a thermocouple, and a stirrer seals the top of the vessel. The autoclave is filled with a reaction mixture and then heated up to reach the temperature required. As the mixture heats up, water evaporates and the pressure increases in the autoclave.

Three basic components, aluminium, silicate and oxygen, are required to form the two distinct building blocks of the zeolites crystals, Figure 4.1. These three components are available in the sodium silicate and the aluminium sulphate which are the reagents used in the zeolite synthesis. The quantities of aluminium and silicate were calculated to obtain a Si/AI ratio of about 20. An organic compound, called tetrapropyl-amonium bromide (TPA-Br), was used as a template for the crystals. The sodium ion, contained in sodium chloride, was used as seeds for the crystals as well as to balance the ionic charges in the crystals formed. All these components when mixed together form a gel that solidifies with time. In order to avoid quick solidification of the gel, sulphuric acid was added to keep the pH low.

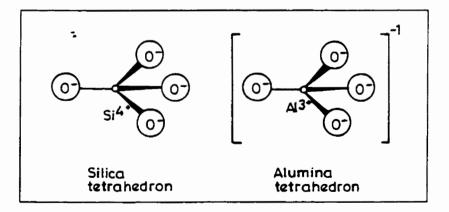


Fig 4.1: Basic Building Blocks of Zeolites

The gel was first stirred for 2 hours at room temperature before closing the autoclave. Following this, the mixture was stirred and heated for 3 to 6 days. X ray diffraction analysis confirmed the nature of the crystal. The X-ray diffraction results obtained are presented in section 4.6.1.

In order to remove the template from the catalyst precursor, calcination of the catalyst must be accomplished. In the present study, calcination was done by keeping the temperature of the catalyst at 500 °C for 12 hours.

#### 4.3 Ion Exchange of the Catalyst

Following the first step of ZSM5 production, described in the previous section, the catalyst is in the Na<sup>\*</sup> form. To obtain the desired H-ZSM-5 acid form, the zeolite had to be ion exchanged. To achieve this, the NH<sub>4</sub>-ZSM-5, precursor of the acid ZSM-5 or H-ZSM-5, had to be formed. Sodium ions, Na<sup>\*</sup>, must be exchanged with NH<sub>4</sub><sup>\*</sup> ions. Solutions of ammonium nitrate, NH<sub>4</sub>NO<sub>3</sub>, or ammonium chloride, NH<sub>4</sub>Cl, are used to perform this ion exchange. The concentration of the NH<sub>4</sub>Cl solution employed was 1 M. The solution was heated with the catalyst at a temperature of 80 °C for 12 hours. To achieve a high degree of exchange of Na<sup>\*</sup> and NH<sub>4</sub><sup>\*</sup>, five ion exchanges were performed as recommended by Hagey (1997), four with the ammonium nitrate and one with ammonium chloride.

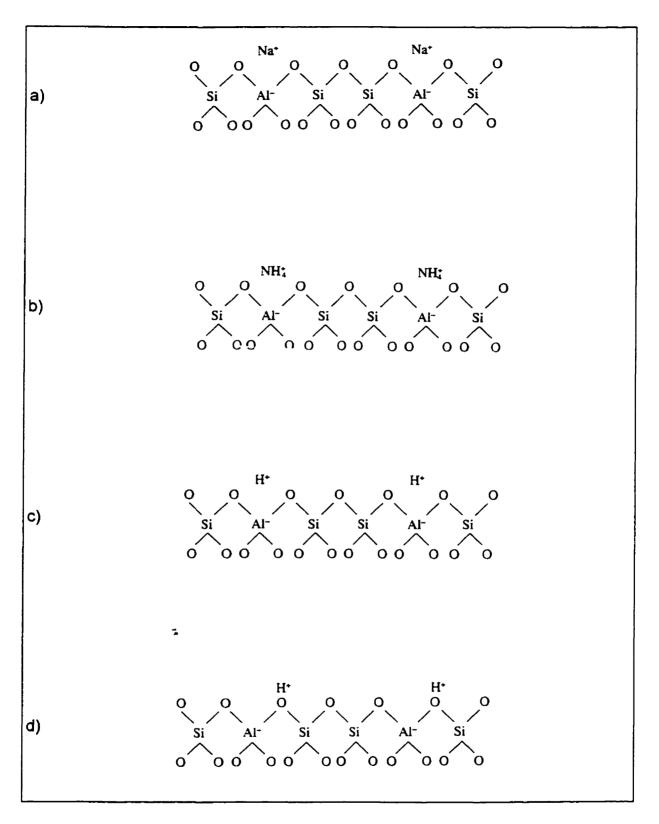


Fig 4.2: Different Ionic Form of the Zeolite H-ZSM-5

# NOTE TO USERS

Page(s) not included in the original manuscript are unavailable from the author or university. The manuscript was microfilmed as received.

UMI

with air at a low pressure, 104 kPa, producing a fine mist that is quickly dried with hot air. The particles obtained are recovered with a cyclone.

The first step, in the catalyst pelletization technique, was to prepare a slurry containing the catalyst (Gianneto, 1993). Sulphuric acid was used to keep the pH low in order to avoid slurry gellification which would eventually plug the injection system. In fact, the pH should be set on the edge of the gellification point to facilitate the formation of the pellets. A pH of 2 was adequate as gellification was observed after 2 or 3 hours. Kaolin, a crystalline form of silicate, was used as binder and also to increase the mechanical strength of the pellets. Sodium silicate was used as a filler. Once all the components were mixed together, the resulting slurry had to be quickly spray dried.

Figure 4.3 shows a side view of the spray dryer available in the CREC laboratory. Two air streams are working together to dry the mist. The entry of one of these streams is located at the top of the spray dryer and distribute air axially through an honeycomb to even the flow across the cylindrical section. The second air supply is located about halfway through the drying chamber and supplies air tangentialy giving a swirling motion to the particles, increasing, as a result, their residence time. In both feeders the air is preheated using a coil of the type found in industrial heat guns with the air coming from the top feeder at 260 °C. A peristaltic pump feeds the slurry to a nozzle assisted by a flow of air at 105 kPa. A cooling jacket keeps the nozzle cold to avoid gellification of the slurry in the injection chamber.

A needle fixed at the end of a rod and going all the way down the nozzle mounting, was pushed periodically through the nozzle tip to avoid plugging. To ensure good operation, the nozzle was removed between each run and completely cleaned as a crust was forming at the tip of the injector.

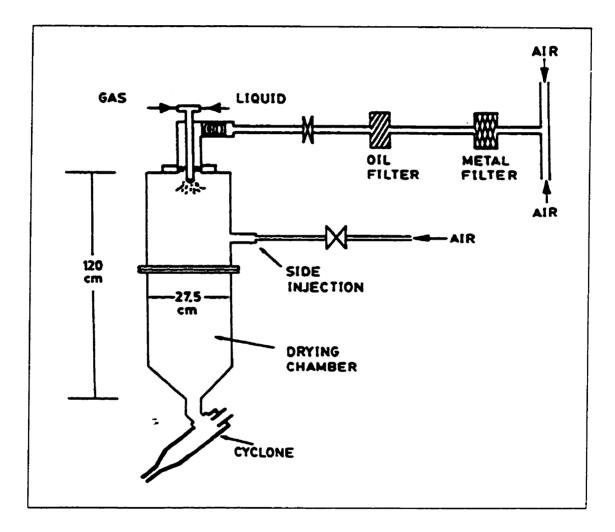


Fig 4.3: Schematic of the Spray Dryer available at CREC Laboratory.

The solid content of the slurry was 51 grams in a total volume of 170 ml. The solid composition of the slurry was 20 wt% of catalyst, 40 wt% of kaolin and 40 wt% of sodium silicate. From these 51 grams about 50 % of solid was recovered. Furthermore, from the final product, 50% had to be discarded after sieving because the size of the particles was too small. Thus, the overall particles yield between 38 and 106 microns was 25 %.

After sieving the final product, the catalyst pellets were washed again with deionized water. The kaolin has a crystalline structure and, following calcination, was returned to an amorphous structure. Two hours at 560 °C was sufficient to perform this task.

An extra ion exchange had to be performed as it was found that the sodium contained in the sodium silicate returned the catalyst to its Na<sup>+</sup> form. The use of an acidic source of the ion NH<sub>4</sub><sup>+</sup> was not allowed as it caused the breakdown of the pellets forming a powder. To avoid this problem a 1 N solution of ammonium hydroxide (NH<sub>4</sub>OH), a weak base, was employed for the ion exchange without causing the pellets to rupture. The ion exchange with NH<sub>4</sub>OH was performed during three days, changing the solution at the beginning of each day and stirring it three times a day.

#### 4.5 Characterisation

Throughout the process of production of the H-ZSM-5 catalyst several characterisation techniques were used to establish the formation of the desired crystals and their degree of crystallinity. The following section describes the techniques used and the results obtained.

# 4.5.1 X-ray Diffraction (XRD)

X-ray diffraction is one of the major techniques used to identify crystalline structures of catalysts. An X-ray diffractometer is composed of a source, a sample holder and a detector. The source and the detector are at a fixed angle from the horizontal while the sample angle, called scattering angle, changes during the analysis. X-rays are emitted toward the sample and are scattered by the electron clouds of the different atoms. This diffraction effect is sensed by the detector. For each scattering angle, the sample is bombarded by X-rays for a fixed period of time. If a specific pattern of atoms appears inside the substance analysed for one or several positions of the sample, the signal from the detector is stronger and shows a sharper peak on the final spectrogram. In the case of a substance which has no crystalline structure, the spectrum gives only a line composed of small peaks with approximately the same intensities. As the structure of the zeolite crystals are tri-dimensionnal, the XRD is a technique of choice. Each atom of the crystal contributes to the observed XRD pattern which is as specific as a fingerprint for a human being. Thus, each type of crystalline structure possesses its own XRD pattern and can be identified by comparison with another available pattern. In a word, the position of the peaks and their relative intensities are specific for each crystalline structure and correspond to a unique catalyst.

Figure 4.4a shows a theoretical calculation of the XRD pattern of H-ZSM-5. Figure 4.4b presents an experimental pattern found in the literature. The XRD pattern of the present catalyst (Figure 4.5c), realised at the Geology Department on the UWO campus, is in good agreement with the two previous patterns. The position of the peak as well as their relative intensities are very similar.

Figure 4.5 presents the XRD analysis at different stages of the pelletization. Figure 4.5a displays the XRD analysis for kaolin alone showing its crystalline structure. Figure 4.5b reports the XRD of the pellets after being washed with deionized water. In Figure 4.5b, the specific peaks of kaolin and H-ZSM-5 appear together. Fig 4.5c shows the final XRD results after the calcination of the pellets at 500 °C. These results clearly indicated that the kaolin structure has completely disappeared and that only the H-ZSM-5 crystalline structure remains in the pellet.

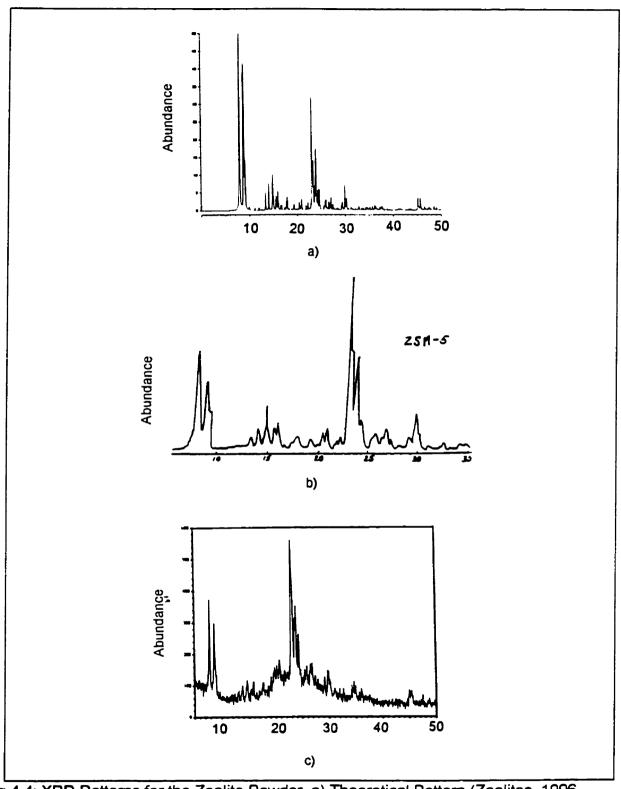
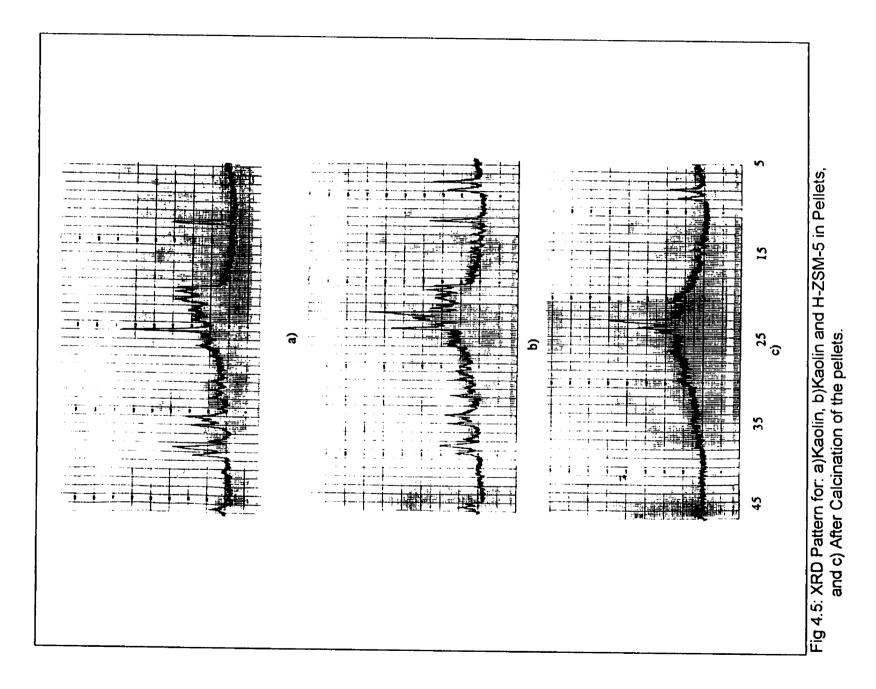


Fig 4.4: XRD Patterns for the Zeolite Powder. a) Theoretical Pattern (Zeolites, 1996, numbers 5-6), b) Experimental XRD Pattern (Wenyang et al, 1989), and c) Experimental XRD from the Present Study.



# 4.5.2 Temperature Program Desorption Analysis (TPD)

TPD analysis was used to determine the strength of the acid sites available on the catalyst as well as their relative densities. To perform this analysis ammonia was circulated through the catalyst and adsorbed by the different acid sites. Ammonia bounds more or less strongly depending on the type of acid site. A brief description of the method used is provided in the following paragraphs.

In order to remove the impurities that may be adsorbed on the catalyst surface, the catalyst was outgassed with helium for 12 hours at 200 °C. Following this operation, the temperature of the furnace was brought down to room temperature. Then, helium, containing 4.3 % ammonia, was circulated over the catalyst for 30 minutes. After the adsorption of ammonia was completed, pure helium was fed to the system for 30 minutes to remove the excess. Finally, the catalyst was heated up to a temperature of 500 °C at a rate of 15 °C/min. This temperature was kept for 30 minutes. As the catalyst was heated up, ammonia desorbed from the catalyst and a Thermal Conductivity Detector, TCD, analysed the resulting gas mixture of helium and ammonia. A constant flow of helium was maintained throughout the desorption of ammonia.

TPD results, Figure 4.6, show two peaks: one at 230 °C and the other at 400 °C. The strength of the acid sites is a function of the temperature: the higher the peak temperature the stronger the acid sites. The results obtained from the analysis correspond to two strengths of acid sites. The relative area of the weaker sites represents 84 % of the total area, the difference being stronger sites. This shows that weaker sites were more abundant than the strong ones.

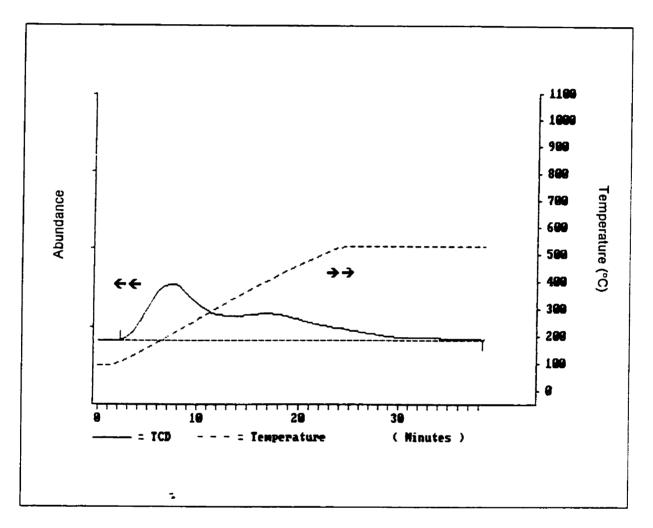


Fig 4.6 Results of the TPD Analysis of the H-ZSM-5

#### 4.5.3 BET Analysis

BET analysis was used to assess the specific area of a catalyst. The surface area of a catalyst is a good sign of its potential activity. The higher the surface area is, the higher the potential catalytic activity and the possibility for reactants to interact. The type of analysis performed in this case is known as single point BET as only one equilibrium pressure is obtained for the adsorption of nitrogen.

Prior to all operation, the sample was weighed. The sample was then outgassed at 200 °C overnight using helium to remove any potential contaminant. Then a mixture of 30 % nitrogen and 70 % helium was circulated through the catalyst. Liquid nitrogen was employed to refrigerate the catalyst to 77 K at which temperature nitrogen was adsorbed onto the catalyst surface. The sample was then heated up using water at room temperature. Because of its high density, water provides an almost instantaneous shift to room temperature. The increase in temperature caused the nitrogen to desorb.

Nitrogen adsorption and desorption decreased and increased the nitrogen concentration in the carrier gas. These changes in concentration were analysed using a thermal conductivity detector. The areas under the desorption peaks of the chromatogram were integrated and , using a calibration, the number of mole of nitrogen were determined. Knowing the approximate saturate pressure of nitrogen at the adsorption temperature, the volume of the nitrogen monolayer was calculated. Using the typical area covered by a

# NOTE TO USERS

Page(s) not included in the original manuscript are unavailable from the author or university. The manuscript was microfilmed as received.

58 thru 60

UMI

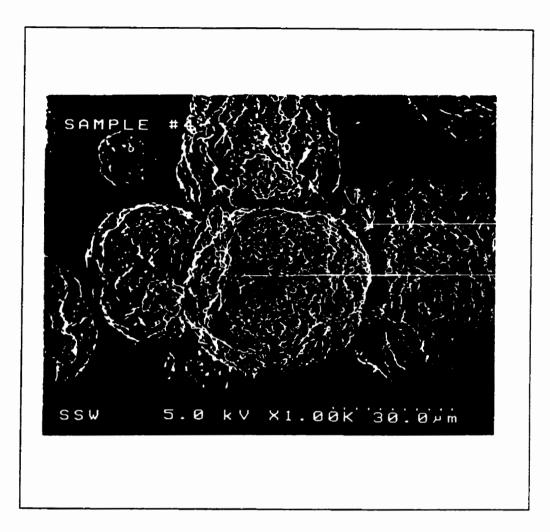


Fig 4.7: Picture of the Pellets

-

# 4.6 Conclusion

Physical characterisation and chemical composition of the catalyst were thoroughly controlled using standard method of analysis available. The X-ray diffraction patterns provided a positive identification of the zeolite crystals. The temperature programmed desorption technique established the relative strength and the distribution of the acid sites.

The BET analysis produced high surface areas typical of zeolite catalysts. The results obtained from the SEM EDX gave the chemical composition of the catalyst showing evidence of the presence of a zeolite type structure. The size and shape of the catalyst were within the range to obtain good fluidization.

On the basis of the good results obtained for the physical and chemical catalyst properties, the experimental program was allowed to continue to the following phase which involved reaction testing.

# Chapter V

# **Experimental Methods**

### 5.1 Introduction

Once the catalyst was synthesized and pelletized the experimental program was ready to proceed. This chapter covers the details of the different experimental steps:

a) development of the analytical method,

b) experiments,

c) analysis of the results.

During the course of the present study, several trials were needed until the preferred experimental method was developed. In order to provide an effective reporting, only the successful experimental techniques are described.

5.2 The analytical Method

The MTBE reaction was conducted in the gas phase in which case gas chromatography (GC) appeared to be the adequate analytical technique. The gas chromatography principle is simple; a carrier gas, in this case helium, dilutes the sample and carries it through a column which elutes the sample into its component. There are two common types of columns: a) the columns filled with a packing component, and, b) the open columns with only a film or a packing on the wall. The first type is called packed column and its diameter is usually greater than 1 mm. The second type is called capillary column and its diameter is usually less than 1 mm. There is also a third type of column called the packed capillary column (Grant, 1996). For every type of column the leading principle remains the same: the material inside the column has different adsorption affinities for the various chemical species of the sample. As a result, chemical species are eluted and are delivered at the end of the column at different times. The time that a chemical takes to go through the column is called the retention time. Finally, a detector located at the end of the column analyzes the concentration of the chemicals contained in the carrier gas.

Gas chromatography has three main advantages: rapid execution, adaptability, and ease of utilization. In this case, the gaseous samples do not need special preparation or treatment. A gas chromatograph, model HP 5890, available at the CREC's laboratory was employed. The gas chromatograph was equipped with two types of column: a) a Poropak Q column in association with a thermal conductivity detector (TCD), and, b) a capillary colum HP-1 linked to a mass spectrometer (MS).

The Poropak Q column with the TCD was mainly used as a tool for quantification of the reaction products. The TCD offers a linear response for the reaction products analyzed which makes it very easy to use.

The HP-1 column associated to the MS was mainly used as an identification tool. As the flow of carrier gas enters the MS vacuum chamber, the molecules are bombarded by an electron beam which causes the molecule to

64

break down. Molecule are decomposed to ionic fragments which are analyzed by a detector. The detector's signal is translated in patterns of different molecular weighs and corresponding abundances. These patterns are compared with data stored in a computerized library file. Results are listed in order of similarity as different compounds may have similar patterns. Similarities of patterns are expressed with a percentage scale.

## 5.2.1 Chemicals to be Analyzed

In order to properly develop the analytical method to be used, it is important to know the products that require identification. Methanol, isobutanol, isobutylene and MTBE are the main four compounds expected during the experiments. As mentioned in the literature review, some byproducts may be encountered: dimethyl ether, diisobutylene (which has different isomers) and MIBE.

## 5.2.2 Retention Time

Knowing the chemicals to analyze, the next step was to establish the retention time for each one of them. All the chemicals listed in the previous section were purchased with the only exception of MIBE which was not available through chemicals suppliers.

Reactants and products were injected one by one using different temperature programs until good peak separation was obtained. Argon which was used as inert gas inside the Riser Simulator and also as internal standard was also analyzed. As experiments were performed, some additional peaks appeared in the chromatogram. Dimethyl ether was then purchased to obtain a clear identification of the unknown species. Figure 5.1 reports the optimized temperature program obtained for the Poropak Q column.

In the case of the capillary column, a constant temperature of 60 °C during the analysis appeared to be the best choice for the separation of the chemicals species. However, methanol, isobutylene and dimental ether showed very close retention times and the HP1 column could not be employed, to obtain their positive identification.

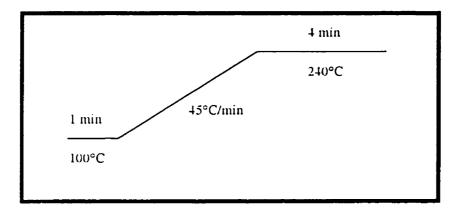


Fig 5.1 Temperature Program for the Poropak Q Column

# 5.2.3 Calibration for the Quantitative Analysis

A first step before proceeding with the quantitative calibration was to develop several tests with similar concentration levels to the ones expected in the gas samples. These quantities were found to be about 10<sup>-6</sup> moles for methanol and isobutylene and 10<sup>-7</sup> moles for MTBE. For isobutylene, being a gas at room temperature, the amount required was related to the volume injected using the ideal gas law. For methanol and MTBE, liquids at room temperature,

the procedure was more complex as injections had to be done in a liquid form and amounts involved were very small. In order to obtain these small amounts, mixtures were prepared by diluting one component into the other. The syringe used for the injections was weighed before and after the injection. The difference between the two measurements represented the mass of liquid injected for the GC analysis. Knowing the mass injected and the weight composition of the calibrated sample, the number of moles injected was calculated. This procedure is explained in greater detail in the Appendix C where calibration curves are also reported. Runs were repeated on a regular basis to ascertain any potential changes in calibration constant.

# 5.3 The Riser Simulator

The Riser Simulator is a novel unit invented at CREC (de Lasa, 1991). The Riser Simulator operates under batch conditions offering a high gas recirculation rate. Its main advantage is to reproduce the reaction conditions in a riser reactor: the catalyst and the reactants are in contact for approximately the same time. After the reaction period the reaction mixture is evacuated, the catalyst can be regenerated and a new reaction cycle is initiated.

A vacuum sampling system allows quick evacuation of the product mixture and as a result a close control of the reaction times. Reaction times can be varied in a broad range being typically set in the order of few seconds to several seconds.

Fig 5.2 shows a schematics of the Riser Simulator. An impeller is located in the unit upper section above a basket containing the catalyst. The catalyst is

maintained in the basket by two porous plates with pores of 20 microns. The basket and the impeller are isolated inside a sealed chamber. During an experimental run, the impeller rotates at high velocity inducing a high upward gas velocity. The high upward gas velocity fluidizes the catalyst and creates high catalyst-gas mixing, which translates into intimate contacting between the reactants and the catalyst. This high degree of mixing offers a uniform concentration inside the reactor at all times. The gas volume of the reactant with the catalyst loading makes it possible to reproduce typical solid hold-ups found in riser units.

However, some of the features found in a riser reactor could not be reproduced in this bench scale unit. For instance, the slip velocities, which is the difference of velocities between the gas and the solid, are not fully equivalent to the ones observed in industrial units and this may affect mass transfer rates. However, Kraemer (1987) shows that the interparticle mass transfer is not a limiting factor for the Riser Simulator. In fact, the reaction rate is the limiting overall reaction step. Thus, slip velocity differences do not affect the overall reaction rate. Furthermore, the solid concentration profile along the axis of a FCC riser, being higher in the bottom of an industrial riser, cannot be represented inside the Riser Simulator. Finally, the wall effects found in a large scale FCC riser reactor cannot be incorporated directly in the Riser Simulator analysis. Wall effects cause recirculation of catalyst, which may produce further formation of coke and catalyst deactivation because of the longer contact time of the reaction gases. Longer contact times may also, in the case of catalytic cracking, cause unwanted lighter hydrocarbons.

68

In spite of these differences the Riser Simulator can contribute to the understanding of catalyst performance as it reproduces residence times found in riser/downer units. Entry or wall effects may be incorporated through potential mathematical modeling of the gas-solid suspension.

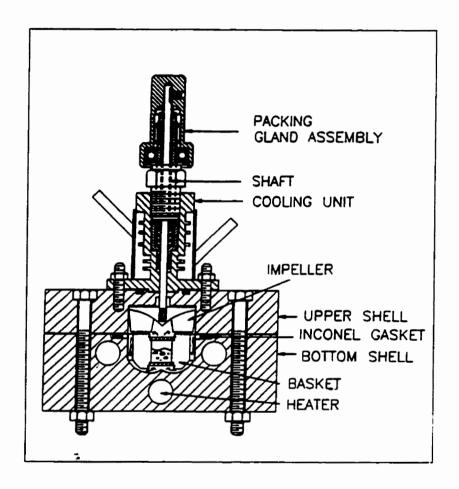


Figure 5.2: Schematic of the Riser Simulator

# 5.3.1 Details of the Riser Simulator

Fig. 5.2 presents a side and a top view of the reactor. The reactor is mainly formed by a bottom shell, an upper shell, a basket containing the catalyst

and an impeller. Heaters are inserted in the bottom and the upper shells. Different orifices are located around the upper shell in order to sample the reactant mixture, circulate gases, and monitor the conditions inside the reactor. A thermocouple is inserted in the middle section of the basket to measure the bed temperature. Another thermocouple is located in the upper section of the reactor. A pressure transducer is connected to the reaction chamber to measure pressure changes. An inlet and an outlet ports allow gases to be fed in the reactor and to be removed from the reactor. Finally, an injection port is located on the bottom shell for reactants injection.

The extent of the fluidization is a function of the gas velocity which is proportional to the impeller speed. The impeller can turn up to a velocity of 10 000 RPM. Earlier experiments showed that the lowest impeller speed to obtain minimum fluidization was 6300 RPM and that the bed was fully fluidized at 7875 RPM (Pekediz. 1993). Higher speed may cause pneumatic transport which is not desirable. Another important aspect that is affected by the impeller velocity is the mixing time. In this type of operation where the reaction time is fairly short, the mixing time may be significant and should be as short as possible. In Pekediz (1993), the mixing time was evaluated to be 0.02 s at 7350 RPM which is well below 1 s and should not affect the overall reaction.

Attached to the Riser Simulator there is a sampling system composed of five components:

- 1) a four port valve,
- 2) a timer coupled to an actuator,
- 3) a sampling bomb,
- 4) a sampling port,
- 5) a vacuum pump.

A schematic of the sampling system is presented in Figure 5.3. The four port valve has two main functions: a) it allows gases to circulate through the reactor, and, b) it isolates the reactor during experiments. The four port valve is coupled to an actuator controlling the valve position. The actuator is connected to a timer controlling the total reaction time. The purpose of the sampling bomb is to collect the sample from the reactor.

Prior to each experiment, the vacuum pump is activated and empties the sampling bomb. Once the reaction is completed the actuator changes the position of the four port valve and the sampling bomb draws the reaction gases. The actuator is activated by the timer which is preset to the desired reaction time. A system of switches associated with the syringe injecting the reactants, turns the timer on and off. Filling the syringe prior to an experiment sets the valve in the reaction mode and zeroes the timer. At the time the syringe is emptied, which corresponds to the beginning of the reaction, the timer is activated by the action of a switch. Once the reaction time is completed, the

timer sends a signal to the actuator which changes the valve position to the purging mode. The sampling bomb is equipped with a septum which allows the use of a syringe to draw the sample.

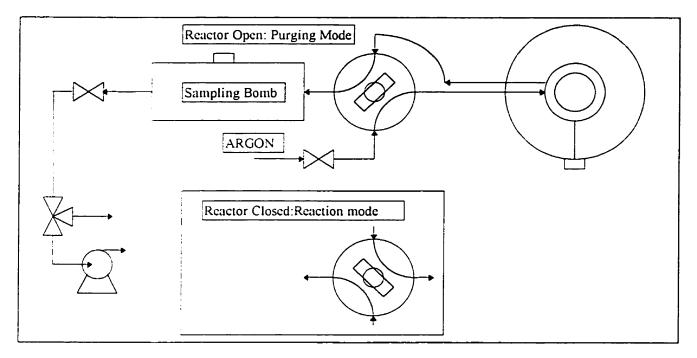


Figure 5.3: Schematic of the Sampling System

Another mode of sampling was also used which consist of drawing a sample directly from the reactor through the injection port. This method was used when it was suspected that species concentrations were smaller than the detection threshold of the GC. In this case, the timing of the reaction was done manually. The syringe was wrapped with insulation material and heated prior to each sampling in order to avoid condensation.

The dew point of the sample mixture was calculated with Hysim and was determined to be 27 °C. The results were confirmed with different properties packages available on Hysim, e.i. Peng Robinson, Activity models.

#### 5.4 The Experimental Procedure

Each experiment was performed in a sequential fashion. The first step of an experiment was to purge the reactor and the sampling bomb using argon as the inert gas. The four port valve was set in the purging mode. This was accomplished by keeping the syringe in the empty position. At the same time, the valve at the exit of the sampling bomb was set in the vent mode. This purging step ensured that the reactor was free of any remnants from previous experiments or contaminants that could have been introduced while opening the reactor to the atmosphere. Ten minutes was judged sufficient to ensure a proper purging of the reactor. The next step consisted in closing the argon flow allowing the pressure to stabilize to the atmospheric level. Once the atmospheric pressure was reached the reactor was closed by setting the four port valve in the reaction position and this was accomplished by filling the syringe.

Once the reactor was purged and brought back to atmospheric pressure, the next step was to prepare the sampling system. The pressure of the sampling bomb was lowered to subatmospheric conditions with the help of the vacuum pump. An absolute pressure of 14 to 15 KPa was judged sufficient to remove the reactor content in a short period of time, less than a second. The gas line coming from the sampling bomb to the vent was diverted to the vacuum pump by setting the three way value in the proper position. Once the targeted pressure was achieved the valve located between the pump and the three way valve was closed.

The syringe, for the liquid reactants injections, had to be calibrated to constantly inject a known weight of liquid. Thus, before the experiment began, several injection volumes were weighed to ensure reproducibility. The balance used to weigh the injection volumes was precise to a 0.001 gram. An average weight was used in all calculations.

With the reactor purged, the sampling vessels evacuated and the syringe calibrated, the timer was set to the desired reaction time. The reactor was then ready for an experimental run. The impeller was spun at 75% of the motor controller scale, 7875 RPM, to achieve good catalyst fluidization. Once the impeller reached steady state, the injection was effected.

At the time the syringe was emptied the reaction time counting started. When the reaction time was completed, the timer sent a signal to the actuator which positioned the four ports valve in the purging mode. Due to the pressure difference, the reactor content was drawn by the sampling bomb. As the reactants were not in contact with the catalyst anymore, the reaction was terminated. At the moment the sampling bomb and the reactor pressures reached equilibrium, the four ports valve was set back to the reaction mode in order to isolate the gas sample from the reactor.

After the sampling procedure completed, the sampling bomb pressure was still lower than atmospheric pressure. The pressure inside the sampling bomb was brought slightly above atmospheric by feeding argon. In this manner, the sample taken by the syringe was above atmospheric pressure. This operation avoided that too much air entered the sampling syringe because of the negative pressure.

In the case of the direct sampling from the reactor, the timing was controlled with a stop watch and all the preparations pertaining to the sampling bomb were not needed.

#### 5.4.1 Different Feedstocks

Two feedstocks were tested during the experimental program: 1) methanol/isobutanol, and 2) methanol/isobutylene. In the case of the second feedstock, methanol and isobutylene, it was not possible to inject the reactant simultaneously since methanol is a liquid and isobutylene is a gas at room temperature. It was then decided to inject the reactants sequentially and in different order to study the effect on the reaction behavior. In the case where methanol was injected first, the timer was activated at the end of the injection of isobutylene. Methanol and isobutanol were simply mixed together in proper proportions and then injected simultaneously.

#### 5.5 Analysis of the GC Results

The GC thermal conductivity detector produces a signal in millivolts proportional to the concentration of chemicals contained in the gas. This signal from the GC was collected under a graphical representation called a chromatogram by an HP integrator, model HP-3393A. Each chemical species was represented by a peak on the chromatogram. The areas of the various peaks were calculated by the integrator. The integration results were used to quantify the different chemicals contained in the reaction mixture.

Two methods were used to determine the concentration of each chemicals species in the reactor: 1) the argon as an internal standard, and 2) the total pressure at the sampling time. These two methods were based on the assumptions that the concentration of argon remained constant and that no leakage took place during the reaction. The two methods offered consistent results, with a maximum difference of 5%.

#### 5.5.1 Argon as the Internal Standard

Argon, being inert, does not react during the reaction or is not adsorbed by the catalyst. The argon partial pressure remains constant throughout the whole reaction time if there are no leaks. The amount of argon was measured using the initial pressure and the reactor volume. Because of the low pressure and temperature, the perfect gas law was applied for all calculations. It was also assumed that the bulk concentration inside the reactor was the same everywhere at all times and that the sample taken with the syringe was a good representation of the reactor content.

Knowing the initial partial pressure of argon, it was a simple matter of making ratios based on argon to calculate the actual concentration of chemicals inside the reactor. An example of these calculations are presented in Appendix A.

## 5.5.2 Pressure at Sampling Time as the Reference Value

The pressure at sampling time gave a mean to calculate the total number of moles of reactants and products that were present in the gas phase at the moment of sampling. Since the partial pressure of argon remained constant throughout the experiment, the difference between the pressure at the sampling time and the partial pressure of argon was a measure of the combined reactants and products partial pressure. The GC analysis of the sample provided the mole fraction of each of the chemical species. From the total number of moles of the reactants and products and their molar fraction, it was possible to calculate the number of mole of each chemical species in the Riser Simulator

#### 5.6 Temperature and Pressure Profile

A computer was used to record the temperature and pressure profiles during the reaction. Signals from the thermocouple inserted in the catalyst bed and the pressure transducer were read by a computer through a data acquisition card. The results were plotted as a function of time and provided information on the reaction behavior. The pressure profile was used to assess the rate of evaporation of liquid reactants. The profile could also provide a good assessment of sampling speeds while using the sampling bomb or the manual sampling.

## 5.7 Molar Balances

The pressure profiles were used to assess the actual molar balances. The pressure profiles measured the pressure rise associated to methanol or isobutylene injections. From these pressure rises, it was possible to calculate the amount of methanol and isobutylene injected. The expected values for the injection were compared to the values calculated from the pressure rise. In the case of isobutylene, these two values were found to have differences of 5 %. In the case of methanol the difference were below 10 %. The greater difference in the case of methanol was due to the increased uncertainty due to the injection of liquids. In both cases, the errors associated to the reactant injections are within experimental errors.

In order to confirm these results, carbon balances were calculated and are reported in appendix H. The carbon balance results ranged between  $\pm$  10 % which was consistent with the errors associated to the injection of methanol and isobutylene.

#### 5.8 Experimental Design

As the use of a Riser Simulator was never attempted before for the MTBE synthesis a large spectrum of operation conditions were chosen. The residence time ranged from 10 to 120 s, the temperature from 80 to 160 °C and two weighs of catalyst were experimented: 0.2 and 1 grams.

Experiments were performed by sets of several runs. A set was composed by a number of runs varying between 3 to 6. Between each run the reactor was swept with argon to remove previous gases and contaminants. Between each set of runs the catalyst was regenerated with air at 450 °C. This method of regenerating the catalyst appeared to be effective as the activity of the catalyst was restored.

## 5.9 Repeatability of the Results

Each experiment was repeated at least one time to ensure reproducible results. Since the catalyst was found to be deactivating, the experiments were also repeated as much as possible for different stages of deactivation of the catalyst. Repeatability insured a good quality of the analysis and of the interpretation of the results.

## 5.10 Conclusion

The Riser Simulator offered a good labscale equipment to perform the experiments involved in the present study as it offers conditions close to industrial riser reactor. The GC/MS association was found to be a powerful tool for the identification of the chemical species contained in the reaction mixture. The packed column, Poropak Q, linked to a thermal conductivity detector provided an easy procedure

# Chapter VI

# **Results and Discussion**

#### 6.1 Introduction

The different results collected during the experimental program are presented and analyzed in this chapter. Two feedstocks were investigated: methanol/isobutanol, and methanol/isobutylene. In the case of the methanol/isobutylene different methodologies of injection were considered. These different methodologies allowed the clarification of reaction mechanisms and strategies of operation.

When the best reaction conditions were identified the residence time, the temperature and the catalyst/reactant ratio were systematically changed to offer a better description of the influence of the operating parameters. From these results, a kinetic model was proposed and kinetics parameters were calculated. Finally, the model was used to predict reaction trends at different operating conditions of potential interest.

80

#### 6.2 Methanol and Isobutanol Feedstock

Methanol and isobutanol, being both liquid at room temperature, were mixed in a 1 to 1 molar ratio. The reaction was carried out at temperatures ranging from 100 to 300 °C. Two catalyst/reactant ratios were used 5 and 0.2 based on the zeolite content of the pellets. In order to achieve these two ratios the masses of catalyst used were 1 g and 0.2 g with masses of reactants of 0.040 and 0.1000 g respectively. Reaction times were also changed from 10 to 60 seconds. Upon injection of the reactants, it was observed that the pressure inside the reactor reached its maximum value within 1 sec. Thus, vaporization effects were considered negligible.

Experimental results obtained are reported in Table 6.1. The goal of these experiments was to demonstrate the feasibility of synthesizing MTBE from a methanol/isobutanol mixture by the direct coupling of these two alcohols. It has to be mentioned that only a qualitative analysis was pursued.

As a summary it can be stated that no experiments led to the production of MTBE from a methanol/isobutanol mixture. On the contrary, MIBE, an isomer of MTBE with a lower octane number, was detected from 100 to 260 °C for a catalyst/reactant ratio of 5. For the catalyst to reactant ratio of 0.2 a similar behavior was observed. The identities of MIBE and MTBE cannot be confused for two reasons: 1) the retention times of both isomers are, in the GC chromatogram, almost 1 minute apart, and 2) the mass spectrometer shows a distinctive fragmentation pattern for the two components: the major m/z peaks for MTBE are at 57 and 73 and for MIBE at 45 (Nunan 1993).

Temperature	Cat/Reactant	Time	MTBE	MIBE	Isobutylene
°C		seconds		*****	
100	5:1	60	NO	YES	NO
120	5:1	30	NO	YES	NO
140	5:1	10	NO	YES	NO
160	5:1	30	NO	YES	YES
180	5:1	60	NO	YES	YES
200	5:1	10	NO	YES	YES
220	5:1	60	NO	YES	YES
240	5:1	30	NO	YES	YES
260	5:1	30	NO	YES	YES
280	5:1	10	NO	NO	YES
300	5:1	60	NO	NO	YES
100	1:5	60	NO	YES	NO
150	1:5	30	NO	YES	NO
200	1:5	30	NO	YES	YES
250	1:5	10	NO	YES	YES
300	1:5	60	NO	NO	YES

Table 6.1 Direct Coupling of Methanol and Isobutanol.

Isobutylene, a product of the dehydration of isobutanol, appeared at 160 °C for the reactant/catalyst ratio of 5 and at 200 °C for the reactant/catalyst ratio of 0.2. The relative quantity of isobutylene while compared with the argon peak increased with temperature. Starting at 200 °C, byproducts were identified and

their quantity and number augmented with temperature. These byproducts were hydrocarbons in the  $C_3$  - $C_8$  range.

During these experiments the catalyst was not regenerated. After its removal a strong change in coloration was noted, from white to dark gray, almost black. This change in color was assumed to be the result of cokefication and that the catalyst was potentially deactivated. It was then decided that for further experiments the catalyst would need periodic regeneration.

# 6.3 Dehydration of Isobutanol

To clarify the dehydration of isobutanol to isobutylene, a set of experiments was developed. Temperatures ranged from 100 to 300 °C. The weight of catalyst loaded in the Riser Simulator was 1 g and the mass of isobutanol injected was 0.040 g giving catalyst/reactant ratio of 5 (based on the zeolite content). The reaction time for all the runs was 60 s. The results of these runs are presented in Table 6.2.

Temperature	isobutylene		
<u> </u>			
100	NO		
120	NO		
140	NO		
160	YES		
180	YES		
200	YES		
220	YES		
240	YES		
260	YES		
280	YES		
300	YES		

Table 6.2: Dehydration of Isobutanol to Isobutylene

These experiments confirmed that the dehydration of isobutanol forming isobutylene occurred above 140 °C. As already advanced in the Literature Review, the synthesis of MTBE appears to require the presence of isobutylene to initiate the MTBE synthesis. Thus, dehydration and etherification reactions are necessary to synthesize MTBE from methanol and isobutanol. However, there are problems with thermal compatibility as isobutylene was only formed above 140 °C. The minimum dehydration temperature was well above 100 °C, the recommended temperature for MTBE synthesis from isobutylene and methanol.

In conclusion, the direct coupling of methanol to isobutanol to obtain MTBE was not very encouraging considering the two different temperature levels required to achieve the two consecutive reactions necessary for the MTBE synthesis.

# 6.4 Methanol and Isobutylene Feedstock-Three Modes of Operation

Three modes of operation were devised where different orders of injection and adsorption of methanol and isobutylene were investigated. It was found that the order of injection and adsorption of the reactants modifies significantly the selectivity toward MTBE. The three modes of operation were as follows:

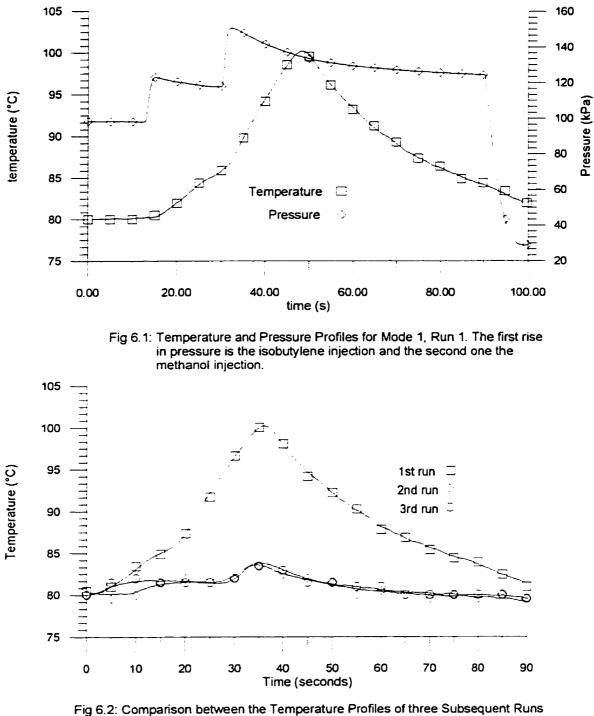
- Mode 1: Isobutylene injection followed after approximately 15 seconds by methanol injection.
- Mode 2: Methanol injection followed after approximately 15 seconds by isobutylene injection.
- Mode 3: Methanol injection with enough time given to methanol adsorption to reach equilibrium. Following this the isobutylene injection was effected.

Temperatures and pressures were recorded during experiments performed for these three modes of operation. Conversions and selectivities obtained for the three modes of operation are going to be presented along with the temperature and pressure profiles.

## 6.4.1 Mode 1 of Operation

The experiments of this section were essentially qualitative and were performed in order to assess the capacity of the catalyst to produce MTBE under operating conditions expected in a riser reactor. Conditions selected for these experiments are based on results found in the technical literature (Chu *et al.*, 1987 and Nicolaides *et al.*, 1993). The Riser Simulator was loaded with 1 g of catalyst. The temperature was set at 80 °C. 10 ml of isobutylene were injected first, followed by 0.0250 g of methanol These quantities of reactants corresponded to a methanol/isobutylene molar ratio of 2.25 and a catalyst/reactant ratio of 4 (based on the zeolite content). The two injections were completed within 15 seconds. The reaction time was set at 60 seconds. The partial pressure of the argon inside the reactor was atmospheric.

Typical temperature and pressure profiles are reported in Figure 6.1. Figure 6.1 describes the first experiment after catalyst regeneration. The first rise in the pressure plot corresponds to the injection of isobutylene. Once isobutylene is injected the pressure reaches a maximum value and then begins to decrease indicating an adsorption process and/or a dimerization reaction. The second rise in pressure corresponds to the methanol injection. The steep increase of pressure, after methanol injection, indicates a fast vaporization. There is also a temperature rise, following isobutylene injection, and this is a



after Regeneration of the Catalyst for Mode 1.

further indication of either an adsorption or a reaction process. When methanol is injected, the temperature of the catalyst has already reached 86 °C. As the

reaction progresses, it peaks at 98 °C. The steady rise in temperature following methanol injection suggests that the MTBE synthesis is taking place.

GC results allowed the identification of two reaction products: MTBE and diisobutylene. This justifies the temperature change during the reaction phase of the experiments. Isobutylene dimerization is an exothermic reaction with a heat of reaction of -87.3 kJ/mole to -79.1 kJ/mole and this depending on the isomer produced (Rehfinger *et al.*, 1990). The exothermic nature of the diisobutylene reaction explains the temperature rise following isobutylene injection. The MTBE reaction is also exothermic with a heat of reaction of -37.7 kJ/moles and this can also explains the temperature rise following the methanol injection.

Fig 6.2 displays the temperature profile of Run 1, from Figure 6.1, accompanied by the temperature profiles for two subsequent runs, Runs 2 and 3. The same conditions were used for each one of the runs. The maximum temperatures reached during Runs 2 and 3 is lower, suggesting potential deactivation of the catalyst. The accuracy of the temperature readings was ± 0.5 °C, and this suggests that Runs 2 and 3 were essentially identical within the experimental error. This similarity between the temperature profiles of Run 2 and 3 led to the conclusion that the catalyst, once Run 1 is completed, may not sustain more significant deactivation.

Following Run 3 the catalyst was regenerated at 450 °C. After the regeneration, the catalyst resumed a very similar behavior as for Runs 1,2 and 3.

Experiments, for which the amount of MTBE produced was quantified, showed that Run 1 produced 2.5% of MTBE based on isobutylene conversion. For the second and third runs the conversion of isobutylene to MTBE reached up to 5%. Diisobutylene was identified for Run 1 as well as for all the subsequent ones.

# 6.4.2 Mode 2 of Operation

The next step in the experimental program was to change the order of the injections: methanol was injected first followed, after 15 seconds, by isobutylene. The amount of methanol injected was 0.0145 g and the amount of isobutylene 11 ml. This represented a methanol/isobutylene molar ratio of 1 and a catalyst/reactant ratio of 5. By decreasing the amount of reactant while compared to the amount of catalyst, the catalyst helped controlling the temperature by adsorbing some of the heat of reaction. The reaction time was 60 seconds. Cycles of 6 runs were performed between each catalyst regeneration.

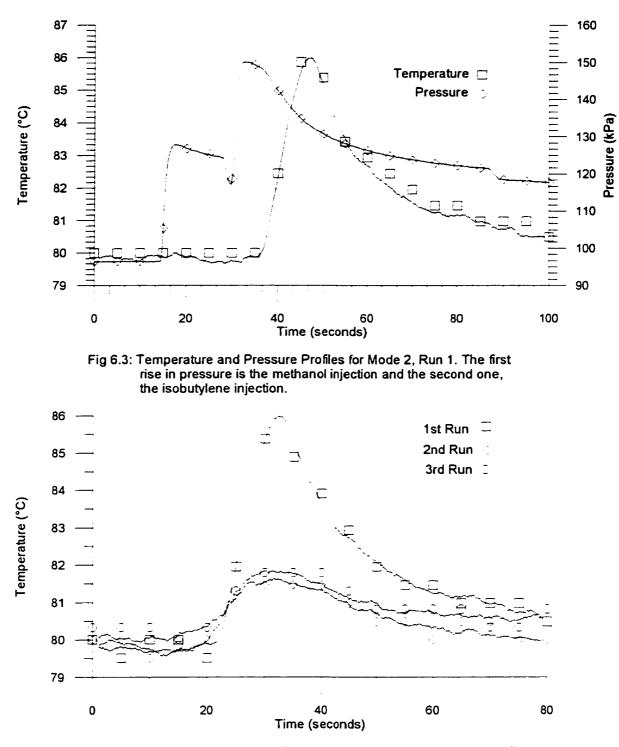


Fig 6.4: Comparison between the Temperature Profiles of the First three Runs after Regeneration for Mode 2

Pressure and temperature profiles for Run 1, following catalyst regeneration, are presented in Figure 6.3. The first rise of pressure is due to the injection of methanol. This steep pressure increase indicates rapid methanol vaporization. The decrease in pressure following methanol injection was related to the adsorption of the alcohol onto the catalyst surface. The second rise of pressure represents the isobutylene injection. This was followed by a pressure decrease after isobutylene injection and this reflects the reaction with methanol and/or the adsorption of isobutylene or methanol. The sharp decrease of pressure before the isobutylene injection is due to the pressure difference between the reactor and the syringe.

Temperatures profiles for Mode 2 of operation were quite different from Mode 1 of operation. There was no significant temperature increase during methanol adsorption and this suggested that no methanol dehydration was occurring. This was confirmed by the GC results not showing any dimethyl ether. Temperature only begun to increase at the time isobutylene was injected. GC results suggested that two reactions were occurring at this point: isobutylene dimerization and coupling or methanol with isobutylene leading to MTBE. This temperature pattern was consistently repeated for the first run, Run 1, of several sets of experiments. MTBE amounts obtained for Run 1 ranged between 2.2 and 2.4 % (based on isobutylene conversion).

91

As explained earlier, up to 6 runs were performed between catalyst regenerations. Figure 6.4 reports the temperature profiles of the first three runs. The maximum temperature reached during Run 1 was very high while compared to Runs 2 and 3. Again, as it happened during the first mode of operation, Runs 2 and 3 showed an approximately identical profile with differences being in the error range of temperature readings. This decrease in the maximum temperature achieved was accompanied by an increase in the MTBE yield and with essentially total disappearance of diisobutylene formation. This decrease of the maximum temperature appears to be related to a decay in the catalyst activity to promote the dimerization reaction. The MTBE yield for the last five runs of this set was between 3 and 4.5% (based on isobutylene conversion).

#### 6.4.3 Mode 3 of Operation

The third mode of injection consisted of a first methanol injection. Methanol was allowed to reach adsorption equilibrium followed by isobutylene injection. The reaction conditions were the same as for Modes 1 and 2. The initial pressure of the reactor was set to atmospheric. The temperature of the reactor was 80 °C. The catalyst/reactant ratio was 5. The volume of isobutylene injected was 11 ml, and the weight of methanol 0.0155 g; for a methanol/isobutylene ratio of 1.06.

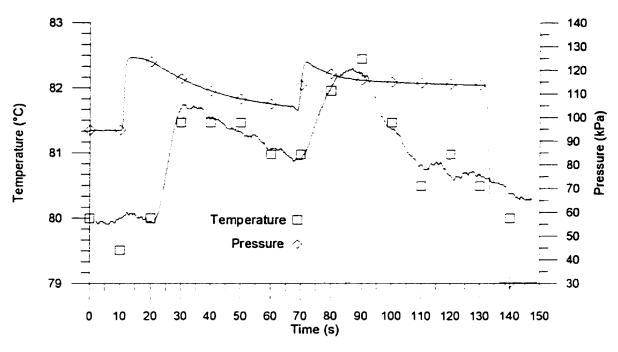


Fig 6.5: Temperature and Pressure Profile for Mode 3, Run 1. The first rise in pressure is the methanol injection and the second one the isobutylene injection.

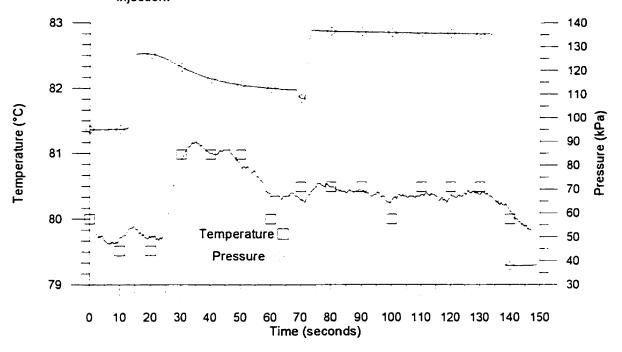


Fig 6.6: Temperature and Pressure Profiles for Mode 3, Run 3. The first rise in pressure is the methanol injection and the second one the isobutylene injection.

Temperature and pressure profiles are presented in Figure 6.5 for Run 1. In this case the first rise in pressure corresponds to the methanol injection. Methanol was allowed to contact the catalyst for 50 seconds. This period of time was judged sufficient for the methanol to reach adsorption equilibrium. The second pressure rise represents the isobutylene injection. Pressure decreased following isobutylene injection and this is an indication that the MTBE synthesis was taking place. In the case of Mode 3, the pressure decrease after isobutylene was not as important as in the two other modes of operation. This lower pressure reduction was the result of methanol already adsorbed onto the catalyst.

Temperature of the catalyst, following the methanol injection, increased about 2 °C after 10 seconds. This suggested that either a reaction was occurring or that heat of adsorption was released. Results from the product analysis favor the later interpretation as no dimethyl ether was detected. Once methanol reached adsorption equilibrium, the temperature was already reduced by about 1 °C. At this time, isobutylene was injected and the temperature increased again and this is consistent with the MTBE synthesis reaction taking place.

Figure 6.6 shows the temperature and pressure profiles for the third run following catalyst regeneration, Run 3. The partial pressure of methanol, after the adsorption equilibrium is reached, remained higher than for the previous experiments. This indicated that a smaller density of active sites were available

onto the catalyst surface. These sites were presumably occupied by either methanol or MTBE strongly adsorbed to the surface. Experiments where only isobutylene was injected, after sweeping the reactor with argon for 45 minutes, showed that a significant amount of MTBE was still produced, up to 5% based on isobutylene conversion. This confirmed the presence of adsorbed methanol on the catalyst surface.

Another major difference between Run 1 and the subsequent runs was the temperature rise following the isobutylene injection. During the first run, Figure 6.5, the temperature increased by almost 2°C, while during subsequent runs, Figure 6.6, the temperature remained essentially constant. Caution must be taken while making this comparison, as the error associated with the temperature measurement is  $\pm 0.5$  °C.

The amount of MTBE produced during Run 1, based on isobutylene conversion, was 2.3-3.1 %, while the amount of MTBE obtained in subsequent runs ranged form 3.8-6.8 %. No other products of reaction were identified for Mode 3 of operation.

### 6.4.4 Comparison Between the Three Modes of Operation

The difference between Modes 1, 2 and 3, is mainly given by the different selectivity toward the reaction byproducts. In the Mode 1 of operation, diisobutylene was identified in every run. For the Mode 2 of operation, diisobutylene was only identified in the first run following catalyst regeneration. In the case of the Mode 3 of operation, no diisobutylene was identified in any of the runs.

In every mode of operation, MTBE was produced in smaller amounts (2-3%) during Run 1. MTBE levels for the subsequent runs reached as much as 6.8%.

Moreover, the changes of catalyst temperature with reaction time appeared to be better controlled when methanol was adsorbed first (Modes 2 and 3). In the case of Mode 1 of operation, the catalyst temperature increased as much as 20 °C above the initial temperature level, of which, 10 °C may be attributed to the diisobutylene formation. In the case of Mode 2 of operation, the temperature increased up to 6°C above the initial temperature. For Mode 3 of operation the temperature increased by 3°C only.

96

Furthermore, for the second and third runs, in the case of the Mode 1 temperature increases with reaction time were limited. This decrease in the maximum temperature may be explained by the selective deactivation of the catalyst. Diisobutylene and higher oligomers were strongly adsorbed onto the catalyst surface thus limiting the access to the acid sites.

Modes 2 and 3 offered 100 % selectivity toward MTBE, excepted for the first run when Mode 2 was used. This confirms that the order of injection is of great importance when selectivity toward MTBE has to be optimized. The effect of temperature on reaction equilibrium is substantial. Thus, it is important to have good temperature control during the reaction.

Overall, Mode 3 of operation appears to provide the best alternative for MTBE synthesis.

### 6.4.5 Variation of the Methanol to Isobutylene ratio

It was decided to study the behavior of the MTBE synthesis, under mode 3 of operation, by changing the reactant ratio. The injection of methanol was kept constant at 0.0161g for all the experiments, and the volume of isobutylene was varied between 2 and 50 ml. In this manner, the molar ratio of methanol to isobutylene ranged within 0.25 and 6.16. During these experiments the catalyst was only regenerated every ten runs. The total reaction time was 60 seconds. Every run was repeated 2 to 5 times, the exception being for the molar ratios 0.25 and 6.16 for which the runs were only effected once. Table 6.3 reports the results of these experiments as an average of the results obtained.

	Molar Ratio	MTBE Yield
	(methanol/isobutylene)	(conversion of
		isobutylene)
		(%)
•	0.25	4.0
	0.31	4.2
	0.41	4.0
	0.62	3.7
	1.12	5.4
	1.54	4.4
	2.46	5.3
	6.16	4.8
-		

Table 6.3: MTBE Yields for Different Methanol/Isobutylene Molar Ratio.

For these runs the only reaction product identified was MTBE. Consequently, the selectivity of the reaction remained 100% and this for all the molar ratios studied. Furthermore, the yield of the reaction appeared to be directly related to the concentration of isobutylene. The amount of MTBE increased or decreased with the isobutylene partial pressure.

Some experiments demonstrated that a minimum methanol partial pressure was necessary to reach 100 % selectivity. Experiments were performed in the following manner: a) methanol was pre-adsorbed onto the catalyst, b) the

reactor was outgassed with helium for 10 minutes, c) isobutylene was injected, and, d) the reaction was completed in 60 seconds. During these runs MTBE was obtained along with diisobutylene. Hence, a minimum partial pressure of methanol is necessary to maintain a high concentration of occupied sites.

### 6.5 Reaction Mechanism

From the results described previously, a first attempt to describe the reaction mechanism can be developed. The reaction involves an adsorbed molecule, methanol, reacting with a second gas phase molecule, isobutylene. Experimental results obtained so far support this mechanism. The results suggest that methanol preadsorbed onto the catalyst surface may block the access of isobutylene to the acid sites. Isobutylene would have no choice but to react with the alcohol to form MTBE.

This mechanism was corroborated by the three Modes of operation described earlier. For Mode 1 of operation, isobutylene is injected first and has access to the active sites thus producing diisobutylene as well as MTBE. For Modes 2 and 3 of injection, methanol is injected first and in the case of Mode 2 methanol has less time to adsorb onto the catalyst surface, thus blocking partially the access of isobutylene to the acid sites. The result is that MTBE is formed along with diisobutylene for the first run. In Mode 3 of injection, methanol

is allowed to reach the adsorption equilibrium, thus blocking more effectively the active sites to isobutylene and consequently giving a 100% selectivity toward MTBE.

These conclusions about the reaction mechanism partly agree with Chu *et al.* (1987) and Kogelbauer *et al.* (1995). Both authors reported 100% selectivity toward MTBE under very specific conditions. In both cases, the experiments were performed in continuous fixed bed reactors while the present study was accomplished in a well mixed batch type reactor, the Riser Simulator.

Chu *et al.* (1987) suggested that the reaction mechanism could be explained by the different diffusion rates of methanol and isobutylene. H-ZSM-5 has two pore sizes of 5.4 x 5.6 Å and 5.1 x 5.5 Å (Chu *et al.*,1987). Methanol a smaller molecule, 3.7 x 4.2 Å, diffuse more easily through the catalyst pores than isobutylene, 3.9 x 5.4 Å. Thus, isobutylene might encounter a large excess of methanol on the catalyst surface and react to form MTBE. However, by injecting methanol and isobutylene simultaneously, Chu *et al.* (1987) were not able to distinguish the effects of methanol or isobutylene adsorption on reaction selectivity. Moreover, Chu *et al.* (1987)did not mention potential effects of initial reactivity when, as demonstrated using Modes 2, it would be more likely to observe diisobutylene along with MTBE production.

Kogelbauer et al. (1995) performed adsorption experiments showing that more molecules of methanol were adsorbed per acid sites than isobutylene. The results were 2.5 molecules of methanol per acid site compared with 1 for isobutylene per acid site for a partial pressure of 20 kPa. Comparative desorption experiments, performed at 100 °C, showed that a larger fraction of methanol than isobutylene would desorb from the catalyst surface. These results suggest that isobutylene is more strongly bonded than methanol onto the catalyst surface. On this basis Kogelbauer et al. (1995) speculated that adsorbing isobutylene first reduces the methanol access to the acid sites. These authors also argued that the larger uptake of methanol by the catalyst is responsible for the lower yields of byproducts such as diisobutylene or larger hydrocarbons. As part of their experimental program, Kogelbauer et al. (1995) reported, following pre-adsorbing of methanol onto the catalyst, 100 % selectivity toward MTBE. On the contrary isobutylene pre-adsorption yielded lower selectivity toward MTBE. This lower selectivity is explained by the presence of diisobutylene or higher hydrocarbons unfavorably affecting catalyst activity. These products could only be removed by high temperature desorption. After regeneration, the catalyst resumed its original activity. Kogelbauer et al. (1995) argue that although ZSM-5 may exhibit some mass transfer limitations, the main factor, for the catalyst favorable selectivity toward MTBE, is the higher affinity of the catalyst for methanol adsorption.

Most of the results of this research are in agreement with the Kogelbauer et al., (1995) with the exception of Modes 1 and 2 of operation. In the case of Mode 1 of operation, isobutylene did not seem to impede the production of MTBE for runs following Run 1. Comparable yields were obtained for the second and third injections of Modes 2 and 3 of operation. In any case, for all the Modes of operation, as reported in this study, methanol adsorbed during the first run of a set of experiments seemed to have a favorable effect on the subsequent runs as the yields of MTBE essentially doubled.

### 6.6 Reactions Testing at Different Conditions of Temperatures, Catalyst/Reactant Ratios, and Reaction Time

Using Mode 3 of operation, several experiments were developed in which temperature, catalyst/reactant ratios and reaction time were changed systematically.

Reaction temperatures were 80, 120 and 160 °C. Lower reaction temperatures were not allowed as methanol and MTBE can condense below 80 °C. Catalyst/reactant ratios were varied by changing the mass of catalyst while keeping the amounts of methanol and isobutylene injected constant. The volume of isobutylene injected was 11 ml and the mass of methanol 0.0154 g. The two mass of catalyst employed were 0.2 and 1 g. In this way the two catalyst/reactant ratios studied were 5 and 1. The times of reaction were 10, 30, 60, and 120

seconds. The catalyst was only regenerated once a full set of experimental runs were completed i.e. for all the temperatures and reaction times for one catalyst/reactant ratio.

Figures 6.7 and 6.8 present the conversion of isobutylene versus the reaction time. Each graph covers one catalyst/reactant ratio. Each reported data point represents the average of two to five experimental results and the error bars represent the sample standard deviation. The reported data points for each temperature are connected by lines. Individual results are reported in Appendix D.

Although no byproducts were observed at 80 °C, dimethyl ether and isobutylene were both identified at 120 and 160 °C. In both cases the quantities increased with the temperature and with the reaction time. While byproducts were not quantified, it appears that increasing reaction temperature may not be favorable for MTBE production as a larger proportion of the feedstock is converted into unwanted byproducts.

Two important comments can be advanced on the basis of the results displayed in Figures 6.7 and 6.8. First, the isobutylene conversion achieved after 120 seconds at 80 °C for a catalyst/reactant ratio of 1 was below the

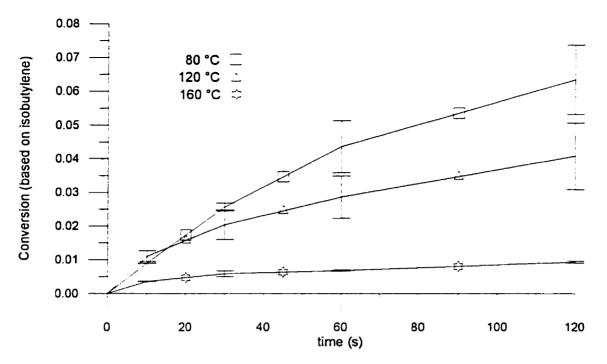


Figure 6.7: Conversion of Isobutylene toward MTBE for a Catalyst/Reactant Ratio of 5. (The error bars correspond to the standard deviation)

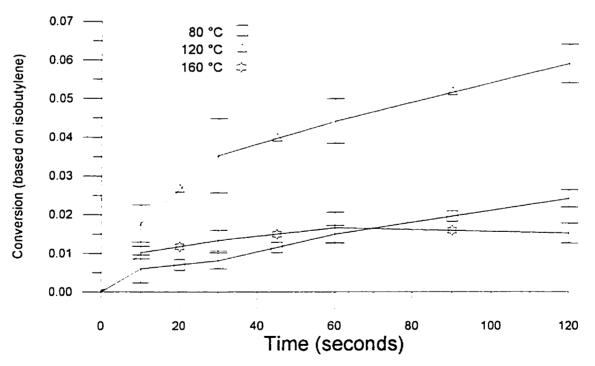


Figure 6.8: Conversion of Isobutylene toward MTBE for a Catalyst/Reactant ratio of 1. (The error bar correspond to the standard deviation)

isobutylene conversion achieved at 120 °C. This conversion was also below the one achieved for a catalyst to reactant ratio of 5 at 120 °C. The conversion at a reaction time of 120 seconds are listed in Table 6.4.

Temperature	Conversion		
°C	% of isobutylene (± SD) catalyst/reactant ratio 5	% of isobutylene (±SD) catalyst/reactant ratio 1	
80	6.4 ± 1.03	2.4±0.23	
120	4.1 ± 0.99	6.0±0.5	
160	0.93 ± 0.03	1.5±0.26	

Table 6.4: Conversion of Isobutylene toward MTBE at a Reaction Time of 120 seconds.

To explain these effects it can be argued that the catalyst/ reactant ratio has a strong effect on the reaction rate at low temperature, 80 °C. As a result, for constant temperature, the increase of catalyst/reactant ratio would increase the rate of isobutylene transformation. A second observation can be drawn from the results at 160 °C for both catalyst/reactant ratio. The curves reach a plateau indicating that reaction equilibrium may be attained. Moreover, the isobutylene conversion is in this case lower for the highest catalyst/reactant ratio. This implies that a larger amount of catalyst, in the case of a constant amount of reactants, decreases the isobutylene equilibrium conversion.

In order to justify the reduction of conversion associated with the catalyst/reactant increase, the isobutylene theoretical equilibrium conversions

were calculated, see Appendix F. To perform these calculations, complementary adsorption experiments were developed to determine the equilibrium adsorption constants of methanol. Details of adsorption experiments are provided in Appendix E.

To develop reaction equilibrium calculations some assumptions are adopted: a) the only reactant or product adsorbed onto the catalyst is methanol and this in agreement with the results obtained in the present study, and, b) the equilibrium constants can be calculated from eq (2.6) (refer to the literature review). The first assumption may be somewhat inadequate at 160 °C when byproducts quantities are more significant. According to Tejero *et al.* (1988), it is reasonable to assume that the fugacity coefficients are close to unity in the case of a gas phase system for the MBTE synthesis.

In summary, the reaction equilibrium conversion can be calculated using the following relation:

$$K_{_{eq}} = \frac{p_c}{p_{_{A}}p_{_{B}}} = \exp(-\frac{\Delta G_{_{R}}}{RT})$$
(6.1)

where  $p_A$ ,  $p_B$  and  $p_C$  are respectively the partial pressure of methanol, isobutylene and MTBE. In the present study there are a number of known parameters  $p_{Ao}$ ,  $\alpha$ ,  $p_{Bo}$ ,  $K_A$ ,  $q_{sat}$ ,  $W_{cat}$ , T, V, eq(6.1) can be modified as follows:

$$K_{**} = \frac{p_{**} X}{(p_{**} - p_{**} X) \alpha p_{**} (1 - X)}$$
(6.2)

with

$$p_{Ao} = \frac{K_A p_A}{1 + K_A p_A} q_{ee} W_{ce} \frac{RT}{V} + p_A$$

A detailled description of the method of calculation is presented in Appendix E. Equilibrium conversions calculated using eqs(6.1) and (6.2) are given in Table 6.5 as well as the corresponding equilibrium constants.

Table 6.5: Equilibrium Constants and Equilibrium Conversions of Isobutylene into MTBE

Temperature	Kea	Catalyst/ re	actant ratio	
°C	kPa <sup>-1</sup>	5	11	
80	3.5046E-2	17.72 %	33.74 %	
120	3.7182E-3	3.78 %	7.77 %	
160	6.0969E-04	0.97 %	1.68 %	

Results reported in Table 6.5 confirm that the catalyst/reactant ratio has an important effect on reaction equilibrium and this was consistently observed for the three thermal levels investigated. In fact, the lower the catalyst/reactant the higher is the expected isobutylene equilibrium conversion. Moreover, when compared with theoretical results, it was observed that reaction equilibrium was essentially reached for the two catalyst/reactant ratios at 160 °C. For 120 °C, the catalyst/reactant of 5 gave a higher reaction rate and reaction equilibrium was approached for the reaction time investigated during the experimental program.

The increase of the catalyst/reactant ratio diminishes the potential achievable equilibrium conversion. On the other hand, increasing the catalyst/reactant ratio increases the rate of reaction. The relative influence of these two factor has to be carefully evaluated if reaction times are going to be below 10 seconds which are potential reaction times for industrial riser reactors.

The augmentation of the catalyst/reactant ratio can be achieved in two manners: a) increasing the catalyst hold-up, or b) increasing the concentration of H-ZSM-5 in the catalyst pellet. The first of these two options presents potential limitations, as current riser reactors have restrictions on the allowed catalyst hold-ups. The exothermicity of the reaction could also impose some restrictions to the implementation of the increase of the zeolite concentration in the catalyst matrix. The temperature profiles would become sharper and depress the equilibrium concentration. However, the two options can be combined using a compromise between higher catalyst hold-ups and limited temperature rise. Future research in this area is needed to clarify these points and to progress on the implementation of these results.

### 6.7 Model of the Reaction

Relatively simple rate models have been proposed for predicting the rates of MTBE synthesis. These rate models were developed using results obtained from a liquid-solid reactor systems using Amberlyst 15.

In spite of the differences with the gas-solid reaction system considered in the present study, the reported rate equations provide a basis for the development of a model with H-ZSM-5. These models, discussed in the literature review, are based on the Langmuir-Hinshelwood and Rideal-Eley mechanistic representations. Both models assume that the reactants and products display an adsorption behavior that can be represented with a Langmuir isotherm.

Rideal-Eley model, derived from the more general Langmuir-Hinshelwood mechanistic formulation, represent the reaction between an adsorbed molecule and a molecule in the gas phase:

$$A(ads) + B(g) \to C(ads)$$
(6.3)

with A and C being respectively methanol and MTBE adsorbed on the catalyst and B being isobutylene present in the gas phase only. Under these constrains the rate equation for MTBE synthesis is as follows:

$$\mathbf{r}_{c} = \mathbf{\vec{k}} \mathbf{\theta}_{A} \mathbf{p}_{B} - \mathbf{\vec{k}} \mathbf{\theta}_{c} \tag{6.4}$$

with  $\theta_A$  and  $\theta_C$  being the fraction of the catalyst sites covered by methanol and MTBE,  $\vec{k}$  and  $\vec{k}$  the forward and backward constants and  $p_b$  the partial pressure of isobutylene in the gas phase. Using the Langmuir isotherm, the fraction of sites occupied by chemical species covering the catalyst surface can be defined as:

$$\Theta_{1} = \frac{K_{1}p_{1}}{1 + \sum_{i=1}^{n} K_{i}p_{i}}$$
(6.5)

with K<sub>i</sub> being the equilibrium sorption constant,  $p_i$  the partial pressure of methanol, isobutylene or MTBE. The fraction of sites occupied by isobutylene and MTBE are assumed to be negligible so that K<sub>B</sub>P<sub>B</sub> and K<sub>c</sub>P<sub>c</sub> are both equal to zero. Once eq (6.5) is substituted in eq (6.4), eq (6.6) is obtained:

$$r_{c} = \frac{\vec{k}K_{A}p_{A}p_{B} - \vec{k}K_{c}p_{c}}{1 + K_{A}p_{A}}$$
(6.6)

At the condition of reaction equilibrium, when the rate of reaction is equal to zero, the constants of the numerator can be related through the following relationship:

$$K_{s_{s}} = \frac{p_{c}}{p_{A}p_{B}} = \frac{\vec{k}K_{A}}{\vec{k}K_{c}}$$
(6.7)

Thus equation 6.6 can be further simplified:

$$r_{\rm c} = \vec{k} K_{\rm A} \left[ \frac{p_{\rm A} p_{\rm B} - p_{\rm c} / K_{\rm eq}}{1 + K_{\rm A} p_{\rm A}} \right]$$
(6.8)

A mass balance is performed around the reactor using the proposed reaction rate model:

$$\frac{\mathrm{d}C_{\mathrm{c}}}{\mathrm{d}t} = r_{\mathrm{c}}W_{\mathrm{cut}} \tag{6.9}$$

The following step requires the modification of eq (6.9) so that the reaction rate is a function of the conversion of isobutylene, x.

$$\frac{1}{W_{at}}\frac{dx}{dt} = K[f(x)]$$
(6.10)

with the function f(x) being defined as :

$$f(x) = K \left[ \frac{(p_{A0} - p_{B} x)\alpha(1 - x) - x_{K_{a}}}{1 + K_{A}(p_{A0} - p_{B} x)\alpha} \right]$$
(6.11)

where:

$$K = \bar{k}K_{A}$$
(6.12)

 $p_{A0}$  represents the hypothetical partial pressure of methanol without catalyst being loaded in the reactor. The parameter  $\alpha$  represents  $p_A/p_A$  which is the fraction between the methanol partial pressure and the hypothetical partial pressure of methanol.

Then, eq(6.9) can be rearranged and integrated as follows:

$$\int_{x=0}^{x_{t}} \frac{dx}{f(x)} = K \int_{t=0}^{t} dt$$
(6.13)

Once the process of integration was completed, the theoretical conversion  $x_{the}$  for a given reaction time was obtained and this theoretical conversion could be used in a regression analysis minimizing the differences between the  $x_{the}$  with the experimental values,  $x_{exp}$ , observed

$$\sum (\mathbf{x}_{_{\mathbf{x}\mathbf{y}}} - \mathbf{x}_{_{\mathbf{t}\mathbf{x}}})^2 = \min \operatorname{imum}$$
 (6.14)

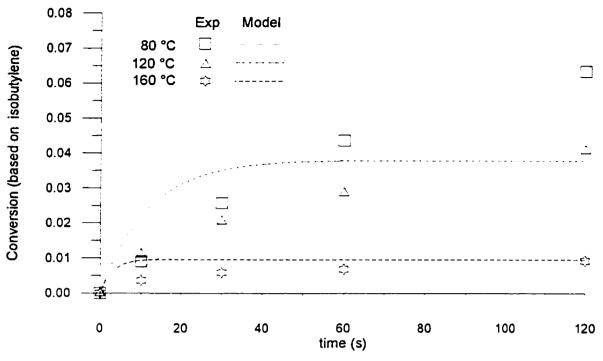
Thus, the numerical procedure was based on adjusting the value of the K constant until the summation of the residuals function was minimized. Additional details of the integration and the residual minimization are provided in Appendix G.

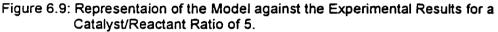
In the present study, for conditions where reaction equilibrium is reached rather quickly, the experimental points available makes, in the case of higher temperature, the evaluation of the initial reaction rates rather difficult. There is a potential risk of underestimating these rates and this may lead to errors in the analysis.

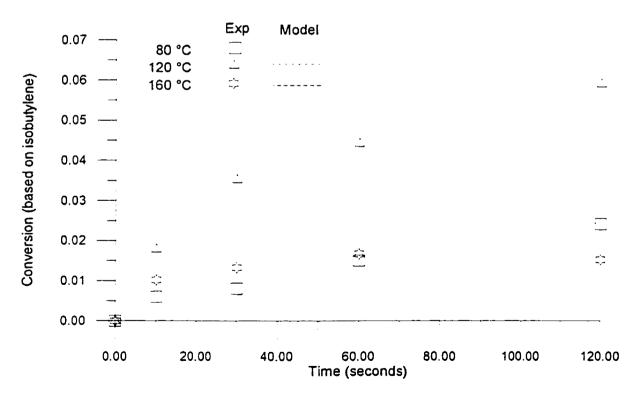
Consequently, it was observed that the use of an integral method of analysis, eq (6.12), versus a differential method, improved accuracy of the fitting process and as a result it was the preferred method for developing calculations.

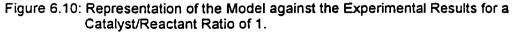
#### 6.8 Fitting Results.

Once the results of the fitting analysis, between the model and the experimental results were completed, a graphical representation was used in order to illustrate the adequacy of the model proposed. Figures 6.9 and 6.10 present the model against the experimental results. The trends found during the experiments are well represented by the model proposed. It appears that the model follows the experimental results with only one exception, the runs with the catalyst/reactant ratio of 5 at 120 °C. The fact that only two runs were done for each of these observations may explain the potential error between the model and the experimental results. Having less observations limits the confidence that can be granted to these observations. Nevertheless, the overall number of observations, 73, used to fit the model, increases significantly the confidence on the final results.









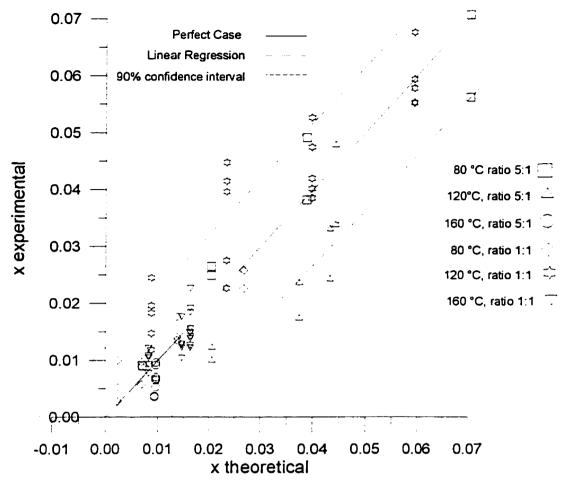


Fig 6.11: Comparison Between the Experimental and the Theoretical conversion.

Figure 6.11 provides a representation of all the experimental points plotted against the theoretical values. The plotted line with the slope of one represents the ideal case where the model would represent perfectly the experimental results. Three broken lines are also plotted. The center broken line represents the results of a linear regression applied to the experimental observations. The error between the slope of the theoretical optimum and the linear regression is 2.2%. The small difference between the slopes shows that the experimental values are well balanced on each side of the theoretical line.

116

The broken line on each side of the linear regression is the result of the calculation of a 90% confidence interval. 68 of 75 of the observations are actually falling inside this interval. This means that 90.6% of the experimental values have a 90% confidence to be well represented by the model. This is also a good evidence of the agreement between the model and the experimental values.

One of the assumptions used during the fitting process was that the forward kinetic constant followed the Arrhenius Law. Figure 6.12 is the representation of an Arrhenius plot. The slope of the line plotted through the three points is the observed energy of activation which is found to be 55 kJ/mole. The values found in the literature, in the case of the liquid phase MTBE synthesis, for Amberlyst-15 range from 82 to 92 kJ/mole. Ali *et al.* (1990) reported a value of 68.9 kJ/mole for the gas phase reaction with Amberlyst-15. This last value is in the same range as the one found in the present study. The fairly good agreement between the two energy of activation reinforces the conclusion that the model proposed represents well to the MTBE synthesis reaction.

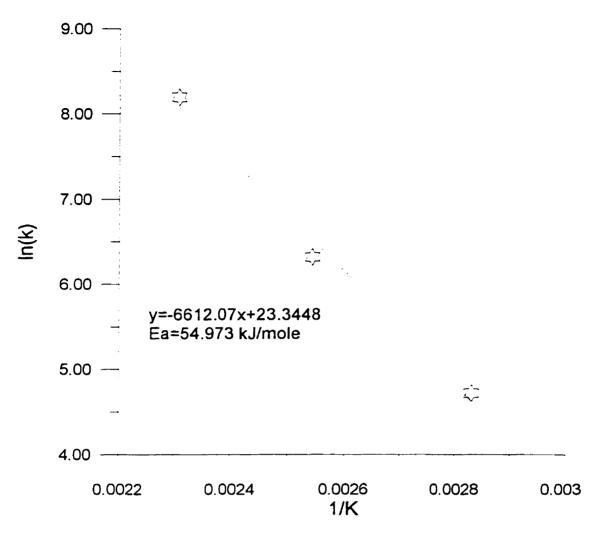


Fig 6.12: Arrhenius Plot of the Forward Kinetic Constant.

### 6.9 Prediction using the Model

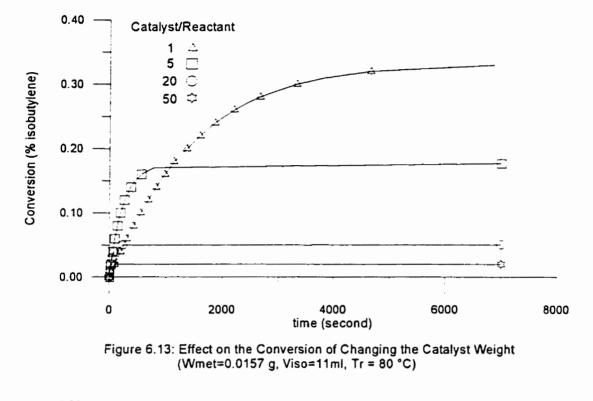
The mathematical model proposed in the present study appears to represent accurately the MTBE synthesis for a zeolite H-ZSM-5 based catalyst. The purpose of this section is to apply this model to predict potential trends while using this catalyst.

Two cases were studied: a) methanol/isobutylene ratio is modified from 1 to 1/4 while keeping the catalyst weight constant at 1 g , b) the weight of the catalyst is varied from 0.2 to 10 grams while keeping the quantity of methanol and isobutylene constant, thus, changing the catalyst/ reactant ratio from 1 to 50. All the simulations were done for a temperature of 80 °C.

Figure 6.13 and 6.14 presents the results of the calculations. The main effect of the operating changes proposed is the influence on reaction equilibrium conversion. It was expected that the rate of reaction would greatly increase, as a result of the higher catalyst loading or the increase of the partial pressure of isobutylene. However, the increase in the reaction rate appears to be offset by the larger amount of methanol adsorbed onto the catalyst surface and by the non proportionnal increase of MTBE obtained at higher isobutylene initial partial pressure. These two cases are reviewed in the following sections.

Changing the catalyst/reactant ratio from 1 to 50 considerably reduces the reaction equilibrium conversion. Having more catalyst means more sites available for methanol to be adsorbed and as a result less methanol is available in the gas phase. It is important to remember that the reaction equilibrium is determined using eq (6.1) with the reaction equilibrium constant being calculated on the basis of free energy of reaction. However, by reducing the partial

pressure of methanol into the gas phase through adsorption lowers the MTBE partial pressure at reaction equilibrium.



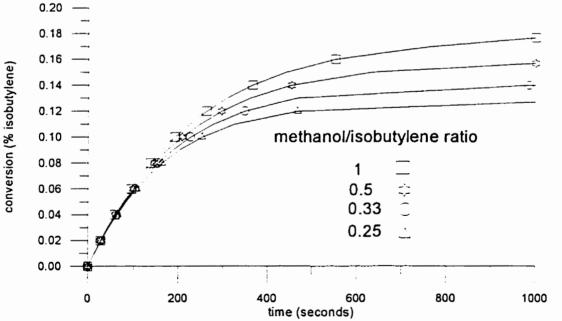


Figure 6.14 Effect of Changing the Methanol to Isobutylene Ratio on the Equilibrium Conversion and the Rate of Reaction (Wcat = 1 gram, Pmet = 28, Tr = 80 °C)

Furthermore, increasing the catalyst/reactant ratio augments the rate of reaction. This change is quite apparent between the 1 and 5 ratio and becomes essentially unnoticeable at 5, 20 and 50 ratios.

The most important effect of increasing the isobutylene partial pressure is the reduction of the equilibrium conversion toward MTBE. The non-proportionnal increase of the isobutylene partial pressure results in an isobutylene conversion decrease. The amount of MTBE produced increases with the isobutylene partial pressure. These results are reported in Table 6.6 in terms of equilibrium conversion and partial pressure of MTBE at equilibrium

Table 6.6: Final Partial Pressure of MTBE when the Partial Pressure of Isobutylene is Increased.

Initial Partial Pressure of Isobutylene kPa	Equilibrium Conversion Based on Isobutylene %	Partial Pressure of MTBE at Equilibrium kPa
25.76	17.7	4.6
50	15.7	7.9
75	14.1	10.6
100	12.7	12.7

Results of this simulation are very important. The first conclusion is that the zeolite H-ZSM-5 in its present form does not seem to offer enough activity for the MTBE synthesis to suit the design criteria of a riser reactor: i.e reach equilibrium conversion within 10 seconds. A potential explanation could be that the amount of catalyst active sites promoting the MTBE synthesis are not available in sufficient concentration. Moreover, the presence on the zeolite H-ZSM-5, of two different types of acid sites adds another unknown to the problem as the present study did not address this potential effect. Downer reactors, offering longer residence time than risers, up to 50 s, could also be considered as a potential option for the development of a new process for the MTBE synthesis.Future studies will be necessary in order to clarify the roles of the two acid sites in the MTBE synthesis.

#### 6.10 Conclusions

Results discussed in this chapter lay the foundation for future research on the MTBE synthesis from H-ZSM-5 catalyst of other zeolites presenting similar properties. The different modes of operation helped clarifying the reaction mechanism which adds to the understanding of the MTBE synthesis. Mode 3 of operation, which offered the best alternative for the reaction, was applied for a wide range of operations and these results were used in the development of a kinetic model. Finally the kinetic model was employed to make predictions for operating condition leading to high yeilds of MTBE. The results obtained may be used to develop future experiments.

## Chapter VII

## **Conclusions and Recommendations**

The production of cleaner burning fuels is an important issue as the public and the government demand more environmentally acceptable fuels. Production of reformulated gasolines is an excellent approach to deal with these requirements. MTBE is one of the main component of reformulated gasoline. Consequently, the demand for MTBE is expected to steadily grow in the coming years.

In addition to this, the current feedstocks for MTBE, methanol and isobutylene will soon no longer be sufficient to meet such a demand. Hence, other alternative sources of MTBE must be found to supplement the actual feedstocks.

One most promising alternatives is the use of natural gas. Natural gas can, through steam reforming, produce synthesis gas (syngas). The reaction of syngas can in turn, under the proper temperature and pressure conditions, and in the presence of appropriate catalysts, yield methanol and isobutanol. Isobutanol can be dehydrated to isobutylene, one of the current chemical species for the industrial MTBE synthesis. Another possible alternative consists on the direct coupling of methanol and isobutanol. A new OXY-CREC reactor concept was recently proposed at CREC-UWO based on a riser/downer configuration. This new MTBE reactor has several advantages. It offers a precise control of the contact time between the reactants and the catalyst thus, avoiding reactions leading to unwanted byproducts. The riser/downer configuration also allows good control of the reaction temperature, avoiding hot spots.

In order to assess the feasibility of MTBE synthesis in a riser/downer reactor; the Riser Simulator, available at the CREC's laboratories, was used in the present study. The Riser Simulator reproduces main conditions of a full scale reactor: a) the contact time between catalyst and reactants, b) the catalyst/ reactant ratios, and, c) the partial pressure of reacting species.

Using these experimental tools the present study shows that the direct synthesis of MTBE from methanol and isobutanol is not viable using H-ZSM-5 catalyst. MIBE, an isomer of MTBE, was the only ether identified. The two reactions leading to the formation of MTBE, dehydration of isobutanol to isobutylene followed by the coupling of methanol to isobutylene, require different thermal levels. The 140 °C dehydration temperature is not compatible with the 90 °C optimum temperature for the etherification reaction. These results indicate that the presence of isobutylene appears to be a process requirement for the MTBE synthesis.

The second conclusion reached in the present study was given by the fact that MTBE synthesis from methanol and isobutylene was viable using H-ZSM-5. Due to the different phase of the reactants at room temperature, methanol a liquid and isobutylene a gas, they had to be injected separately. This situation led to interesting findings concerning the selectivity of the reaction for MTBE. Three modes of operation were investigated a) Mode 1, isobutylene is injected followed by the methanol injection after approximately 15 seconds; b) Mode 2, methanol is injected followed by isobutylene after approximately 15 seconds, c) Mode 3, methanol is injected allowing enough time, approximately 50 seconds, for methanol adsorption onto the catalyst surface to reach equilibrium. After this the isobutylene injection was effected.

Mode 3 of operation appeared to be the most promising one with 100% selectivities toward MTBE. It was observed that methanol adsorption was the most important factor to reach high MTBE selectivities.

On this basis, a series of experiments, with different methanol/isobutylene ratios, were developed and this demonstrated that as long as methanol was preadsorbed onto the catalyst surface, the selectivity remained 100 %. These last results also reinforced the conclusion that methanol pre-adsorption was a very important step to achieve a 100 % selectivity toward MTBE. Once it was established that methanol preadsorption yielded MTBE with a 100 % selectivity, Mode 3 of operation was used during the reminder of the experimental program. In this section of the program, reaction conditions were systematically varied as follows: 1) Temperature: from 80 to 160 (C, 2) Catalyst/reactant ratios: 5 and 1 levels were selected, 3) Reaction times: from 10 to 120 seconds. These runs confirmed that the yield of MTBE diminished while the reaction rates augmented with increasing temperature. It was also established that the variation of the catalyst/reactant ratio, the amount of methanol adsorbed increased and this translated in a reduction of the reaction of the catalyst/reactant ratio, the amount of methanol adsorbed increased and this translated in a reduction of the reaction equilibrium conversion, lowering the yield of MTBE. In summary, increasing the catalyst/reactant ratio may increase the reaction rate while at the same time reduce the potential maximum allowed equilibrium conversion.

From these experimental results a rate equation based on the Rideal-Eley mechanistic formulation was developed. The model offered good representation of the experimental results. From the forward reaction kinetic constant and based on the Arrhenius relationship the apparent energy of activation was calculated. The valued for the apparent energy of activation was 55 kJ/mole value was obtained.

Finally, the kinetic model was used to develop reactor simulation for various conditions: a) catalyst/reactant ratio, and, b) methanol/isobutylene ratio. The main consequence of increasing the catalyst/reactants ratio or the methanol/isobutylene ratio decreased the maximum equilibrium conversion.

It appears that the H-ZSM-5 based catalyst of this study, while valuable to demonstrate the MTBE formation and the optimum conditions for MTBE synthesis, did not provide the reaction rates required for typical riser operation (e.g. 10s). Therefore, downer reactors allowing for longer reaction times (e.g. 50 s) may be required to implement this technology.

Reviewing the results of the present study the following recommendations can be advanced:

a) To modify the catalyst used, H-ZSM-5, by increasing the Si/Al ratio. This could potentially reduce the density of acid sites while increasing the sites strength. The overall effect would be to increase the potential equilibrium conversion by having less methanol adsorption with an overall increased catalyst activity. A preferred procedure would be to increase the Si/Al by catalyst dealumination using mild steam treatment (Nikopoulos, 1996)

- b) To extend future experimental programs to other zeolites offering similar physical and chemical properties, small pores size and acidity, such as ZSM-11 already mentioned in the literature review section.
- c) To further investigate the compatibility of downflow reactors not so restricted as in the case of riser units on the allowed reaction times.
- d) To further explore MTBE synthesis from methanol and isobutanol using a different reaction path. Methanol/isobutanol etherification reaction yields MIBE. MIBE can be in turn isomerized to MTBE. The lack of knowledge on the thermodynamic equilibrium between MTBE and its isomer MIBE seems to be an obstacle to better assess this approach. The investigation of this particular alternative may lead, perhaps, to the development of a bifunctional catalyst which could catalyze both the etherification and the isomerization reactions to form MTBE.

# References

O.C. Abraham, G.F. Prescott, <u>Make Isobutylene from TBA</u>, Hydrocarbon Processing, 1992, February, pp 51-54

A.M. Al-Jaralah, M.A.B. Siddiqui, A.K.K. Lee, <u>Kinetics of Methyl Tertiary Butyl Ether</u> <u>Synthesis Catalyzed by Ion Exchange Resin</u>, The Canadian Journal of Chemical Engineering, 1988, vol 66, pp 802-807

A. Ali, S. Bhatia, <u>Methyl\_Tertiary Butyl Ether Formation in a Catalytic Bed Reactor-Kinetic</u> and <u>Modelling Study</u>, The Chemical Engineering Journal, 1990, vol 44, pp 97-106

J.R. Anderson, K.C. Pratt, Introduction to Characterization and Testing of Catalysts, Academic Press, 1985

F.G. Anthony, P.E. Thomas, <u>Make Isobutylene from Methanol</u>, Hydrocarbon Processing, 1984, November, pp 95-96

S. Bhatia, Zeolite Catalysis Principles and Applications, CRC Press, 1990

L.S. Bitar, E.A. Hazbun, W.J. Piel, <u>MTBE\_Production\_and\_Economics</u>, Hydrocarbon Processing, 1984, October, pp. 63-66

S.A. Bradley, M.J. Gattuso, R.J. Bertolacini, <u>Characterization and Catalyst Development-An</u> interactive Approach, American Chemical Society, ACS Symposium Series, 1989

H.L. Brockwell, P.R. Sarathy, R. Trotta, <u>Synthesize Ethers</u>, Hydrocarbon Processing, 1991, September, pp. 133-141

A.C. Butler, C.P. Nicolaides, <u>Catalytic Skeletal Isomerization of Linear Butenes to</u> <u>Isobutenes</u>, Catalysis Today, 1993, vol 18, pp 443-471

R. Schmitt, <u>Alkylation of MTBE\_Raffinate Increases Octane Unloads Alky Unit</u>, Oil and Gas Journal, 1991, November, pp. 99-100

E.J. Chang, S.M. Leiby, <u>Ethers Help Gasoline Quality</u>, Hydrocarbon Processing, 1992, February, pp. 41-44

P. Chu, G. H. Kühl, <u>Preparation of Methyl tert-Butyl ether (MTBE) over Zeolite Catalysts</u>, Industrial Engineering Chemistry Research, 1987, vol 26, pp 365-369

F. Colombo, L. Corf, L. Dalloro, P. Delogu, <u>Equilibrium Constant for the Methyl tert-Butyl</u> <u>Ether Liquid Phase Synthersis by Use of UNIFAC</u>, Industrial and Engineering Chemistry Fundamentals, 1983, vol 22, pp 219-223 Facts and Figures from the Chemical Industry, Chemical and Engineering News, 1996, vol 24, nu 26, p 38-79.

H.I. de Lasa, Industrial Catalysis E.S. 417A-Course Notes, University of Western Ontario, Fall 1995

H. de Lasa, Canadian Patent 1,284,017 (1991), USA Patent 5,102,628 (1992)

F. Niu, H. Hofmann, <u>Activity and Deactivation Behavior of Various Zeolite Catalysts</u>, Applied Catalysis A: General, 1995, vol 128, pp. 107-118

G.L. Frischkorn, P.J. Kuchar, R.K. Olson, <u>Butane Isomerization Technology: Now and for</u> the Future, Energy Progress, 1988, September, pp. 154-159

A. Gianetto, <u>Novel Cracking Catalyst for the Production of Reformulated Gasoline</u>, Thesis (M.E.Sc.), University of Western Ontario, 1993

A. Gicquel, B. Torck, <u>Synthesis of Methyl Tertiary Butyl Ether Catalyzed by Ion-Exchange</u> <u>Resin. Influence of Methanol Concentration and Temperature</u>, Journal of Catalysis, 1983, vol 83, pp 9-18

D.W. Grant, <u>Capillary Gas Chromatography</u>, Separation Science Series, John Wiley and Sons, 1996

L.H. Hagey, <u>Compound Catalyst for the Production of C<sub>1</sub>-C<sub>4</sub> Hydrocarbons from Synthesis</u> <u>Gas</u>, Thesis (M.E.Sc.), University of Western Ontario, 1997

G.J. Hutchings, C.P. Nicolaides, M.X. Scurrel, <u>Developments in the Production of Methyl</u> tert-Butyl Ether, Catalysis Today, 1992, vol 15, pp 23-49

K. Klier, R.G. Herman, O.C. Feeley, M.A.Johansson, <u>High Octane Ethers from Synthesis</u> <u>Gas Derived Alcohols</u>, Liquefaction Contractors' Review Meeting, September 22-24 1992, pp 291-320

H. Knözinger, H. Bühl, K. Kochloefl, <u>The Dehydration of Alcohols on Alumina XIV.</u> <u>Reactivity and Mechanism</u>, Journal of Catalysis, 1972, vol 24, pp 57-68

A. Kogelbauer, A.A. Nikopoulos, J.G. Goodwin Jr, G. Marcelin, <u>Reactant Adsorption and its</u> <u>Impact upon MTBE Syntesis on Zeolites</u>, Journal of Catalysis, 1995, vol 152, pp. 122-129

A. Kogelbauer, M. Öcal, A.A. Nikopoulos, J.G. Goodwin Jr, G. Marcelin, <u>MTBE Synthesis</u> on <u>Partially Alkali-Exchanged HY Zeolites</u>, Journal of Catalysis, 1994, vol 148, pp. 157-163

D. Kraemer, <u>Catalytic Cracking of Hydrocarbons in a Riser Simulator: Design and Testing</u>, Thesis (M.E.Sc.), University of Western Ontario, 1987 M.R. Ladisch, R.L. Hendrickson, M.A. Brewer, P.J. Westgate, <u>Catalyst-Induced Yield</u> <u>Enhancement in a Tubular Reactor</u>, Industrial Engineering Chemistry Research, 1993, vol 32, pp 1989-1996

M. Matouq, T. Tagawa, S. Goto, <u>Combined Process for Production of Methyl tert-Butyl</u> <u>Alcohol and Methanol</u>, Journnal of Chemical Engineering of Japan, 1994, vol 27, pp 302-306

Micromeritics, TPD/TPR 2900 Analyzer-Operator's Manual, 1992

J.L. Monfils, S. Barendregt, S.K. Kapur, <u>Upgrade Isobutane to Isobutylene</u>, Hydrocarbon Processing, 1992, February, pp. 47-50

C.P. Nicolaids, C.J. Stotijn, E.R.A. van der Veen, M.S. Visser, <u>Conversion of Methanol and</u> <u>Isobutanol to MTBE</u>, Applied Catalysis A: General, 1993, vol 103, pp. 223-232

A.A. Nikopoulos, A. Kogelbauer, M. Öcal, J.G. Goodwin Jr, G. Marcelin, <u>Effect of</u> <u>Dealumination on the Catalytic Activity of Acid Zeolites for the Gas Phase Synthesis of</u> <u>MTBE</u>, Applied Catalysis A: General, 1994, vol 119, pp. 69-81

J.G. Nunan, K. Klier, R.G. Herman, <u>Methanol and 2-Methyl-1-Propanol (Isobutanol)</u> <u>Coupling to Ethers and Dehydration over Nafion H: Selectivity, Kinetics, and Mechanism</u>, Journal of Catalysis, 1993, vol 139, pp. 406-420

A. Pekediz, D.W. Kraemer, J. Chabot, H.I. de Lasa, <u>Mixing Patterns in a Novel Riser</u> <u>Simulator</u>, Chemical Reactor Technology for Environmentally Safe Reactors and Products, Kluwer Academic Publishers, 1993, pp. 133-146

A. Rehfinger, U. Hoffmann, <u>Kinetics of Methyl Tertiary Butyl Ether Liquid Phase Synthesis</u> <u>Catalyzed by Ion Exchange Resin-I. Intrinsic Rate Expression in Liquid Phase Activities</u>, Chemical Engineering Science, 1990, vol 45, pp. 1605-1617

R.C. Reid, J.M. Prausnitz, B.E. Poling, <u>The Properties of Gases and Liquids</u>, Fourth Edition, McGraw-Hill Book Company, 1987

A.K. Rhodes, <u>U.S. Refiners Choose Variety of Routes to MTBE</u>, Oil and Gas Journal, 1992, September, pp.36-41

C.N. Satterfield, <u>Heterogeneous Catalysis in Practice</u>, McGraw-Hill Book Company, 1980

D. Seddon, <u>Reformulated Gasoline</u>, <u>Opportunities for New Catalyst Technology</u>, Catalysis Today, 1992, Vol 15, pp 1-21

J.M. Smith, <u>Chemical\_Engineering Kinetics</u>, Third Edition, McGraw-Hill Book Company, 1981

A.B. Stiles, F. Chen, J.B. Harrison, X. Hu, D.A. Storm, H.X. Yang, <u>Catalytic Conversion of</u> <u>Synthesis Gas to Methanol and Other Oxygenated Products</u>, Ind. Eng Chem. Res., 1991, vol 30, pp 811-821

J. Tejero, F. Cunill, J.F. Izquierdo, <u>Equilibrium Constant for the Methyl tert-Butyl Ether</u> <u>Vapor Phase Synthesis</u>, Industrial Engineering Chemistry Research, 1988, vol 27, pp 383-343

M.M.J. Treacy, J.B. Higgins, R. von Ballmoon, Zeolite, 1996, vol 16, nu 5-6

T. Zhang, R. Datta, <u>Integral Analysis of Methyl tert-Butyl Ether Synthesis Kinetics</u>, Industrial Engineering Chemistry Research, 1995, vol 34, pp 730-740

X. Wenyang, L. Jianquan, L. Wenyuan, Z. Huiming, L. Bingchang, <u>Nonaqueous Synthesis</u> of <u>ZSM-35</u> and <u>ZSM-5</u>, Zeolites, 1989, Vol 9, pp 468-473

Appendices

#### Appendix A: <u>BET Analysis: Results and Calculations</u>

The BET basic principles have already been reviewed in Chapter IV: <u>Catalysis Synthesis, Pelletization and Characterization</u>. The purpose of this appendix is to present the graphical results and the calculations necessary to analyse these results.

Figure A.1 is the BET experimental result for the catalyst zeolite H-ZSM-5. All the positive peaks on this figure are desorption peak, except the first one. According to Micromeritics (1992), the desorption peaks should be utilized to determine the specific area of the catalyst

Figure A.3 is the BET experimental result for the pelletized zeolite H-ZSM-5. The first peak of Figure A.3 is not used. The second, third and fourth positive peaks are desorption peaks. The other peaks are calibration results.

Figures A.2 and A.4 provides the integration report of Figures A.1 and A.3 respectively. The integration reports include the area of each peaks of the two chromatograms.

Even though some calibration of the response of the TCD with nitrogen was done in Fig A.3, a more thorough calibration was performed. This complete calibration is presented in fig A.5 and suggest that the TCD detector offered a linear response for nitrogen in the range necessary for the BET analysis. A linear regression through the origin was calculated. The resulting slope was used to calculate the number of mole from the desorption peaks of figure A.1 and A.3. These results are presented in Table A.1

The following calculations were based on the technique described in Micromeritics (1992). First the volume of nitrogen was converted to the conditions of standard temperature and pressure using equation A.1.

$$V_{STP} = V_N \times \frac{273.2K}{273.2 + T_{room}} \times \frac{P_{ATM}}{760}$$
(A.1)

Where  $T_{room} = 22$  °C and the  $P_{atm} = 750$  mm Hg. The calculated values of the volume at standard temperature and pressure are listed in Table A.1. Then the volume of the nitrogen monolayer was calculated as follow:

$$V_{m} = V_{STP} \left[ 1 - P_{N} / P_{N0} \right]$$
 (A.2)

Where  $p_N$  is the partial pressure of Nitrogen.

In this case the fraction of nitrogen contained in the gas mixture is 0.3. Thus the partial pressure is 225 mm Hg, i.e.  $P_{atm} \times 0.3$ .  $p_{w}$  is the saturation pressure of nitrogen. According to Micromeritics (1992), the saturation pressure of nitrogen is equal to the atmospheric pressure plus 15 mm Hg.

Values of the volume of the monolayer are given in Table A.1.The final calculation was to convert the volume into the surface area and to divide this area by the mass of catalyst to obtain the specific surface area with equation A.3.

$$S_{A} = \frac{V_{m} \times 6.023 \times 10^{23} (molecule / mole) \times 16.2 \times 10^{-20} (m^{2} / molecule)}{22 \ 414 (cm^{3} / mole) \times W_{cat}}$$
(A.3)

The values of the specific surface area are given in table A.1.

Zeolite	Area	W <sub>cat</sub>	V <sub>N</sub>	V <sub>STP</sub>	V <sub>m</sub>	S <sub>A</sub>
(-)		g	cm <sup>3</sup>	cm <sup>3</sup>	cm <sup>3</sup>	m²/g cat
Powder	1.83975 E7	0.0375	3.665	3.34	2.36	274
Pelletized	8.6257 E6	0.0370	1.718	1.57	1.11	131.3

Table A.1: Experimental values and results of the calculations.

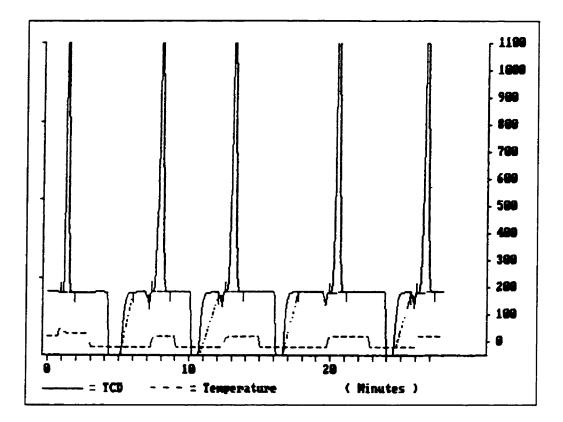


Figure A.1: Chromatogram of the BET Analysis of the Zeolite H-ZSM-5.

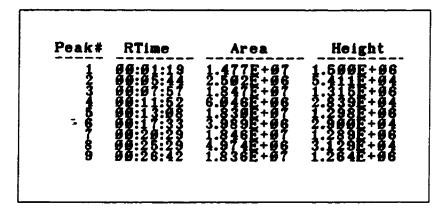


Figure A.2: Integration Report of the Chromatogram of the BET Analysis of the Zeolite H-ZSM-5.

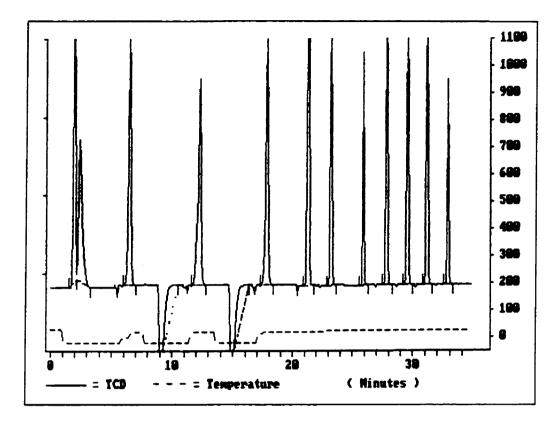


Figure A.3: Chromatogram of the BET Analysis of the Pelletized Zeolite.

RTime	Area	Height
	1.004E+07 6.801E+06 8.723E+06	9.024E+05 3.791E+05 7.334E+05
	4.431E+06 8.556E+06	2.765E+04 5.974E+05
	8.598E+46 2.629E+47	6.891E+05 3.186E+06
	4.332E+96 9.287E+96	1.3084E+95 1.493E+96
00:31:08 00:32:49	9.230E+06 3.978E+06	1.397E+06 1.390E+06 6.153E+05
	497-64 5112-64 5112-64 5112-64 5112-64 511-11-15 512-511-11-54 50 50 50 50 50 511-11-15 51-57 50 50 50 50 50 50 50 50 50 50 50 50 50	999941154         1.99941154           999941154         1.99941154           999941154         900723154           999941154         900723154           999941154         900723154           999941154         900723154           999941154         900723154           999941154         900724           999941154         900724           999941154         900724           999941157         900724           999941157         900724           999941157         900724           999941157         900724           999941157         900724           999941157         900724           9009941157         900724           9009941157         900724           9009941157         900724           9009941157         900724           900994157         900734           900994157         900734           900994157         900734           900994157         900994           90099417         90094           90099417         90094           900994334         90094           900994334         90094           90094         90094

Figure A.4: Integration Report of the Chromatogram of the BET Analysis of the Pelletized Zeolite.

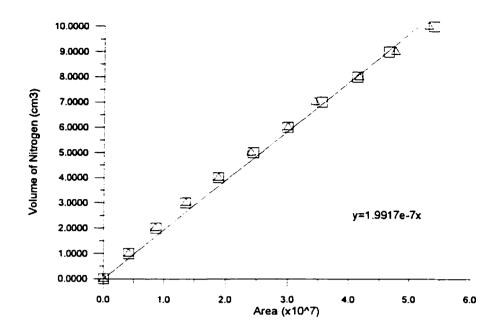


Fig A.5: Calibration of Nitrogen for the BET Analysis.

## Appendix B: Calibration of the Reactor Volume

This appendix describes the procedure involved in the determination of the volume of the reactor. First, the initial pressure in the reactor was recorded. A syringe of 50 cm<sup>3</sup> was then used to sequentially inject volume of 10 cm<sup>3</sup> of air. The pressure of the reactor was recorded after each injection. Series of 5 to 7 injections were done and 2 sets of 3 series were completed: one at the beginning of the experiments and the other at the end. As the pressure stays in the neighborhood of the atmospheric value, the ideal gas law was used to relate the reactor volume to the pressure increase.

$$PV = nRT$$
 (B.1)

As the temperature and the volume of the reactor remain constant, the pressure is directly related to the number of moles injected:

$$\frac{\Delta P}{\Delta n} = \frac{RT}{V} = m \qquad (B.2)$$

The pressure difference was plotted against the number of moles of air injected. The best fit slope was calculated using the linear regression technique. As R and T were known, it was simple to determine the volume from the slope.

Date →	September 25 <sup>th</sup> 1996			September 25 <sup>th</sup> 1996 May 1		
Volume cm <sup>3</sup>	Pressure psi	Pressure psi	Pressure psi	Pressure psi	Pressure psi	Pressure psi
0	14.17	14.17	14.16	13.65	13.65	13.65
10	17.18	17.04	17.16	16.69	16.68	16.75
10	20.09	19.96	19.89	19.69	19.68	19.72
10	22.98	22.78	22.82	22.59	22.65	22.63
10	25.85	25.58	25.63	25.47	25.65	25.48
10	28.68	28.35	28.28	28.30	28.56	28.40
10				31.15	31.34	31.17
10				33.94	34.14	33.72

Table B.1: Results of the observation of the calibration of the reactor volume

The temperature used to calculate the volume was 21.5 °C and the gas constant R=8314 cm<sup>3</sup> kPa/(mol K).

Figure B.1 and B.2 present the results of the fitting process. The results for the volume of the reactor with a confidence interval of 90 % are given in Table B.2. An average value of 51.1 cm<sup>3</sup> for the reactor volume was used for the reminder of the calculations.

Date of Calibration	Slope PSI/mole	Volume cm <sup>3</sup>
September 1996	6893.63 ±44.79	51.6±0.3
May 1997	7038.02±37.45	50.5±0.3

Table B.2: Results for the Volume for the two Calibrations.

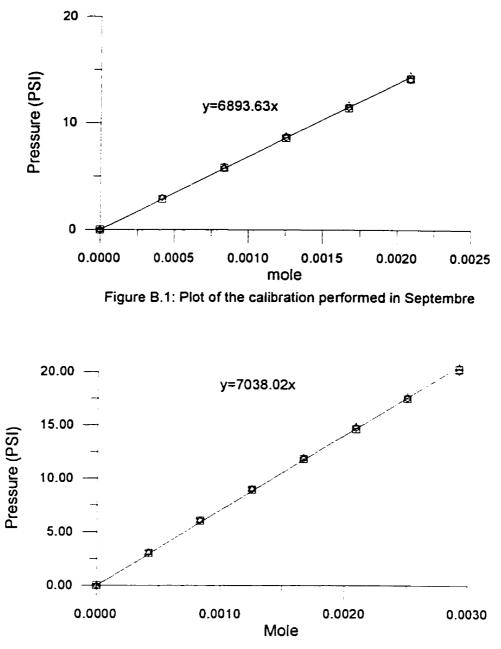


Figure B.2: Plot of the calibration performed in May

# Appendix C:<u>Calibration of the Gas Chromatograph and Calculation of the Concentration from the Chromatogram Results.</u>

C.1 Calibration

Figure C.1, C.2, C.3, and C.4 report the calibration for methanol, isobutylene MTBE and argon. The number of moles is plotted against the corresponding chromatogram areas.

In the case of isobutylene and argon, gases at room temperature, the calibration was done with a gas tight syringe. The number of moles was then calculated using the ideal gas law : PV = nRT.

For methanol and MTBE, liquids at room temperature, the quantities injected were weighed and then the number of moles were calculated. The syringe containing methanol and MTBE was weighted before and after injection with a digital balance having a precision of  $\pm 0.0001$ g.

Obviously small quantities are difficult to measure even with this type of balance. Thus, a dilution technique was used where methanol and MTBE were diluted with each other. The dilution ratio was about 1/10 in either case.

#### C.2: Calculation of Concentration

The final concentration of reactants and products in the reactor can be calculated in two ways: 1) from the argon used as an internal standard, 2) from the sampling pressure.

Both calculation techniques are based on the assumption that the amount of argon inside the reactor remains constant. Thus, the two techniques work satisfactorily if there is no leakage and if argon does not react either by adsorption or reaction with the reactants. The fact that argon is an inert prevents any reaction.

To illustrate these two techniques the same run is going to be used. The chromatogram for this run is presented in Figure C.5

#### C.2.1: Argon as Internal Standard

The calculation process is quite simple, with all the results presented in Table C.1.

The first step is to calculate the number of moles of each chemical species contained in the sample using the calibration data. Then, eq C.1, is used to calculate the total number of moles of products in the reactor:

$$N_{iT} = n_{iS} \times \frac{N_{ar}}{n_{arS}} \qquad (C.1)$$

with  $N_i$  being the total number of moles of i chemical species in the reactor,  $n_{is}$  being the number of mole of the i chemical species in the sample,  $N_{ar}$  being the number of mole of argon in the reactor, and  $n_{Ars}$  being the number of moles of argon in the sample. Results of the calculation are reported in Table C.1.

Chemical	Chromatograph results	Quantity	n;/N <sub>ar</sub>	n <sub>i</sub> /n <sub>ar</sub> *N <sub>ar</sub>
(-)	area	moles	(-)	moles
Argon	892998	6.45E-05	1.0000	1.74E-03
Methanol	145677	7.47E-06	0.1159	2.02E-04
Isobutylene	548372	1.58E-05	0.2448	4.27E-04
MTBE	24874	5.74E-07	0.0089	1.55E-05

Table C.1: Results for the Calculation Based on the Argon Content.

### C.2 Sampling Pressure

The difference between the reactor pressure, at the time of sampling, and the argon partial pressure allows to calculate the composition of the reaction mixture. Thus, the following equation can be applied:

$$N_{rp} = \frac{(p_{st} - p_{AR})V_{R}}{RT} \quad (C.2)$$

with  $N_{rp}$  being the total number of moles of reactants and products in the reaction mixture at the time of sampling;  $p_{sr}$  being the pressure at the sampling time; and  $p_{sr}$  being the partial pressure of argon.

If  $p_{sr}$  equal to 135.1 kPa and  $p_{sr}$  to 95.54 kPa, the total number of mole of product and reactants is equal to 6.9119 10<sup>-4</sup> moles.

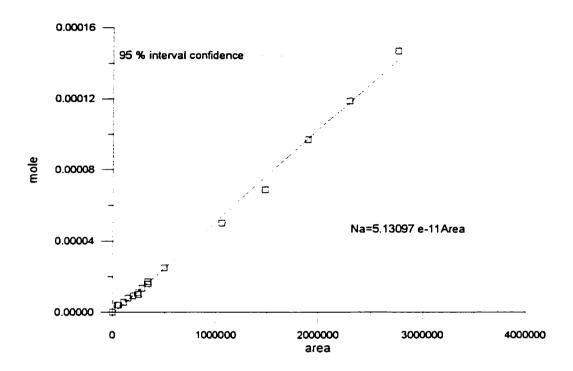
Then, the molar fraction, y<sub>i</sub>, of methanol, isobutylene and MTBE can be calculated. Note that the number of moles of each chemical species is given by the molar fraction of this chemical species times the total number of moles. Results are presented in Table C.2.

## C.3. Conclusions

Chemical	Chromatograph Results	Quantity	у,	y <sub>i</sub> xN <sub>rp</sub>
(-)	(area)	moles	(-)	moles
Methanol	145677	7.47E-06	0.3136	2.1675E-04
Isobutylene	548372	1.58E-05	0.6623	4.5779E-04
MTBE	24874	5.74E-07	0.0241	1.6654E-05
	Total	2.38E-05	1	6.9119E-04

Table C.2: Results for the Calculation based on the Sampling Pressure.

It can be observed that the two techniques provide essentially the same results and this justify the methodology proposed for calculating the various fractions of chemical species in the Riser Simulator in the case of the MTBE reaction.





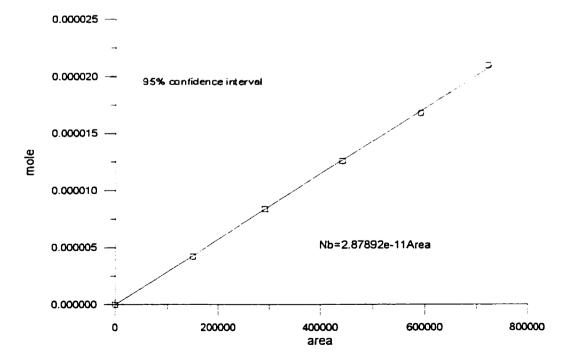


Fig C.2: Calibration of Isobutylene.

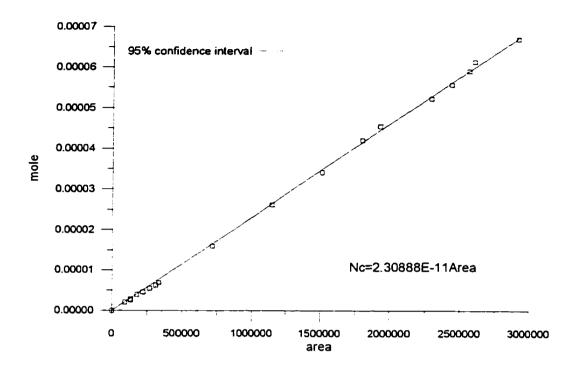


Figure C.3: Calibration of Isobutylene.

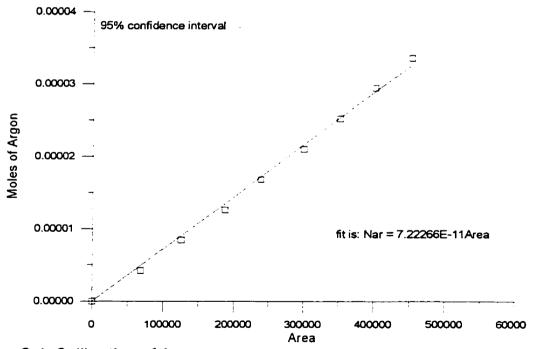


Figure C.4: Calibration of Argon

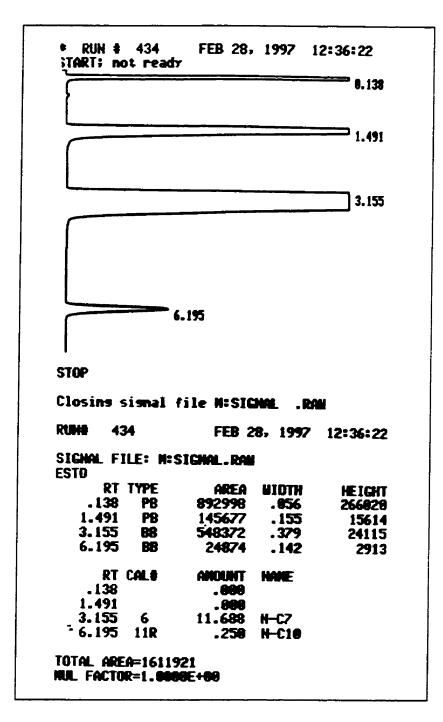


Figure C.5: Chromatogram of the example. The first peak is argon, the second methanol, the third isobutylene and the fourth MTBE

## Appendix D: List of the experimental observations used to plot Figures 6.7 and 6.8. Calculation of the average conversion for the different conditions.

This appendix includes a listing of all the experimental observations used

to calculate the average points of Figures 6.7 and 6.8. The experimental points

are classified by catalyst/ reactant ratio and then temperature.

Temperature °C	Time s	first % iso-C₄ <sup>■</sup>	second % iso-C₄ <sup>≢</sup>	average % iso-C₄ <sup>*</sup>	SSD % iso-C₄ <sup>■</sup>
80	10	0.0090	0.0091	0.0090	0.0001
80	30	0.0265	0.0249	0.0257	0.0011
80	60	0.0491	0.0382	0.0436	0.0077
80	120	0.0708	0.0563	0.0635	0.0103
120	10	0.0100	0.0122	0.0111	0.0016
120	30	0.0173	0.0236	0.0205	0.0044
120	60	0.0242	0.0330	0.0286	0.0062
120	120	0.0338	0.0478	0.0408	0.0099
160	10	0.0037	0.0035	0.0036	0.0001
160	30	0.0053	0.0065	0.0059	0.0008
160	60	0.0070	0.0067	0.0069	0.0002
160	120	0.0091	0.0095	0.0093	0.0003

Table D.1: Conversion of the reactant to MTBE based on isobutylene for the Catalyst to Reactant ratio of 5:1:

temperature °C	time s	first % iso C₄ <sup>■</sup>	second % iso C₄	third % iso C₄ <sup>■</sup>	fourth % iso C₄ <sup>■</sup>	fifth % iso C₄ <sup>■</sup>	average % iso C <sub>4</sub>	SSD % iso C₄ <sup>■</sup>
80	10	0.0099		0.0052		0.0028	0.0060	0.003629
80	30	0.0096		0.0089		0.0057	0.0081	0.002085
80	60	0.0135		0.0176		0.0140	0.0150	0.00225
80	120	0.0226		0.0258			0.0242	0.002253
120	10	0.0118	0.0245	0.0183	0.0196	0.0147	0.0178	0.004838
120	30	0.0275	0.0448	0.0396	0.0415	0.0226	0.0352	0.009584
120	60	0.0402	0.0385	0.0526	0.0474	0.0420	0.0441	0.005796
120	120	0.0552	0.0676	0.0553	0.0594	0.0578	0.0591	0.005101
160	10	0.0106	0.0122	0.0094	0.0079	0.0109	0.0102	0.001624
160	30	0.0130	0.0178	0.0128	0.0105	0.0123	0.0133	0.002696
160	60	0.0185	0.0228	0.0143	0.0128	0.0149	0.0167	0.004031
160	120	0.0157	0.0193	0.0139	0.0123	0.0150	0.0153	0.002581

Table D.2: Conversion of the reactant to MTBE based on isobutylene for the Catalyst to Reactant ratio of 1:1:

#### Appendix E: Adsorption Experiments and Related Calculations

Experiments to obtain the adsorption isotherms were performed for the three temperatures: 80, 120 and 160 °C. The Riser Simulator was used to conduct the adsorption experiments. The weight of catalyst was 1 gram. The methanol was injected using a 1 ml syringe. The quantity of methanol injected was weighted with a digital balance with a  $\pm 0.0001$  g precision. Measuring the weight instead of the volume offered more accuracy.

The weight of the syringe was measured before and after the injection. Once the injection was completed, the system was allowed to reach adsorption equilibrium conditions. The adsorption equilibrium was reached within 2 to 3 minutes. The number of moles of methanol adsorbed onto the catalyst surface was defined as the difference between the initial number of moles injected and the number of moles present in the gas phase at adsorption equilibrium. The final reactor pressure minus the pressure before injection was used to calculate the number of moles of methanol in the gas phase.

As the behavior of gases may be approximated with the ideal gas law at the conditions of the experiments, pressure between 100 and 200 kPa and temperatures between 80 and 160 °C, the number of mole of methanol in the gas phase was calculated as PV=nRT.

152

Tables E.1, E.2 and E.3 report the various parameters involved in this calculation.

The experimental points are plotted in Figures E.1, E.2 and E.3. The curves for temperature 80 and 120 °C reach a plateau where the monolayer is assumed to be completed. Condensation seems to be responsible for the second adsorption rise. In the case of 160 °C, experiments were not done up to the point where the curve reaches a plateau but the same behavior was assumed to occur.

In any case, it has to be mentioned that the methanol partial pressure during the MTBE synthesis experiments was always smaller than 35 kPa. Thus, the condensation phenomena is far from the methanol maximum value employed in the present study . A Langmuir isotherm is thus, appropriate for modelling adsorption at equilibrium. The Langmuir isotherm is described by the following mathematical formula:

$$\theta_{\star} = \frac{K_{\star}P_{\star}}{1 + K_{\star}P_{\star}}$$
(E.1)

with  $K_A$  being the adsorption constant for methanol and  $\theta_A$  is the fraction of the monolayer covered by methanol

$$\theta_{\star} = \frac{q}{q_{\pm}}$$
 (D.2)

q is the amount of methanol amount by unit mass and  $q_{sat}$  is the maximum methanol amount adsorbed by the monolayer.  $q_{sat}$  is assumed to be the value reached at the plateau of the three curves.

The calculated isotherms are represented in Figures E1, E.2 and E.3 and compared to the experimental data.

The model is fitted to the experimental data by adjusting the  $K_A$  and  $q_{sat}$  parameters. Values of  $K_A$  and  $q_{sat}$  are listed in table E.4. While  $q_{sat}$  can vary in a fairly wide range another fitting criteria was that the adsorption constant,  $K_A$ , gave a value consistent with the Arrhenius law as shown in Figure E.4.

W <sub>A</sub> gram	N <sub>Ai</sub> mole	P₄ kPa	N <sub>agp</sub> mole	q mole/g cat
0.0102	0.00032	6.20	0.00011	0.00021
0.0161	0.00050	9.17	0.00016	0.00034
0.0699	0.00218	62.73	0.00110	0.00109
0.1085	0.00339	73.75	0.00129	0.00210
0.0704	0.00220	61.35	0.00107	0.00113
0.2079	0.00650	75.82	0.00132	0.00517
0.2525	0.00789	91.12	0.00159	0.00630
0.0210	0.00066	12.20	0.00021	0.00044
0.0303	0.00095	25.02	0.00044	0.00051
0.0455	0.00142	43.77	0.00076	0.00066

Table E.1: Observations for the adsorption experiments at 80 °C.

Note:  $W_A$  = weight of methanol;  $N_{al}$  = initial number of mole of methanol;  $P_A$  = partial pressure of methanol;  $N_{agp}$  = number of mole in the gas phase; q = coverage of the catalyst surface by methanol.

W <sub>A</sub> gram	N <sub>Ai</sub> mole	P₄ kPa	N₃gp mole	q mole/g cat
0.0753	0.002353	83.89	0.00119	0.00116
0.0268	0.000838	29.98	0.00043	0.00041
0.0209	0.000653	16.54	0.00024	0.00042
0.0137	0.000428	13.10	0.00019	0.00024
0.0292	0.000913	34.81	0.00050	0.00042
0.0359	0.001122	43.43	0.00062	0.00050
0.0518	0.001619	57.90	0.00082	0.00079
0.0654	0.002044	77.89	0.00111	0.00093
0.0852	0.002663	104.77	0.00149	0.00117
0.1209	0.003778	149.58	0.00213	0.00165

Note: W<sub>A</sub> = weight of methanol; N<sub>at</sub> = initial number of mole of methanol; P<sub>A</sub> = partial pressure of methanol; N<sub>agp</sub> = number of mole in the gas phase; q= coverage of the catalyst surface by methanol.

W <sub>A</sub> gram	N <sub>Ai</sub> mole	P <sub>▲</sub> kPa	N <sub>agp</sub> mole	q mole/g cat
0.0378	0.00118	31.71	0.00050	0.00068
0.0177	0.00055	13.79	0.00022	0.00034
0.0169	0.00053	15.16	0.00024	0.00029
0.0546	0.00171	61.69	0.00097	0.00074
0.0729	0.00228	85.47	0.00134	0.00094
0.0878	0.00274	106.15	0.00167	0.00108
0.1147	0.00358	137.17	0.00215	0.00143
0.1261	0.00394	143.37	0.00225	0.00169
0.1943	0.00607	169.15	0.00265	0.00342
0.2122	0.00663	172.60	0.00271	0.00392
0.2313	0.00723	178.53	0.00280	0.00443
0.0104	0.00033	8.27	0.00013	0.00020

Table E.3: Observations for the adsorption experiments at 160 °C.

Note: W<sub>A</sub> = weight of methanol; N<sub>a</sub> = initial number of mole of methanol; P<sub>A</sub> = partial pressure of methanol; N<sub>agp</sub> = number of mole in the gas phase; q = coverage of the catalyst surface by methanol.

Table E.4: Values of KA and qsat for the three temperatures.

Temperature °C	K₄ kPa <sup>-1</sup>	q <sub>sat</sub> mole/g cat		
80	0.1222	0.0007		
120	0.0549	0.0009		
160	0.00416	0.004		

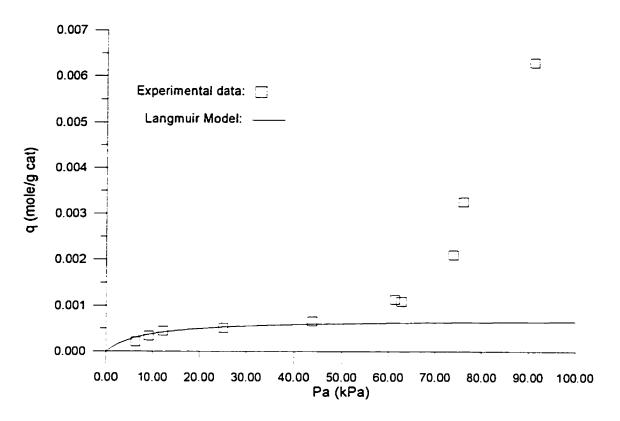


Figure E.1: Experimental observations and Langmuir Model at 80°C

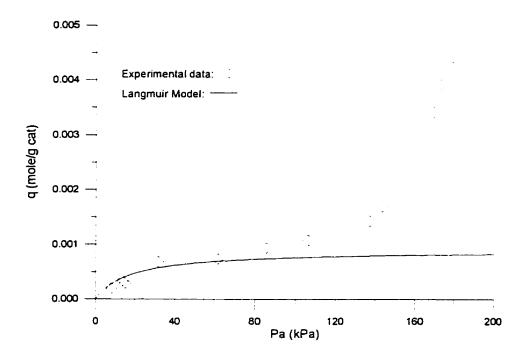


Figure E.2: Experimental observations and Langmuir Model at 120°C

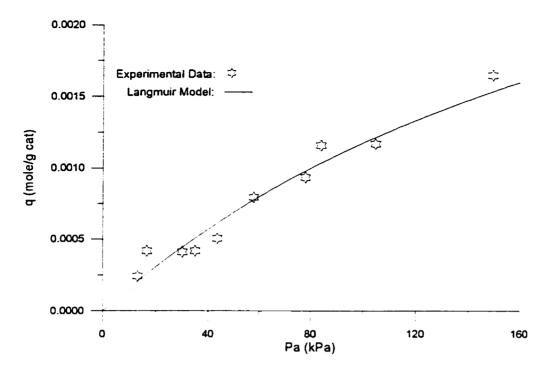


Figure E.3: Experimental observations and Langmuir Model at 160°C

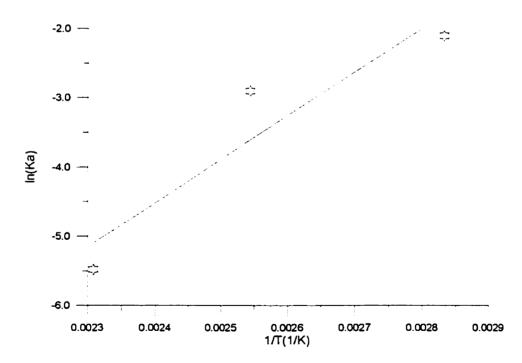


Figure E.4: Arhenius Plot of the adsorption constant (K<sub>A</sub>) against the inverse of temperature.

#### Appendix F: Equilibrium Conversion Calculation

The equilibrium conversion calculation is based on the following equation:

$$K_{s_{a}} = \frac{p_{c}}{p_{A}p_{B}} = \exp(-\Delta G_{R}) \quad (F.1)$$

where p<sub>A</sub>, p<sub>s</sub> and p<sub>c</sub> are the partial pressures of methanol, isobutylene and MTBE.

It was assumed that isobutylene and MTBE did not adsorb onto the catalyst surface according to the experimental results. The equation was then changed to have  $K_{eq}$  as a function of the conversion of isobutylene, x.

$$K_{u} = \frac{p_{Bo}x}{(p_{Ao} - p_{Bo}x)\alpha p_{Bo}(1-x)}$$
(F.2)

 $p_{A0}^{*}$  is the initial equivalent partial pressure of methanol having the reactor empty with no catalyst.  $\alpha$  is equal to  $p_{A}/p_{A}^{*}$  with  $p_{A}$  being the partial pressure of methanol.  $p_{A}^{*}$  is calculated using the following mole balance based on the partial pressure of methanol.

$$\mathbf{p'}_{\star} = \frac{K_{\star}\mathbf{p}_{\star}}{1 + K_{\star}\mathbf{p}_{\star}}\mathbf{q}_{\star}\mathbf{W}_{\star}\frac{\mathbf{RT}}{\mathbf{V}_{\star}} + \mathbf{p}_{\star}$$
(F.3)

The first term of equation F.3 represents the equivalent partial pressure of the methanol adsorbed on the catalyst surface.  $K_A$  is the adsorption constant determined in appendix E.

 $P_A^*$  was evaluated using the solver function on Excel 5.0. First several values of  $p_A^*$  were assumed starting from  $p'_{A0}$  and then going down by decrements of 0.1 kPa. Then the solver approximates the values of  $p_A$  for each value of  $p'_A$ . The value of  $\alpha$  was calculated from the values of of  $p_A$  and  $p'_A$  obtained.

An iteration process was then used to calculate the equilibrium conversion. In order to make a first approximation of the equilibrium conversion, an average value of  $\alpha$  was used. Then, the equilibrium conversion found was used to calculate p'<sub>\*</sub> from which a new value of  $\alpha$  was evaluated. After two of three iterations the value of the equilibrium conversion did not change anymore and it was judged the solution was found.

Equation 2.6, based on the assessment of the free energy change of reaction was used to calculate the value of the equilibrium constant  $K_{eq}$ :

$$\ln K = 7340T^{-1} - 4.749(\ln T) + 1.169 \times 10^{-2}T - 4.339 \times 10^{-6}T^{2} + 2.514 \times 10^{-9}T^{3} + 4.65$$
(2.6)

The initial partial pressures used to complete the calculation are given in

table F.1. The results of the equilibrium conversion are given in table F.2

Temperature °C	W <sub>cat</sub> gram	Cat/Reactant (-)	p*₄ kPa	p*₌ KPa
80	1	5:1	28.00	25.76
120	1	5:1	30.60	28.73
160	1	5:1	33.84	31.09
80	0.2	1:1	28.50	25.76
120	0.2	1:1	30.60	28.68
160	0.2	1:1	34.49	31.59

 
 Table F.1: Initial Partial Pressures and Weights of catalyst for the Calculation of the Equilibrium Conversion

 Table F.2: Equilibrium Conversions for the different Catalyst to Reactant Ratio

 and Temperature.

Temperature °C	Cat/Reactant	α	Conversion % isobutylene		
80	5:1	0.2622	17.72		
120	5:1	0.3581	3.78		
160	5:1	0.4773	0.97		
80	1:1	0.7338	33.74		
120	1:1	0.7981	7.77		
160	1:1	0.8270	1.66		

# Appendix G: Fitting of the Data to the Rate Model

The following is the proposed rate equation for MTBE formation:

$$r_{c} = \vec{k}K_{A} \left[ \frac{p_{A}p_{B} - p_{c}/K_{a}}{1 + K_{A}p_{A}} \right]$$
(G.1)  
$$K = \vec{k}K_{A}$$
(G.2)

This equation can be further simplified by using the initial equivalent partial pressure of methanol,  $p_{\infty}^*$ , which is the equivalent partial pressure of methanol without the catalyst loaded in the reactor (no adsorption) and the initial partial pressure of isobutylene. In this manner the equation becomes function of only the conversion of isobutylene, x.

$$p_{B0} \frac{dx}{dt} = \vec{k} K_{A} \left[ \frac{(p_{A0}^{*} - p_{B0}^{*} x) \alpha p_{B0}^{*} (1 - x) - p_{B0}^{*} x / K_{eq}}{1 + K_{A}^{*} (p_{A0}^{*} - p_{B0}^{*} x) \alpha} \right]$$
(G.3)

with  $\alpha$  being the p<sub>A</sub>/p<sup>\*</sup><sub>A0</sub> ratio.

Further simplification of eq (G.3) leads to:

$$\int \frac{[l/\alpha + K_{A}p_{B0} x] dx}{p_{B0} x^{2} - (p_{A0}^{*} + p_{B0} + l/K_{R0} \alpha)x + p_{A0}^{*}} = \int K dt \qquad (G.4)$$

This equation may be integrated and tables of integration were used to obtain the final result:

$$\left(l/\alpha + K_{A}p_{A0}^{*} - \frac{K_{A}}{2}(p_{A0}^{*} + p_{B0} + l/(\alpha K_{eq}))\right)A - \frac{K_{A}}{2}ln(p_{B0}x^{2} - (p_{A0}^{*} + p_{B0} + l/QK_{eq})x + p_{A0}^{*}) = Kt \quad (G.5)$$

Where A is:

$$A = \left[\frac{1}{\sqrt{(P^{*}_{**} + P_{**} + 1/(\alpha K_{*}))^{2} - 4P^{*}_{**} P_{**}}} \ln\left(\frac{2P_{**} - (P^{*}_{**} + P_{**} + 1/(\alpha K_{*})) - \sqrt{(P^{*}_{**} + P_{**} + 1/(\alpha K_{*}))^{2} - 4P^{*}_{**} P_{**}}}{2P_{**} - (P^{*}_{**} + P_{**} + 1/(\alpha K_{*})) + \sqrt{(P^{*}_{**} + P_{**} + 1/(\alpha K_{*}))^{2} - 4P^{*}_{**} P_{**}}}\right)\right]$$
(G.6)

The parameter K is adjusted until the sum of the square of the residuals,  $(x_{exp}-x_{the})^2$ , is the smallest possible. The values of  $x_{the}$  are evaluated using the eq (G.5).

The values of K also had to follow an Arhenius type of equation. The fitting process was performed manually on an Excel spreadsheet. This allowed the evaluation of eq (G.5) through the adjust function available on Excel. The results obtained from the fitting exercise are listed in Table G.1, G.2 and G.3. The results of the forward reaction kinetic constants are given in Table G.4.

Cat/react	/react temp		K*t	function (G.5)	Xexp	X <sub>the</sub>	(X <sub>exp</sub> -X <sub>the</sub> )	
-	°C	S						
5/1	80	10	101.51	101.51	0.0090	0.0070	4E-06	
5/1	80	30	304.53	304.53	0.0257	0.0203	2.92E-05	
5/1	80	60	609.05	609.05	0.0436	0.0385	2.65E-05	
5/1	80 120 1218.11	1218.11	1218.11	0.0635	0.0693	3.4E-05		
	aka ka ana arawa			unter e e e non e non e e e e e e e e e e e e		sum (x <sub>exp</sub> -x <sub>exe</sub> ) <sup>2</sup>	9.37E-05	
1/1	80	10	20.30	20.30	0.0060	0.0021	1.49E-05	
1/1	80	30	60.91	60.91	0.0081	0.0063	3.11E-06	
1/1	80	60	121.81	121.81	0.0150	0.0126	6.09E-06	
1/1	80	120	243.62	243.62	0.0242	0.0247	2.55E-07	
		···				sum (x <sub>exp</sub> -x <sub>the</sub> ) <sup>2</sup>	2.43E-05	

Table G.1: Results of the Fitting Procedure at 80 °C.

Table G.2: Results of the Fitting Procedure at 120 °C.

Cat/react	temp	t	K⁼t	function (G.5)	Xexp	Xthe	(X <sub>exp</sub> -X <sub>the</sub> )	
-	°C	S						
5/1	80	10	304.81	304.81	0.0111	0.0221	1.20E-04	
5/1	80	30	914.42	914.42	0.0205	0.0353	2.19E-04	
5/1	80	60	1828.84	1745.56	0.0286	0.0378	8.42E-05	
5/1	80	120	3657.67	1745.56	0.0408	0.0378	8.90E-06	
					<u> </u>	sum $(x_{exp}-x_{the})^2$	0.000433	
1/1	80	10	60.96	60.86	0.0178	0.0094	7.00E-05	
1/1	80	30	182.88	182.89	0.0352	0.0250	1.03E-04	
1/1	80	60	365.77	365.77	0.0441	0.0422	3.80E-06	
1/1	80	120	731.53	731.53	0.0591	0.0618	7.23E-06	
						sum (x <sub>exp</sub> -x <sub>the</sub> ) <sup>2</sup>	0.000184	

Cat/react	temp	t	K⁺t	function (G.5)	X <sub>exp</sub>	Xthe	(X <sub>exp</sub> -X <sub>the</sub> ) <sup>2</sup>
•	°C	S					_
5/1	80	10	151.01	151.01	0.0036	0.0094	3.29E-05
5/1	80	30	453.02	207.62	0.0059	0.0096	1.39E-05
5/1	80	60	906.04	207.62	0.0069	0.0096	7.44E-06
5/1	80	120	1812.08	207.62	0.0093	0.0096	7.12E-08
			. <u></u>			sum $(x_{exp}-x_{the})^2$	5.42E-05
1/1	80	10	30.20	30.12	0.0102	0.0081	4.56E-06
1/1	80	30	90.60	90.60	0.0133	0.0145	1.45E-06
1/1	80	60	181.21	181.21	0.0167	0.0165	1.3E-08
1/1	80	120	362.42	242.42	0.0153	0.0168	2.39E-06
						sum (x <sub>exp</sub> -x <sub>me</sub> ) <sup>2</sup>	8.42E-06

Table G.3: Results of the Fitting Procedure at 160 °C.

Table G.4: Values of the Forward Reaction Kinetic Constant.

Т	
°C	1/(mol g cat s)
80	83
120	555
160	3630

# Appendix H: Carbon Balances

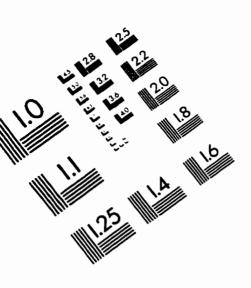
This appendix gives a listing of typical carbon balances

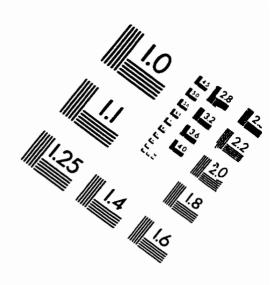
Temperature		80				120				160			
Time	10	30	60	120	10	30	60	120	10	30	60	120	
Before													
Methanol	0.0005	0.0005	0.0005	0.0005	0.0005	0.0005	0.0005	0.0005	0.0005	0.0005	0.0005	0.0005	
Isobutylene	0.0018	0.0018	0.0018	0.0018	0.0018	0.0018	0.0018	0.0018	0.0018	0.0018	0.0018	0.0018	
Total	0.0023	0.0023	0.0023	0.0023	0.0023	0.0023	0.0023	0.0023	0.0023	0.0023	0.0023	0.0023	
After													
Methanol	0.0004	0.0004	0.0004	0.0004	0.0005	0.0004	0.0003	0.0005	0.0005	0.0005	0.0004	0.0004	
Isobutylene	0.0020	0.0019	0.0020	0.0018	0.0019	0.0016	0.0016	0.0016	0.0020	0.0018	0.0015	0.0018	
MTBE	0.0000	0.0001	0.0001	0.0001	0.0000	0.0001	0.0001	0.0001	0.0000	0.0000	0.0000	0.0000	
Total	0.0024	0.0024	0.0025	0.0023	0.0025	0.0021	0.0020	0.0022	0.0025	0.0023	0.0019	5.0023	
Difference	3.0709	-3.2123	-8.3598	-0.2466	-8.2482	9.9900	10.3305	4.0188	-9.1853	0.9802	16.1832	0.8124	

## Table H.1: Carbon Balances for a Catalyst/Reactant ratio of 5.

Table H.2: Carbon Balances for a Catalyst/Reactant ratio of 1.

Temperature		80				12	0		160			
Time	10	30	60	120	10	30	60	120	10	30	60	120
Before										<u> </u>		
Methanol	0.0005	0.0005	0.0005	0.0005	0.0005	0.0005	0.0005	0.0005	0.0005	0.0005	0.0005	0.0005
Isobutylene	0.0018	0.0018	0.0018	0.0018	0.0018	0.0018	0.0018	0.0018	0.0018	0.0018	0.0018	0.0018
Total	0.0023	0.0023	0.0023	0.0023	0.0023	0.0023	0.0023	0.0023	0.0023	0.0023	0.0023	0.0023
After												
Methanol	0.0005	0.0005	0.0005	0.0005	0.0005	0.0005	0.0005	0.0005	0.0005	0.0004	0.0004	0.0004
Isobutylene	0.0020	0.0020	0.0020	0.0018	0.0021	0.0018	0.0018	0.0018	0.0021	0.0020	0.0019	0.0018
MTBE	0.0000	0.0000	0.0000	0.0001	0.0000	0.0001	0.0001	0.0001	0.0000	0.0000	0.0000	0.0000
Total	0.0025	0.0025	0.0026	0.0024	0.0026	0.0024	0.0025	0.0024	0.0026	0.0024	0.0023	0.0022
Difference	-10.75	-9.36	-12.05	-4.33	-14.96	-4.52	-6.68	-3.34	-13.69	-6.48	-1.54	3.14





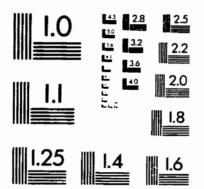
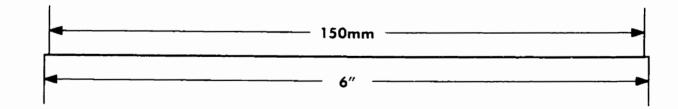
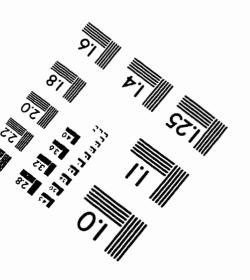


IMAGE EVALUATION TEST TARGET (QA-3)







© 1993, Applied Image, Inc., All Rights Reserved

